Cartography M.Sc.

Master Thesis

Precision Mapping of Apple Proliferation using Multi- and Hyperspectral Data

Ben Alexander McLeod

2021

Precision Mapping of Apple Proliferation using Multi- and Hyperspectral Data

submitted for the academic degree of Master of Science (M.Sc.)
conducted at the Department of Aerospace and Geodesy
Technical University of Munich

Author	Ben Alexander McLeod
Study Course	Cartography M.Sc.
1st Supervisor:	Holger Kumke, Dr.-Ing. (TUM)
2nd Supervisors:	Ekaterina Chuprikova, Dr.-Ing (Eurac Research)
	Abraham Mejia Aguilar, Ph.D (Eurac Research)
Reviewer:	Barend Köbben, M.Sc. (UT-ITC)
Chair of the Thesis Assessment Board:	Prof. Dr. Liqiu Meng
Date of submission:	10.10.2021

Statement of Authorship

Herewith I declare that I am the sole author of the submitted Master's thesis entitled:

"Precision Mapping of Apple Proliferation using Multi- and Hyperspectral Data"

I have fully referenced the ideas and work of others, whether published or unpublished.
Literal or analogous citations are clearly marked as such.

Munich, 10.10.2021 Ben Alexander McLeod

Acknowledgments

I see my thesis as the result of so much support I received from so many people throughout the master's programme and particularly during this past semester, which I am very grateful for.

First and foremost, I would like to thank Ekaterina for her close supervision during the whole thesis. I appreciate your openness and directness regarding the work, but even more outside of the project, having an open ear for issues that were on my mind and not always academic. Looking back, I remember you not only as a supervisor, but a mentor during this challenging time. I won't forget you welcoming me warmly on my first day in Bolzano and showing me around the city (and luckily also one of the best ice-cream places in town, where I happen to pass by when returning home from the library).

Secondly, I am thankful for Abraham's support throughout the thesis, particularly for organising the logistics involved in the field campaigns and supporting me with the processing of the UAV imagery. I like to think back of our open and direct chats during our drives from Fragsburg back to Bolzano once the field work was finished that day. Thanks for letting me learn from you.

In terms of logistics, a huge 'Thank you' also goes to the wonderful women at library at Eurac, giving me a place to study during the pandemic, particularly Antje, Elisabetta and Gerlinde for your support with literature. Thanks to the Center for Sensing Solutions at Eurac, especially Andrea for your support with the Spatial Data Infrastructure, Simone for helping me out with Git and Maura for organising all the administration.

I would like to extend my gratitude to the colleagues from the Plant Genomics Department of the Laimburg Research Centre, particularly Dana and Massimiliano for your support during the field campaigns, as well as Evi and Christine; Katrin and Ulrich I would like to thank you for your initial input in our research collaboration and providing me with relevant literature on Apple Proliferation.

I am very thankful for being part of the Cartography Master's which has turned out to be a challenging, yet unique experience, offering space to learn and grow. Special thanks goes to Juliane for her support throughout! I would also like to thank the European Union and the ERASMUS+ Student Mobility Program for granting me the funding to undertake this research. I would like to thank my classmates with whom I had the pleasure to share this journey. I learned a lot about me through you during this time.

Last, but certainly not least, I would like to thank my Mama, Papa and Carina for always supporting me in what I am aiming at, for bearing my moods and waves of over-excitement, for listening when I needed to talk, for believing in me – for your love.

Abstract

Precision maps have found wide applicability and are predominantly used in precision agriculture, which relies on the visual communication of relevant, high-resolution, environmental data, obtained through sensing systems to the end-user (Sishodia et al., 2020). Despite being treated as a map, the precision map contemporarily exists outside of a theoretical cartographic framework. This study aims at developing a cartographic understanding and methodology for producing precision maps to support local, technology oriented farmers, scientists, and authorities in plant disease management.

As an interdisciplinary domain, cartography bears a huge potential in meeting the increasing demand for the decision-supporting visualisation of Geospatial Big Data (Coetzee et al., 2020; Robinson et al., 2017) and thus may contribute to the development of more sustainable agriculture. Particularly, plant pests endanger tree health and harvest, thus highlighting farmers' vulnerability to plant diseases and ultimately undermining Sustainable Development Goals (SDGs), such as *Zero Hunger*, and food security (Savary et al., 2012). In contrast to traditional plant disease management, plant health monitoring through hyperspectral data enables stakeholders to detect plant stress outside the range of visible light, and hence, at an early disease stage.

This experimental study is expected to encourage future application of cartographic generalisation in agriculture and foster cartographic understanding in precision mapping using multi- and hyperspectral data. In the course of the study, it is argued for the adoption of a multi-scale mapping approach in order to visualise different spatial granularities at respective levels of detail within a precision map. Using the case study of an orchard in South Tyrol (Italy), this research focuses on developing a multi-scale precision map of Apple Proliferation (AP), a phytoplasma-induced disease transmitted through insects. It is believed that precision maps are a cartographic tool that can be part of an environmentally sustainable disease and pest management programme with the potential to minimise yield losses and foster food security.

Keywords: *Sensor-Driven Mapping*, *Plant Disease Mapping*, *Precision Map*, *Hyperspectral Data*, *Agriculture Mapping*

Acronyms

AP Apple Proliferation.

ATP Adenosine triphosphate.

C. melanoneura Cacopsylla melanoneura.

C. picta Cacopsylla picta.

Ca. P. mali Candidatus Phytoplasma mali.

CSS Center for Sensing Solutions.

DEM Digital Elevation Model.

F. florii Fieberiella florii.

GIS Geographic Information Systems.

GNSS Global Navigation and Positioning Satellite System.

IoT Internet of Things.

LiDAR Light Detection and Ranging.

NIR near-infrared.

PCA Principal Component Analysis.

PCR Polymerase Chain Reaction.

SAR Synthetic Aperture Radar.

SDG Sustainable Development Goal.

SDI Spatial Data Infrastructure.

SfM Structure from Motion.

SVM Support Vector Machine.

SWIR shortwave infrared.

UAV unmanned aerial vehicle.

VI Vegetation Index.

VIS visible light spectrum.

List of Figures

List of Tables

Contents

1 Introduction

The general notion of precision mapping has been around for at least the past 40 years when the idea of technology-driven precision agriculture has gained momentum in the 1980s (Directorate-General for Internal Policies of the Union [DGIPU], 2014). With the pressing urge to increase global food production, precision agriculture was envisaged to keep up with the increasing demand for crops in light of global population growth (Delgado et al., 2019). It might come as a surprise though, that in the past 10 years precision mapping experienced a major boost (Huang & Brown, 2018).

Particularly, the combination of scientific and technological advancements, especially in remote sensing and the domain of photogrammetry, have made platforms such as unmanned aerial vehicles (UAV's) or different kinds of high-resolution optical sensors more affordable targetting a wider audience (Szabó et al., 2017). Consequently, precision mapping has become more appealing outside of the agricultural sector, as it serves a wide range of applications, and hence, has turned into a buzzword also in other industries or scientific fields like the automotive sector or the construction business (Liu and Liu, 2018; Casagrande, 2017). Sensors, for example, are deployed on autonomous vehicles to produce HD (high definition) street maps (Liu & Liu, 2018) or 3D renderings of construction sites with high precision (Casagrande, 2017). Subsequently, different understandings of precision mapping have developed across industrial sectors. What they do have in common, is the increased demand for exact (near-real-time) environmental data and information throughout their working processes, documentation, monitoring, prediction and eventually overall-performance. High spatial accuracy and precision are immensely facilitated through past advancements in GPS technologies, even offering sub-centimetre positioning. Precision is therefore considered as a game-changer: the more exact the data, the more precise the information at hand, the better the final outcome.

The use of new technologies has opened new possibilities in mapping and map making, also for the agricultural sector. Precision agriculture is not only limited to yield maps, which was at the heart of precision farming in its infancy but precision mapping is adopted for various purposes within agriculture. By and large, precision mapping includes the location and visualisation of soil types and properties (soil moisture, fertility, nutrient content, etc.) or phenotyping (identifying different types of vegetation), amongst others. The latter makes it possible to differentiate between weeds and crops in remotely sensed imagery, which in turn, allows a precise estimation of weed spread and adequate planning of management practices like the spraying of pesticides (Yao et al., 2018).

Another field of interest in precision agriculture is the mapping and monitoring of plant health, which is inevitable as diseases and pests pose a fundamental threat to crop losses resulting in food shortages. Crop loss due to plant diseases and pests is estimated to be around 20-30% globally (Savary et al., 2019), highlighting farmers' vulnerability to plant diseases and ultimately undermining Sustainable Development Goals, such as Goal 2 ("Zero Hunger") (United Nations General Assembly [UNGA], 2015). and more broadly food security (Savary et al., 2012). Hence, early detection of plant diseases through precision mapping can support minimizing crop losses and ultimately pave the way to a more sustainable agri-

culture.

On-site visible inspections and follow-up laboratory analysis by plant disease experts are rather considered as time and resource-costly practices, which do not guarantee an early detection of plant diseases, especially that not all pant diseases and pests manifest themselves through an early onset of symptoms that are visible to the human eye. Unlike traditional monitoring strategies, plant diseases can be detected at an early stage through remote sensing. Remote sensing techniques allow assessing the plant's physiological state through spectral analysis of the sunlight reflectance behaviour at the leaf or canopy level (Blackburn, 2006). Conventionally, multispectral data was and still is used in spectral band analysis and for computing respective vegetation indices (VI's) to assess plant physiology. However, the development of hyperspectral narrowband sensing systems has offered new opportunities in plant monitoring. Hyperspectral data is characterised not only by narrower bandwidths, but at the same time covers a larger extend within the electromagnetic spectrum (Thenkabail et al., 2018). Recording electromagnetic reflectances in finer bandwidths, allows the identification of small nuances within the electromagnetic spectrum, which has become even more promising for plant health monitoring through precision mapping.

Despite being a cartographic product in the end, the precision map, although widely in use, contemporarily exists outside of a theoretical cartographic framework. On the other hand, Geographical Information Science and Remote Sensing have primarily found entry in agricultural practices (Usery et al., 1995; Papp et al., 2021), consequently laying the foundation for precision agriculture (Sishodia et al., 2020). The intrinsic nature of a map, however, aims at communicating spatial information visually through abstraction and generalisation of what would be too big or complex to be understood in its raw format (Robinson et al., 2017). Cartography as an interdisciplinary domain bears a huge potential in meeting the increasing contemporary demand for automated spatial information extraction and visual communication, especially, when dealing with Big Data, for decision making (Coetzee et al., 2020; Robinson et al., 2017), and hence, may drive progress towards more sustainable agriculture.

This research aims at developing a cartographic understanding and methodology for producing precision maps to support local, technology oriented farmers, scientists, and authorities in making spatial decisions. The methodological framework for precision mapping shall be developed at the example of Apple Proliferation in the Upper Adige Valley in South Tyrol, Italy, using multi- and hyperspectral imaging techniques for classifying (un)infected plants as a non-destructive method and early-warning detection.

1.1. Motivation

AP is considered to be amongst the most hazardous apple plant diseases, bearing enormous environmental, economic and social costs on apple growing regions across Europe and also in the Middle East (Janik et al., 2020). This phytoplasmal disease – a phytoplasma being a cell wall-less bacterium – causes significant yield loss, as it impairs fruit quality, size and weight in affected trees (Janik et al., 2020), resulting in severe economic losses. In Italy alone, for instance, the yield deficit caused through AP is estimated to account for an equivalent of around 100 million Euro in economic loss for 2001 only (Strauss, 2009). Consequently, AP is not only considered a severe plant disease, but even a plant pest in the agricultural sector. Adequate plant disease control and pest management are inevitable to reduce impacts caused through AP by containing and removing affected trees, as well as identifying trees in an early stage of contamination.

Formerly, traditional plant disease management required labour intensive monitoring based on expert knowledge, ideally present on-site regularly or even daily. Additionally, biological and laboratory Polymerase Chain Reaction (PCR) analysis have been developed in recent years, which are very accurate in detecting plant diseases such as AP, but in turn are destructive methods, as plant samples are needed for biogenetic analysis. As the biochemical analysis follows an invasive procedure or having a plant pathologist or an expert in the field of plant diseases present at the orchard seems impractical and costly, farmers are left with few alternatives. One of them is the extensive use of pesticides to cover especially large areas of apple orchards. However, as spraying of pesticides is commonly applied on a large scale, it seems rather inefficient, let alone environmentally harmful in greater quantities over a longer period of time (Sishodia et al., 2020).

Therefore, more sustainable practices need to be developed to minimise costs associated with AP (i.e. uneconomical expenditure on and use of pesticides, resulting in an inefficient pest control and if left unmonitored implying significant environmental and economic damage, once trees at an advanced disease stage face uprooting). Technology and data-driven strategies may aid in designing pest control more efficiently as less time and labour is required in the field and losses are being minimised through identification of AP in its early stages (Janik et al., 2020).

Precision farming, also referred to as precision agriculture, may be considered as a possible solution in reducing crop losses caused through AP, following a non-invasive method for collecting environmental data. Precision agriculture is understood as a '*whole-farm management approach*' (DGIPU, 2014), ranging from the remote and proximal sensor-based data collection in combination with Global Navigation and Positioning Satellite System (GNSS) to the derived precision maps, which are sensor-driven, large scale maps.

Particularly, the use of hyperspectral data for precision mapping is considered promising for early detection of AP, due to the narrowband spectral resolution extending the visible light spectrum (VIS) and near-infrared (NIR) spectrum. To the author's knowledge, there is currently no other research activity with the focus on detecting AP through hyperspectral data for precision mapping.

Contemporarily, precision maps are used to convey spatial information to the end-user, commonly presenting sensor-derived, raw data containing a lot of detail at high spatial resolution. However, maps are considered as powerful visual tools to communicate space as they only

depict a selection or in other words an abstraction of the conceived environment (Kraak & Fabrikant, 2017). Seemingly, there is a need for further research to establish a cartographic foundation for existing precision maps, as cartographic principles are neglected within their creation. Guided by this research interest, this thesis is aiming at the development of a framework for precision maps, to serve as tools for spatial decision making regarding plant pest control. Hence, this thesis is viewed as a cartographic contribution in realising sustainable agriculture as precision maps enable early plant disease detection and, therefore, may aid in pursuing food security in the long-term.

1.2. Research Scope

In line with the proposed scientific contribution, the scope of this thesis is set around the establishment of a methodological framework which shall enrich the contemporary understanding for precision mapping by a cartographic perspective. For this purpose, the concept of the visualisation pipeline (Haber & McNabb, 1990), which shall be elaborated in the course of the thesis, will be adopted as a guiding structure for precision map making. In brief, this conceptualisation summarises the visualisation process as a logical sequence of working stages, beginning with the collection of data, in this case remotely sensed, its processing, analysis, visualisation, and finally, the accessibility by the intended users. Therefore, the breadth of this research spans the entire data life cycle, from 'cradle to adolescence'.

Following an interdisciplinary approach might seem a crux at first, but is indispensable herein, as the interplay of remote sensing, image processing, photogrammetry and cartography allows developing a reproducible, data-driven and non-invasive mapping strategy of AP. Expert knowledge on AP is additionally provided by the Department for Plant Genomics of the Laimburg Research Centre (LRC). However, the thesis is not understood as a piece of work placed directly in plant pathology, per se, but the biological knowledge is fundamental for gaining insight from the hyperspectral data analysis. Consequently, this research is based on findings from previous plant pathology studies of AP in order to reason the possible effects of the plant disease on the plant's spectral characteristics.
Additionally, the investigation of other biotic and abiotic plant disease stressors is out of thesis scope. This means, that neither biotic (e.g. plant age and constitution, insect count on orchard, etc.), nor abiotic (e.g. soil properties, altitude, exposition, geological context, etc.) were investigated as environmental vectors potentially favouring the spread of AP. The thesis is also not considered as a feasibility study for precision mapping of AP, but rather an experimental study. Currently, there is no other research on precision mapping of AP undertaken in the face of cartographic visualisation that is known to the author.

By implementing a multi-scale view in precision maps, scientific innovation is aimed at in the field of cartography. The precision map-making of AP disease spread is based on multimodal data acquisition using remote sensing techniques. This includes a ground sensing approach, to obtain individual leaf spectral signatures with a field-spectroradiometer, as well as airborne proximal sensing adopted on the orchard level using multi- and hyperspectral cameras mounted on an UAV. Insights gained through the spectral data analysis are supposed to serve as the basis for subsequent multi- and hyperspectral waveband selection and composition of adequate vegetation indices that aid in detecting AP infested plants. Additionally, with the use of a machine learning technique, the support vector machine, it is expected to ensure a reproducible and accurate image classification of the aerial imagery in order to delineate infected from uninfected trees based on a robust field-derived training dataset. Spatial granularity shall be integrated within the precision maps by means of abstraction along the interconnected spatial scales (from a high-resolution leaf layer to an object-oriented orchard layer). Finally, the precision maps will be made accessible through open-source geospatial soft-and hardware, ensuing the idea of open science proposed by Coetzee et al. (2020).

The experimental research is coordinated and supervised by colleagues at the Center for Sensing Solutions (CSS) at Eurac Research in Bolzano, located in South Tyrol, Italy. The CSS is a competence centre that aims at establishing innovative technological solutions to

monitor and understand key environmental dynamics in sensitive mountain regions. This includes the design and implementation of environmental and data-driven services by integrating multi-source and multi-scale information (remote, proximal, ground sensing techniques) with interdisciplinary approaches.

1.3. Research Questions and Objectives

In achieving the development of a cartographic methodology for producing multi-scale precision maps of AP, the underlying research objectives are identified as follows:

Research Objectives	
RO.1	Develop a cartographic understanding and definition for a precision map.
RO.2	Identify relevant spectral bands and VI that meaningfully discriminate between leaves infected from AP vs. uninfected leaves (binary and multi-class discrimination).
RO.3	Implement a robust and reproducible image classification procedure based on a machine learning approach specifically for the identification of AP on varying levels of detail (at the leaf, tree, and orchard level).
RO.4	Establish a mapping technique to produce precision maps dedicated to AP on different levels of detail.

Respectively, the research questions are formulated like so to answer the above stated objectives:

Research Questions	
RQ.1	How can a precision map be defined from a cartographic understanding?
RQ.2	Which meaningful spectral bands from the hyperspectral range and which AP can be identified, or computed, respectfully, from the spectral signature of a diseased leaf.. (a) to reflect changes caused through AP? (b) to therefore be an indicator for the presence of AP? (c) to ultimately be used to distinguish between healthy and diseased leaves [binary classification]? (d) additionally: to distinguish degree of disease severity from healthy leaf [multi-class classification]?
RQ.3	Which machine learning approach produces a robust multi-/ hyperspectral image classification for identifying and classifying AP on different scales (leaf, tree and orchard)?
RQ.4	How can multi-scale data be effectively visualised on various granularity levels?

1.4. Thesis Outline

The structure of the proceeding discourse follows a logical set-up that aims to establish a cartographic understanding for precision mapping of plant diseases and exemplify the experimental methodological framework for precision mapping of AP infected trees based on hyperspectral data. For this purpose, the scope and intended contribution of the thesis needs to be contextualised first.

Hence, in Chapter 2 the need for precision mapping in sustainable agriculture shall be reasoned and the gap for cartographic research identified. Thereafter follows a scientific background on remote sensing applications for precision agriculture as precision mapping itself starts with the collection of data. Subsequently, state of the art in hyperspectral data analysis for plant disease detection shall be outlined, which eventually leads to the visualisation techniques adopted in precision mapping and the need for cartographic approaches in precision agriculture. A brief excursion on the effects, symptoms and overall context on AP is made, concluding the literature review.

In Chapter 3, the methodological approach is defined, which adopts the concept of the visualisation pipeline and delineates the subdivided work stages for precision mapping.

The elaborated methodology is then investigated in the *Case Study* on AP detection in South Tyrol and its workflow described in Chapter 4.

The derived findings from the spectral analysis, image classification and the precision mapmaking itself will be presented under *Results*, Chapter 5.

These will set the basis for the follow-on discussion in Chapter 6, where the findings will be placed in context with the previously defined research objectives.

In *Limitations and Paths for Future Research* (Chapter 7), shortcomings faced during this scientific work are reflected and outlook for future research suggested before concluding the thesis in Chapter 8.

2 Foundations and State of the Art

Plant diseases, pests and pathogens, as well as animals, are considered to cause yield losses estimated between 20 and 40% of global agricultural production (for example Oerke, 2006). It can be assumed, that the herein stated direct economic losses imply far more adverse indirect effects on public health, the textile industry, livelihoods, and more broadly speaking societies as well as the environment (Savary et al., 2012). Hence, the true costs can be considered to exceed those of agricultural productivity as crop losses due to plant diseases and pathogens compromise on food availability, ultimately undermining food security. The latter is commonly understood as the ability to have access to food, following the definition from the 1996 World Food Summit (Food and Agriculture Organization of the United Nations [FAO], 1996), which states that food security '*exists when all people, at all times, have physical and economic access to sufficient, safe, and nutritious food to meet their dietary needs and food preferences for an active and healthy life*'. According to Ingram (2011), food security has commonly been framed as a logistical matter when referring to access to food, but concepts such as productivity or agriculture are neither included in the formulation by FAO (1996), nor in other definitions. However, it is important to account for agricultural productivity when conceptualising food security, as this state of basic need is a mutual interdependence of food production and consumption, or in other words, producer and consumer patterns within a political context. The need to account for production patterns when referring to food security and thus adopting Ingram's 2011 review on the term becomes more clear when looking, for instance at the SDG 2 - *End hunger, achieve food security and improved nutrition and promote sustainable agriculture* is directly linked to it (UNGA, 2015). More precisely, the SDG 2 is broken further down into sub-targets of which Target 2.3 and Target 2.4 directly address an increase in agricultural productivity and a transition to agricultural sustainability (Table 2.1). Furthermore, synergetic effects between the

Sustainable Development Goals - Goal 2	
Target 2.3	*By 2030, double the agricultural productivity and incomes of small-scale food producers, in particular women, indigenous peoples, family farmers, pastoralists and fishers, including through secure and equal access to land, other productive resources and inputs, knowledge, financial services, markets and opportunities for value addition and non-farm employment*
Target 2.4	*By 2030, ensure sustainable food production systems and implement resilient agricultural practices that increase productivity and production, that help maintain ecosystems, that strengthen capacity for adaptation to climate change, extreme weather, drought, flooding and other disasters and that progressively improve land and soil quality*

Table 2.1: SDGs - Goal 2 (End Hunger) - Targets 2.3 & 2.4 (UNGA, 2015, p.15)

17 SDG's exist, which means that they are highly interrelated and interdependent and thus when working towards one goal, another goal or several are also tackled at the same time. This, for instance, is the case in the pursuit of Goal 2 ('*End hunger*'), as targets from Goal

12 - *Ensure sustainable consumption and production patterns* can be addressed at the same time (Table 2.2).

Sustainable Development Goals - Goal 12	
Target 12.2	*By 2030, achieve the sustainable management and efficient use of natural resources*
Target 12.4	*By 2020, achieve the environmentally sound management of chemicals and all wastes throughout their life cycle, in accordance with agreed international frameworks, and significantly reduce their release to air, water and soil in order to minimize their adverse impacts on human health and the environment*

Table 2.2: SDG - Goal 12 (Ensure sustainable consumption and production patterns) - Targets 12.2 & 12.4 (UNGA, 2015, p.22)

In sight of an increasing world population and subsequently increased demand for alimentation, food productivity needs to be upscaled to meet current demands and those of future generations. Considering that natural resources are finite, the amount of arable land, soil capacity as well as the quantities of water used for irrigation are limited. This means that agriculture sees itself in need of rethinking and -shaping. Having undergone various transformations (i.e. the Green Revolution in the 1960s – 1980s) in the past due to technological development, agriculture, as we know today, will need to incorporate strategies to overcome food insecurity by maintaining food production, minimizing crop losses during growing, processing and post-harvesting stages (UNGA, 2015).

What is also referred to as agriculture 4.0 (Tappeiner et al., 2020) needs to be based on efficient food production, using available resources reasonably well, and minimize the risk of food shortages due to plant diseases or pests that undermine SDGs, and subsequently, is idealized as sustainable agriculture. How is sustainability understood, though, and what is meant particularly with sustainable agriculture? The definition of sustainability per se is an entire discourse itself and shall not be the focus of this literature review; however, it is important to be aware of its meaning and how it is been understood throughout the thesis. Hence, the definition of the Brundtland Report (United Nations Secretary-General & World Commission on Environment and Development [UN][& WCED], 1987) sets the theoretical frame for the concept of sustainability used within this thesis, in which *sustainable development* aims to '*ensure that it meets the needs of the present without compromising the ability of future generations to meet their own needs*'. Furthermore, any action undertaken towards sustainable development must address its three dimensions, which again are interrelated and interdependent: environment, society and economy (UNWCED, 1987).

How does this apply to agriculture, and what does sustainable agriculture mean then? Different concepts and terms have developed around the notion of sustainability in agriculture, such as community-based, ecological, environmentally sensitive, extensive, organic, and permaculture, to name a few amongst the wide terminological range (Pretty, 2008). All of them touch upon aspects of sustainability, but it is open to debate whether the above qualify as sustainable.

Therefore, Pretty (2008) (p.451) identified the following key principles for agricultural sustainability:

- *integrate biological and ecological processes such as nutrient cycling, nitrogen fixation, soil regeneration, allelopathy, competition, predation and parasitism into food production processes,*
- *minimize the use of those non-renewable inputs that cause harm to the environment or to the health of farmers and consumers,*
- *make productive use of the knowledge and skills of farmers, thus improving their self-reliance and substituting human capital for costly external inputs, and*
- *make productive use of people's collective capacities to work together to solve common agricultural and natural resource problems, such as for pest, watershed, irrigation, forest and credit management*

The FAO defines their five key principles more broadly, but highlights more the balance between the social, economic and environmental dimensions of sustainability (FAO, 2014, p.7) :

- *improving efficiency in the use of resources;*
- *conserving, protecting and enhancing natural ecosystems;*
- *protecting and improving rural livelihoods and social well-being;*
- *enhancing the resilience of people, communities and ecosystems; and*
- *promoting good governance of both natural and human systems.*

Sustainable agriculture can therefore be considered as a key for economically stable and less volatile production, an environmentally friendlier cultivation and a practice to ensure livelihood for people employed in the agricultural sector – especially those who live of what they harvest.

Striving towards sustainability, which is described rather as a process than a state (UNWCED, 1987), and thus progressing towards agricultural sustainability, the use of technologies and the promotion and implementation of innovations take a special role within this transformation (Pretty, 2008; FAO, 2014; Tappeiner et al., 2020, amongst others). Adapted to the local circumstances, technologies like in-field irrigation systems, crop harvesting, but also monitoring and imaging systems using (geospatial) sensors pose opportunities for an agriculture 4.0. These cite specific farming measures are all techniques covered under the umbrella term precision farming or precision agriculture (both terms are used synonymously within the context of this thesis). According to DGIPU (2014), the US House of Representatives firstly defined precision agriculture in 1997 as '*an integrated information-and production-based farming system that is designed to increase long term, site-specific and whole farm production efficiency, productivity and profitability while minimizing unintended impacts on wildlife and the environment*' (p.11). This core concept of precision farming is still valid today, but the field of applications of precision agriculture has diversified in light of technological advancements, such as the inclusion of GNSS, Geographic Information Systems (GIS), remote sensing based not only on satellites, but also on unmanned aerial vehicles, as

well as the presence of Internet of Things (IoT) (Thenkabail et al., 2018). Precision agriculture implies farming with precise knowledge of the within-field variability (Thenkabail et al., 2018).

In terms of sustainable agriculture, precision farming can offer a toolset to pursue sustainable development within the agricultural sector (Directorate-General for Parliamentary Research Services [DGPRS], 2019). Amongst others, it is expected that precision agriculture can contribute to a more efficient resource management (DGPRS, 2019), decreasing the use of and thus the expenses for pesticides due to an early detection of plant diseases, which is expected to reduce production costs in the long-term, and more importantly decrease crop loss due to pests and pathogens (Al-Saddik et al., 2018). Particularly, remote sensing techniques that are deployed in precision agriculture, allow sensing plants' constitution or crop health adopting a non-invasive, reproducible as well as time and cost efficient approach (for example Thenkabail et al., 2018; Yao et al., 2018; Lowe et al., 2017; Al-Saddik et al., 2018). In order to utilize the remotely sensed data, the spatial information needs to be communicated visually and prepared in a way that spatial information can be used by involved stakeholders who can rely on the this approach in their spatial decision making, when it comes to disease and pest control and the choice in adequate management practices. To convey spatial information in an usable manner, maps or rather precision maps are an integral part in precision agriculture. The word *precision* is being given also another meaning when high-resolution cameras mounted on UAVs are deployed for precision agriculture, instead of using satellite-derived images. Large scale precision maps can, therefore, cover a small area of interest with a high amount of detail. However, this poses a dilemma from a cartographic point of view, as the shear amount of data, what one could also refer to as Big Data, cannot be displayed in its raw form, but cartographic abstraction and generalisation is required in order to communicate spatial information through maps. Consequently, the contemporary notion of precision maps exists outside a cartographic understanding.

To address this issue in a logical manner, the following literature review will focus on the development of a cartographic methodological framework for future precision map-making, which sets the scope for this thesis. In the course of the following chapters, an understanding for precision mapping through a cartographic lens shall be elaborated by firstly highlighting the importance of remote sensing applications for data collection in precision agriculture. Thereafter, state of the art in hyperspectral data analysis for plant disease detection shall be outlined, followed by a review of visualisation techniques currently adopted in precision mapping and the need for cartographic approaches in precision agriculture. A brief outline of the research on AP and a summary of intended research ideas conclude the literature review.

2.1. Remote sensing in Precision Agriculture

According to Robinson et al. (1995, p.127) remote sensing can be described as the '*process of collecting, storing, and extracting environmental information from images of the ground acquired by devices not in direct physical contact with the features being studied*'. Initially, the potential of remote sensing was perceived in bridging the lack of detailed geographic information, that could eventually be overcome with the first photographic images taken from aircraft in the late 1930s, when remote sensing was in its beginnings (Robinson et al., 1995). Particularly, topographic mapping profited from remote sensing in the early stages, as cartographers were now given new tools for designing large scale and detailed topographic maps (Robinson et al., 1995). Since the initial stages of remote sensing, its techniques have found entry in various fields, of which precision agriculture is one of them, which in turn sees remote sensing techniques deployed in various formats and for a range of applications. For instance, field sensors are mounted on tractors during harvest, to map high-yielding and low-yielding areas (Environmental Systems Research Institute [ESRI], 2006), variable rate fertilisation systems used to execute site specific nutrient input (ESRI, 2006), satellite derived imagery is used to assess soil properties, such as moisture content (Yao et al., 2018), or airborne sensors are operated to estimate crop damage across the field (Yao et al., 2018). Recent technological advancements enabled the increased production of high-tech devices available on the mass market. This includes the development of cameras that over the years have offered higher resolution imagery due to constantly shrinking pixel size, as well as the design of low-cost UAVs for producing high-resolution digital orthophotos and Digital Elevation Model (DEM) (Casagrande & Gusto, 2017). Consequently, the advantage of affordable UAV-installed cameras is self-evident, as low-cost maps can be produced, for example of the vegetation, highlighting healthy and unhealthy plants on a cultivated area (Candiago et al., 2015). The use of UAVs as a portable platform for mounting sensors is trending within precision agriculture as it allows cite-specific, remote sensing at low altitude (10–100 m above ground typically) (Yao et al., 2018). UAVs exist in all sorts of shapes, such as fixed-wing airframes, helicopters, and multirotors (e.g. quadrotor, hexcopter, octocopter), on which portable sensors, like digital cameras, multispectral broadband cameras, thermal cameras, hyperspectral cameras, Light Detection and Ranging (LiDAR) and Synthetic Aperture Radar (SAR) sensors are mounted. The above stated definition of remote sensing has changed with time as machine-mounted and especially hand-held proximal sensing typically with a spatial resolution in the range of 0.001–0.01 m extends the understanding of (aircraft or satellite) remote sensing applications which are in the order of 0.1–100 m spatial resolution (Oerke et al., 2014)(Fig. 2.1).

However, at the very core of remote sensing data analysis is the interpretation of spectral information (Robinson et al., 1995). Deriving the essential information about the vegetation from remote sensing data depends on sensor specifications, radiation interaction with a vegetation canopy and the methods adopted (Curran, 1989). The spectral signal that is recorded at the sensor carries information of the land's surface that is not necessarily visible to the human eye (Robinson et al., 1995). When referring to the spectral signal, it is understood as the reflectance of light at an object's surface that is measured along specific wavelengths either in micro or nano metres within the electromagnetic spectrum (Robinson et al., 1995). The latter, is divided into certain spectral ranges, such as the VIS (400–700 nm), NIR range (700–1300 nm,) and the shortwave infrared (SWIR) region (1300–3000 nm), amongst others (Schowengerdt, 2006)(Fig. 2.2).

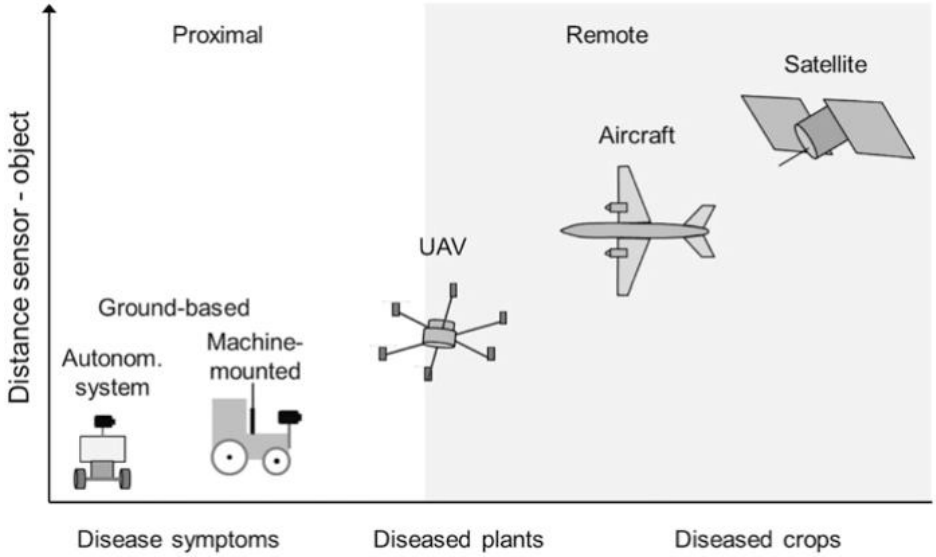

Figure 2.1: Proximal and remote sensing platforms (adopted from Oerke et al., 2014, p.57)

According to Yao et al. (2018), relative reflectances have been used in several studies with the intention to minimize the impact of variable lighting conditions, as well as relative positioning variation between sensor and object. However, it is worth mentioning at this point, that developing a robust, in-field plant spectral sensing technique is subject to variable lighting (i.e. varying sunlight conditions), which poses a challenge (Yao et al., 2018). Unlike data collection under laboratory conditions with an artificial light-source, outdoor, passive remote sensing commonly depends on ambient sunlight. Thus, the spectral signature that is recorded at the sensor is subject to the sun's illumination intensity at a given point that changes according to the time of day, atmospheric effects, such as absorption or scattering of light. The object's surface composition (e.g. flat, rugged, smooth, undulated or multiple stories in case of vegetation canopy), orientation of the object, presence of non-leaf elements, as well as the reflection angle determine the recorded object's radiance (Lowe et al., 2017; Blackburn, 2006).The measured radiance of an object at the Earth's surface is consequently the result of an interplay of several factors, that eventually shape the objects spectral signature, which is essential for remote sensing data analysis.

Due to the high correlation between an object's reflectance and its physical and chemical composition (Curran, 1989), spectral signals are considered as indicators for plant physiology (Peñuelas and Filella, 1998; Wegmann et al., 2016). Multispectral cameras for instance, produce imagery that commonly cover a wider range within the electromagnetic spectrum and therefore typically produce imagery composed of red, green and blue spectral bands, but also within the NIR and thermal domain (Yao et al., 2018). Generally, in the red portion (630–690 nm) sunlight is absorbed by healthy vegetation, but reflected in the NIR (>760–920 nm). In-between the red and NIR range in the electromagnetic spectrum is the so called red edge (>690–760 nm)(Fig. 2.3). This is a very characteristic feature in vegetative spectral reflectances, because a swift change occurs from red with high absorption to high reflectance rates in the NIR. For healthy vegetation a red shift in the red edge portion can be observed. On the contrary, a blue shift in the red edge portion can occur with stressed plants (Thenkabail et al., 2018).

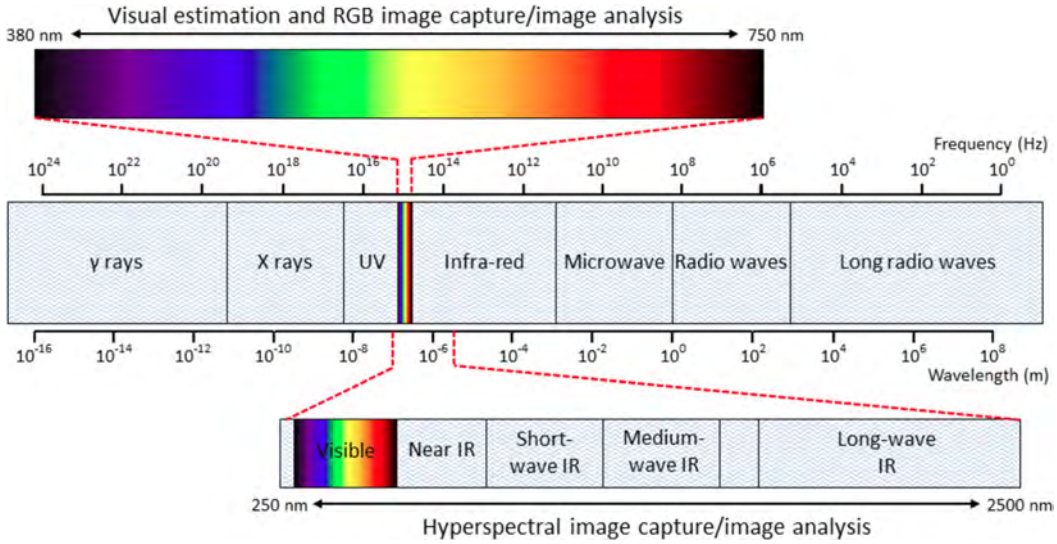

Figure 2.2: Electromagnetic spectrum (adopted from Bock et al., 2020, p.2)

Plant reflectance is governed by leaf surface properties and internal structure, as well as by the concentration and distribution of biochemical components (Peñuelas & Filella, 1998). Within the visible blue electromagnetic spectrum, reflectance ratios are affected for instance by carotenoid and chlorophyll absorption, whereas in the visible red, absorption is only driven by chlorophylls mainly (Peñuelas et al., 1994). The 'red edge' has been viewed as a good indication of chlorophyll content at the leaf level, but also at the canopy level (Fiella & Peñuelas, 1994). In the NIR spectral range, reflectance correlates to structural composition (Fig. 2.4) and changes found in the leaf and generally there are no prominent absorption features in this spectral range. On the other hand, absorption characteristics of a leaf is driven by water and other compounds in the middle infrared region, resulting in varying reflectance values (Peñuelas & Filella, 1998).

This means, that remotely sensed data is not only used for categorising vegetation form the physical contents of canopies, but also considered as an indicator for its chemical composition (Curran, 1989). In the visible spectrum, leaf reflectance is low because of absorption by photosynthetic pigments (Peñuelas & Filella, 1998), primarily by carotenoid and chlorophyll concentrations, the most important solar light absorbing pigments (Blackburn, 2006). Chlorophyll *a* and *b* are both indicators of plant stress and phenological stage, whereas carotenoid concentrations disclose ancillary information on vegetation physiological status (Young and Britton, 1990, cited by Blackburn, 2006, p.856). Furthermore, anthocyanins are the third major pigment group in leaves which can regulate the light environment within the leaf and exhibit a photoprotective function (Steyn et al., 2002; Close and Beadle, 2003) by regulating photosynthesis through limiting photoinhibition and photobleaching (Barker et al., 1997). Generally, it may be difficult to pinpoint a specific reflectance to a particular concentration of a plant pigment as they and other constituents show overlapping absorption features (Blackburn, 2006).

The absorption effects of the chlorophyll can be observed at 675 nm and 550 nm, whereas the former is considered as the wavelength, where maximum absorption occurs and thus sensitive to reflectances even at very low concentrations.

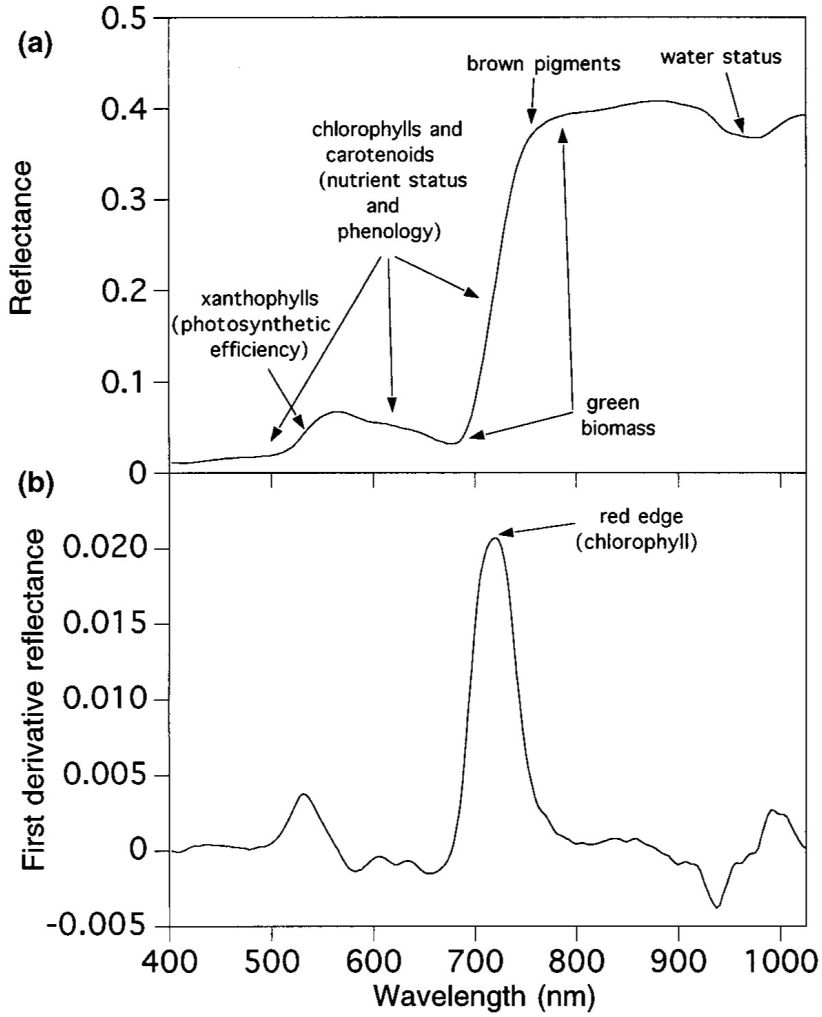

Figure 2.3: Spectral signature of a leaf and characteristic features (adopted from Peñuelas and Filella, 1998, p.152)

At 550 nm, reflectance sensitivity is higher for medium-to-high chlorophyll concentrations (Peñuelas & Filella, 1998). Reflectance values within single spectral wavebands are therefore seen as indicators for plant physiology, but also VI are seen as insightful, where several of these wavebands are included, each of them correlating to a certain biophysical or biochemical trait of a plant (Filella et al., 1995). A VI is a ratio of reflectances (Yao et al., 2018), which are commonly used in precision agriculture for monitoring vegetation physiology and more specifically disease infestation, and shall be further elaborated in the following chapter.

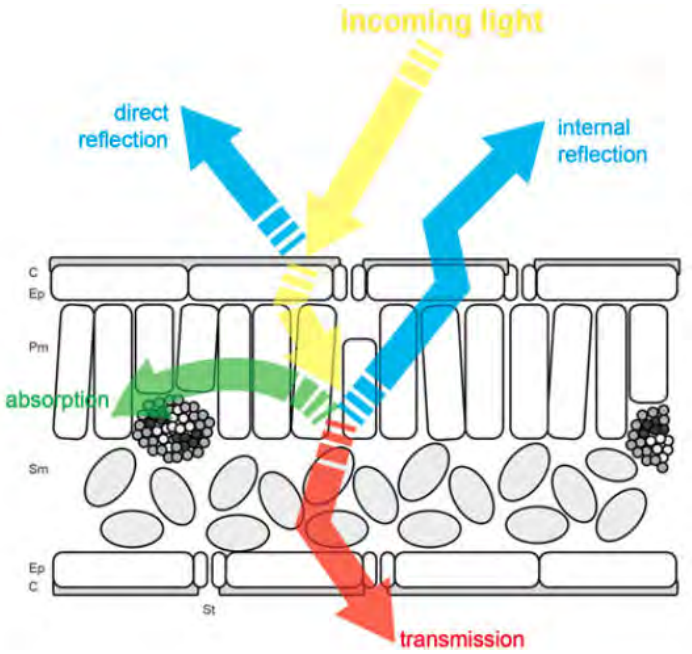

Figure 2.4: Profile of a leaf and illustration of light interaction (adopted from Mahlein, 2016, p.243)

2.2. Plant Disease Detection and Mapping based on Hyperspectral Data

In contrast to multispectral broadband images, which cover a wider electromagnetic spectrum, hyperspectral narrowbands offer a higher spectral resolution which allows spectral analysis of reflectances at single wavelengths. This is of particular interest for precision farming, as not only high spatial resolution is taken into consideration, but also high spectral resolution, which enables the identification of fine nuances within the spectral signatures. Especially the identification of plants that are affected by plant diseases profits from the use of hyperspectral data analysis, as slight changes within the spectral signature that are caused by infestation can be detected.

Typically, hyperspectral data can be obtained with handheld devices, such as spectroradiometers with a very fine resolution (1 to 10 nm bandwidths covering the electromagnetic spectrum between 400 – 2500 nm). Per se, this is not considered as spatial data, but can be understood as single point measurements from which spectral vectors can be obtained that ultimately are used to compute the spectral signature of that point measurement. Spatial data can be obtained through image spectroscopy, or in other words, hyperspectral imaging. In precision agriculture, this is commonly used to cover a certain area of interest and is also deployed with other precision farming applications that make use of additional thermal or LiDAR sensors (Thenkabail et al., 2018).

As mentioned already in the preceding section, hyperspectral data distinguishes itself from multispectral data in respect to the bandwidth at which spectral signals are recorded. As a consequence of this very fine separation of the electromagnetic spectrum, a hyperspectral data set is also considered as high dimensional. Dimensionality here refers to the number of spectral bands used. For instance, in case of a single point measurement using a

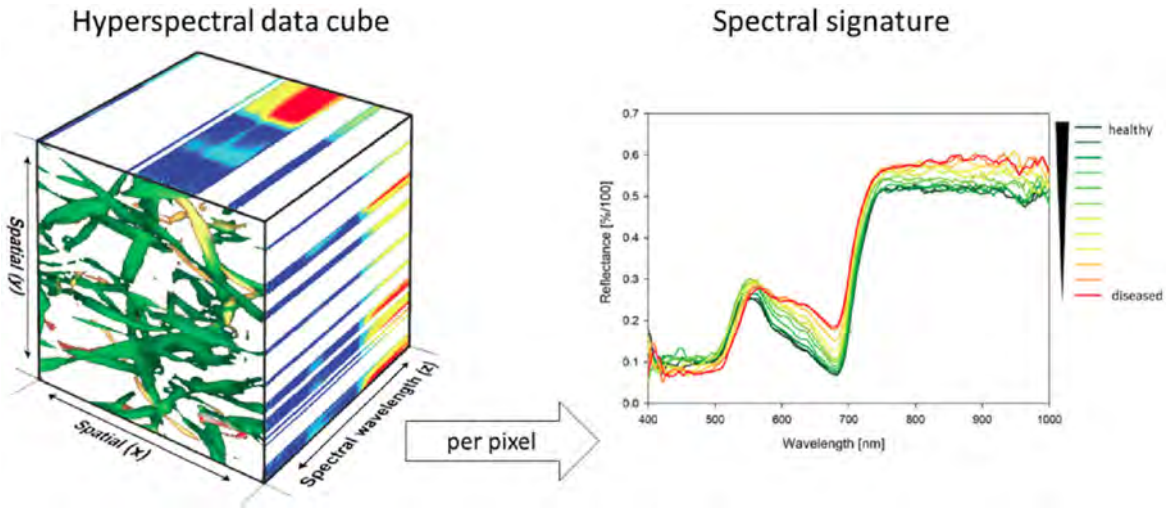

Figure 2.5: Illustration of a hyperspectral data cube (adopted from Bock et al., 2020, p.13)

hand-held device, one obtains a vector with reflectance values for each spectral narrowband. Regarding the hyperspectral imagery, however, one can envision the whole data set as a three-dimensional data set, a data cube (Fig. 2.5). The third dimension consists of two-dimensional images (e.g. 20 – 30 or even more) stacked to a data cube, where a single image represents a narrowband at which reflectance values are recorded. A pixel, therefore, can be understood as a data vector, which comprises of several reflectance values across the feature space. The latter refers to the detection range or window of recorded wavebands within the electromagnetic spectrum (Yao et al., 2018). What does this now mean for precision agriculture?

Hyperspectral imagery can potentially provide more information for precision agriculture due to the high data volume (Yao et al., 2018). Some applications even allow UAV-derived hyperspectral imaging in the fields to be processed even in real-time, through advances in cloud computing, machine learning and artificial intelligence that all have contributed to a paradigm shift in remote sensing: data availability and processing at any place anytime, considering that one can also collect, operate and process (UAV-based) data (Thenkabail et al., 2018). Despite both multispectral and hyperspectral systems being used for plant and weed sensing in the field within the VIS-NIR spectral range, hyperspectral sensors allow in comparison to broadband multispectral cameras the detection of subtle changes in plant spectral narrowbands (Yao et al., 2018). In combination with UAV flights, the operation of hyperspectral cameras for precision agriculture has the additional advantage of increasing the spatial resolution of the imagery, which typically ranges between 5 mm – 5 cm per pixel, allowing in-field variability detection with a high amount of detail. Despite being limited in water stress detection of plants when compared to thermal imaging systems, hyperspectral sensors may identify plant disease and pest infestation at high spatial and spectral resolution. This, in turn, means that the data quantity from hyperspectral sensors is generally larger than that of multispectral broadband images (Yao et al., 2018). Nevertheless, hyperspectral imaging is considered a fast and economical acquisition of detailed field data (Yao et al., 2018), which makes this technology very versatile and suitable for different applications (Mulla, 2013). In precision agriculture, for instance, hyperspectral systems are deployed for a range of pur-

poses like the assessment of plant nitrogen content (as plant nitrogen is crucial for crop productivity); estimation of the effects of heavy metals on vegetation reflectance; mapping abundance and distribution of flowering plants; quantifying litter and invasive species; weed sensing; phenology and seasonal vegetation pattern identification; soil management zoning and crop herbicide damage detection through pesticide spray drift, to name a few (Yao et al., 2018).

More important for this thesis is the detection of plant diseases through remote sensing applications, particularly as their reliable detection and identification remain a challenge in agriculture (Savary et al., 2012; Oerke, 2006, amongst others). Remote sensing of plant diseases bare the huge potential to be utilized at an early plant pathological stage (Oerke et al., 2014), where symptoms are not clearly visible to crop agronomists or farmers but only display visible symptoms at middle or late stages of infection (Lowe et al., 2017). Thus, using remote sensing techniques for plant disease detection can definitely be argued for being at least a complementary practice to the existing methods of in-field visual assessment or laboratory, but meanwhile also in-field, diagnostic testing by experts (Lowe et al., 2017). Manual disease identification and monitoring is considered as rather time-consuming and demanding, hugely depending on the size of the arable land and the crop type (Lowe et al., 2017). Hence, identifying plant diseases at an early stage would allow early action in controlling and preventing the spread of infection (Lowe et al., 2017). Apart from (a) an early detection of the onset of an attack, plant disease identification should also be considering the following aspects, according to Mahlein (2016): (b) *separability of different diseases*, (c) *differentiation of biotic and abiotic stress*, and (d) *disease severity quantification*. Bock (2011) defines disease severity as '*the area (relative or absolute) of the sampling unit (leaf, fruit, etc.) showing symptoms of disease and is often expressed as a percentage or proportion*' (p.2).

To be able to take a stance on these aspects, it is essential to understand the complexity of hyperspectral data from which to obtain insight into the effects of plant diseases. Primarily, it can be said that hyperspectral data is complex in nature. This is due to the aforementioned, large data volume, which was also referred to as a dimensionality issue. Hence, the increased number of dimensions in a hyperspectral data set is adding complexity to the data analysis, may it be multivariate analysis of hyperspectral vector data or image processing (Thenkabail et al., 2018). However, there is a considerable amount of redundancy within a hyperspectral data set, as spectral autocorrelation is evident within sensed reflectance values from adjacent narrow wavebands. Therefore, it is necessary to eliminate redundancies for the follow-on spectral analysis by adopting dimensionality reduction techniques, where the main spectral variability within the data set is preserved. Dimensionality or feature (a feature being a dimension or an image band) reduction techniques focus on the identification of wavebands with maximum information (Blackburn, 2006) to reduce image-processing complexity and increase image-interpretation accuracy (Yao et al., 2018). By and large, Richards and Jia (2006) distinguish between two types of feature reduction methods: feature selection and feature extraction. The former aims at evaluating the image bands in a hyperspectral data-set to select the most effective or discriminating features by removing the least effective. Feature extraction, on the other hand, involves a transformation of pixel vectors into a new set of coordinates. This allows a subsequent feature selection to be more evident as the transformation amplifies feature discrimination within the data set. Common techniques for feature-extraction in remote sensing are PCA, wavelet trans-

forms, spectral angle mapping, or arithmetic transformations such as VIs (Yao et al., 2018). Common VIs, such as the well established Normalised Difference Vegetation Index (NDVI), The Photosynthetic Reflectance Index (PRI) and the Red Edge Vegetation, are not diseases specific (Mahlein et al., 2013). However, the broad range of VIs offers a first glance of the vegetative physiology, highlighting particular properties of vegetation (apart from chlorophyll and carotenoids, also water content, cellulose, lignin, dry matter, etc.). 'Spectral pigment indices' are ratios of narrowbands that are more sensitive to pigments and those spectral areas that are not sensitive or related to another control reflectance (Blackburn, 2006). In general, three bands have been found to be sufficient for the composition of VIs on the leaf level, whereas at the canopy VIs comprising of three and four bands have been developed (Blackburn, 2006).

Disease-centred studies focused on creating disease-specific VIs (Lowe et al., 2017), which to a large extend make use of hyperspectral data. Hyperspectral VIs are viewed as a central method (Izenman, 2008) and their computation is considered fairly simple in order to extract information (Yao et al., 2018). However, the specificity of a vegetation index for delineating a specific disease according to their spectral characteristics or, in other words, the classification accuracy is decisive. According to Bendel et al. (2020), classification accuracy is defined as the '*ratio calculated from the number of samples correctly classified among all possible samples*' (p.7). A common approach is the assessment of spectral bands for disease specificity following the interest in detecting infected, but symptomless plants, at an early disease stage. Up to this point, there was no differentiation between the type of disease, which Yao et al. (2018) identified as a pest, fungal or bacterial. This needs to be considered for the hyperspectral analysis as well because disease types impact the plant material differently (attacking the plant organism in various ways, causing diverse plant reactions and disease symptoms), consequently affecting the spectral reflectance properties of the plant individually. Scientific research has focussed on developing crop and disease-specific indices for quick and reliable assessment of hyperspectral data. Therefore a combination of dimensionality reduction techniques for feature extraction with a follow-on machine learning classification approach is contemporarily considered as state of the art procedure in identifying and detecting plant diseases. However, machine learning models underlie different mathematical algorithms, which is why it is difficult to determine beforehand which approach performs best for hyperspectral data analysis. It is a common approach to compare different algorithms regarding their classification accuracy for a specific disease (Bendel et al., 2020). Often used classification algorithms include, linear or stepwise discriminant analysis, partial least squares, spectral mixture analysis, artificial neural networks or Support Vector Machine (SVM), amongst others (Yao et al., 2018).

Rumpf et al. (2010), for instance, usedSVM classification to differentiate healthy from three different fungal diseased sugar beet leaves. Also Al-Saddik et al. (2018) adopted the SVM classification, a discriminant analysis as well as VIs to compare to a novel approach in feature selection termed Successive Projection Algorithm to assess classification accuracy and propose a multi-class classification regarding disease severity of *Flavescence dorée*. It is a disease where phytoplasma colonises plant cells of grapevine, which is transmitted through leaf sucking insects that pass on the disease with their infected saliva while feeding on the sap. In the European Union *Flavescence dorée* is declared a reason for quarantine due to its infectiousness. In their study, they were using hyperspectral data collected with a portable, in-field spectroradiometer (350 – 2500 nm) to propose an alternative, and particularly,

reliable and early identification in comparison to the naked eye disease assessment. Visual inspection still being the most common technique use for grapevine monitoring (Al-Saddik et al., 2018). Albetis et al. (2017) also performed remote sensing studies on *Flavescence dorée*, but following a proximal sensing approach with an UAV collecting multispectral imagery of the orchard under field conditions. The authors were comparing spectral bands, VIs and biophysical parameters in combination with machine learning classification, amongst them the SVM classifier to assess classification accuracies. One of their recommendations for future studies, is the investigation of hyperspectral data on the leaf level for improving knowledge about spectral responses of the phytoplasmal disease (Albetis et al., 2017). Mahlein et al. (2013) computed disease-specific VIs based on hyperspectral data that were superior to pigment-related VIs in delineating infected plants from uninfected plants.

Bock et al. (2020) conducted a study also concerned with plant disease detection and arguing for the use of hyperspectral data, but set the focus on plant disease severity classification and visual representation. It is one of the few studies encountered in the literature review of this thesis, that addressed the concept of visualisation in the context of plant diseases detection and identification. The authors also promote the adoption and at the same time argue for the need for further research on automated image processing techniques for classifying and recognising disease severity, using different supervised and unsupervised machine learning approaches (Bock et al., 2020). Moreover, the authors address further classification concerns regarding the severity rating of plant diseases such as the classification scheme (nominal or ordinal, quantitative or qualitative), the number of classes and class intervals, as well as how accurate disease severity can be represented independent of scaling. Additionally, the authors addressed questions regarding usability, when intending to develop mobile applications for plant disease severity classifications, bearing in mind visual user-oriented communication.

Cartography typically addresses questions regarding usability, classification and an adequate number of classes, colour scheme, generalisation and abstraction of spatial data and how to communicate these visually. Hence, the following chapter will shine some light on precision mapping in agriculture from a cartographic perspective and to which extend cartographic principles have been adopted in precision mapping for plant disease detection.

2.3. Precision Mapping and Cartography

By and large, cartography has not yet lived up to its potential in agriculture. Surveying, GIS and remote sensing, on the other hand, have already found an entry and are integrated in common agricultural practices since the 1980s (Thenkabail et al., 2018). Cartography, *the art, science and technology of reading and producing maps* (Kraak, 2019), bears a great chance for improving visual communication of spatial information in agriculture. Mapping is fundamental for spatial decision making and sets the basis for crop monitoring, including plant disease management. Due to the limited use, perhaps even awareness of the strengths in implementing cartographic techniques, not much scientific literature has been produced on what could be termed *agricultural cartography*, or perhaps even *precision cartography* in the face of precision agriculture. In respect to the detection and visualisation of plant diseases, there is a rather overseeable amount of scientific publications and reporting of successful implementations dedicated to cartography in plant disease mapping. Particularly, precision maps, which are widely used in agriculture but have hardly received attention from a cartographic perspective. Hence, their nature and the cartographic requirements from its making to the final use of precision maps are core to this chapter. In order to develop a cartographic understanding of how precision maps are perceived and what expectations exist towards precision mapping, it is important to firstly capture the notion of precision maps from their making to their use in the past, as well as at present. These different notions of precision mapping need to be perceived with respect to their mapping context. Especially that precision mapping is used as a buzzword in different domains and it is closely associated with UAV-based applications, it is crucial to look at the current precision map users and map makers. Only then a contemporary understanding of precision mapping within precision agriculture for plant disease identification and mapping can be synthesized.

In the introductory session to this literature review, it was mentioned that precision mapping is currently used in the construction business, as well as in the automotive sector, for example. The latter has also adopted the term *HD maps*, or *high definition* maps (Liu & Liu, 2018). Autonomous driving, in particular, sets the present vision of the future expectations towards cars and, therefore, the need to develop sensors attached to the car in order to perceive the vehicle's environment and in real-time. High definition mapping is therefore understood in the automotive industry as data collection of the vehicle's environment at high spatial resolution, the real-time processing of the data to be made available either for the vehicle's computer for spatial decision making or as a visual representation of the street and the car's surrounding (Liu and Liu, 2018; Geospatial Media, 2019). Generally, the spectrum of applications the use of high-resolution imagery for their mapping purposes is wide and ranges from Structure from Motion (SfM) of UAV imagery of a construction site for assessment of ongoing construction work to the identification of potential sources of infection of schistosomiasis in Cameroon (Tchuenté et al., 2018). What they do have in common though, is the need for high-resolution imagery. Here, it is important to stress that high-resolution imagery should not be misleadingly set equal to a precision map. Moreover, the high-resolution imagery rather sets the basis for the final map. In terms of resolution, spatial resolution is considered foremost for precision applications.

However, spatial resolution is also relative to the are of interest or the scale of mapping. Tchuenté et al. (2018) for instance, describe precision mapping in their attempt to delineate

areas with potential infection risk of schistosomiasis as '*conducting sampling at a much finer geographical resolution*' (p.1). In their study, high spatial information was defined on the level of health districts and subdistricts of Cameroon to delineate high-risk zones of infection. In another study also dedicated to schistosomiasis, but in Senegal, Wood et al. (2019) used UAV-derived imagery to perform habitat mapping of the disease transmitting snails and delineate high-risk of infection zones along the shores of a lake. Here, precision mapping is understood as mapping an area less than one hectare, a very large scale map on the basis of high resolution imagery. Kim et al. (2021) conducted precision mapping related to child undernourishment across India, where the smallest unit is at the level of the village. From the authors' point of view, the smallest plausible spatial to be used for this study with the given data, was the village units from which clusters could be generated. At the same time, Kim et al. (2021) distance themselves from other studies conducted on the African continent where a spatial resolution was conceived differently for their precision mapping. In a review on high resolution, but thematically different maps produced in three publications (Walker et al., 2016; Osgood-Zimmerman et al., 2018; Graetz et al., 2018) on the African Continent, Reich and Haran (2018) refer to the produced maps as 'precision maps', where the smallest spatial unit is a 5x5 km 'pixel'. Perhaps a more virulent topic in times of a global pandemic in 2021, locales vulnerable to the Coronavirus disease 2019 (COVID-19) have been visually displayed on district levels of South Korea in what the authors refer to as a methodological approach to be used for precision mapping of pandemics (Weinstein et al., 2021). Precision in the sense of spatial resolution is conceived differently when looking at the above mentioned examples and studies, where spatial units of reference vary from intra-state mapping (Kim et al., 2021), to 5x5 km pixel as the smallest spatial reference (Walker et al., 2016; Osgood-Zimmerman et al., 2018; Graetz et al., 2018) or even decimetre mapping of snail habitats that pose infection risk zones of schistosomiasis disease (Wood et al., 2019). All aforementioned studies, however, claimed to produce high-resolution maps or precision maps. What then is precision in a map? Is high precision the same as high resolution? And is it possible to define precision mapping with this variety of use cases and understandings?

According to Raposo (2017), precision can be defined in cartography as '*[t]he repeatability of similar measures or representations; the granularity or frequency at which distinctions can be made by a sensor or display medium*'. Closely related to this definition of precision is also the cartographic understanding of resolution (Raposo, 2017), which the same author defines as follows: '*The degree of detail to which a phenomenon is detected or represented. Data are stored and rendered at some degree of representation resolution*'. In terms of resolution, Raposo (2017) differentiates between raster sensor arrays and vector geospatial data. The latter, resolution is defined by both '*by the spatial precision to which vertices are defined and how densely vertices are posted, though both measures can vary greatly throughout a single dataset*'. Resolution from raster sensor arrays '*is defined by the dimensions of the individual sensors in terms of ground units (i.e. the width of one pixel in meters on the Earth)*'. Both precision and resolution are both variables in an interplay with scale, particularly in cartography, where map scales refer to the abstraction of space defined by its areal extent. Raposo (2017) again defines scale as a '*measure of relative size, of objects or representations*'. Herein, Raposo (2017) distinguishes between phenomenon ('*relative spatiotemporal sizes at which objects and processes occur in the natural world*'), analysis ('*relative spatiotemporal sizes over which something is studied or simulated*') and cartographic scale ('*ratio between the size of an object and its representative symbol on a map*'). In cartography

particularly, the balance between scale and detail is or rather should ideally be considered in the map making process, as '*cartographic scale is correlated to resolution*' (Raposo, 2017), which means that at a smaller map scale less detail is shown in the map, than at a large scale.

Generally, a map is understood as being '*a visual representation of environment*' (Kraak and Fabrikant, 2017, p.14), whereas the physically available space on a map is limited, which is why real world objects, that need to be represented on a map have to be scaled accordingly to be visible (Weibel, 1997). At this point it is necessary to acknowledge, that there is a range of definitions and a whole discourse on what a map is supposed to be (Kraak & Fabrikant, 2017), especially that the demand for maps, the basis as well as the media for map making, map use itself, and ultimately the understanding of maps has changed over time. However, this thesis is not aiming at entering this discourse in depth, but adopting this less-specific definition above, which allows maps in general wider applicability (Kraak & Fabrikant, 2017), which can already be seen from the broad range of '*precision mapping*' examples pointed out in the beginning of this chapter.

By and large, any kind of map though, has to implement cartographic scale reduction, which is also referred to as *generalisation*, map generalisation or cartographic generalisation. Generalisation ontologies and the implementation of automatic digital generalisation are complete research areas for themselves embedded in the cartographic domain. This research, however, is merely tapping into some aspects of this domain and its scientific literature. By highlighting and linking core aspects of cartographic generalisation that are fundamental to map making the need for generalisation shall be argued for, particularly in precision mapping. According to Weibel (1997), generalisation '*encompasses a reduction of the complexity in a map, emphasizing the essential*' (p.101). Without doubt, what is being referred to as '*the essential*', is subject to the map maker and the map's purpose. Raposo (2017) defines the process of generalisation as '*abstracting and transforming geospatial data in order to reduce their detail and generate versions that instead retain only their main, common, or principal components or forms*'. Broadly speaking, generalisation techniques have been addressed in the scientific cartographic literature with a strong research focus on vector feature generalisation, GIS supported automation of feature generalisation, and more recently also web-based, real-time generalisation, also for mobile mapping applications.

The range of adopted techniques (Table 2.3) and the respective terminology has grown particularly with the advent of GIS favouring digital generalisation in map making. Hence, since the past century generalisation ontologies and respective terms have changed over time, which is nicely compiled in various studies, of which Roth et al. (2011) shall be highlighted. Roth et al. (2011) surveyed generalisation typologies and respective terms used cartography, giving a good overview of the different understandings of generalisation techniques. Despite the authors' conclusion from the survey that there is a very heterogeneous perception and even disagreement among the prominent cartographers regarding the terminology on generalisation techniques, they stress the intrinsic interrelation between generalisation and scaling. Frank and Timpf (1994) already identified the benefits of applying generalisation iteratively (not restricted to a single generalisation technique, but also in combination), creating multiple representations of the same data set, where the rendered representation of real-world phenomena would de adequately displayed balancing the level of detail and viewing scale. Furthermore, they identified '*zoom*' as the dominant operation in moving in-between mapping scales and viewing the visual representations at varying levels of detail.

Cartographic Generalisation Techniques	
Simplification	*The reduction in sinuosity or complexity of a linear or polygonal shape, usually involving a reduction in vertices along its constituent polylines*
Aggregation	*The combination of polygon symbols into a smaller number, usually by filling space between the initial polygons to create a lesser number of contiguous polygons*
Smoothing	*The replacement sharp angles in a polyline or polygon with curves so that the overall shape is softened*
Selection/Elimination	*The retention of certain features and rejection of others*
Typification	*The transformation of detailed polygonal features into canonical, usually simpler versions of the type of object being represented (e.g. complex buildings to simple rectangles)*
Displacement	*Moving features away from their planimetrically-accurate locations for legibility or to emphasize a spatial relationship (e.g., moving a building closer to or further away from a road)*
Exaggeration	*Adding visual emphasis, usually with increased symbol size, to an object*
Classification	*Reducing the variety of measures in a dataset by binning similar measures together*
Trend Calculation	*A relatively severe generalization of a surface into a mathematically simple function approximating it, commonly defined by a lower-order polynomial*
Opening and Closing (Expand and Shrink)	*The increasing or decreasing dilation, respectively, of the set of areas of a given class in a classified dataset. Often employed on classified raster regions, opening and closing tends to produce simplified region boundary geometries. The two operations are not commutative*
Resampling	*Changing the unit of aggregated data by recollecting source data in differently-sized units (e.g. changing the resolution of a raster dataset)*

Table 2.3: An overview of cartographic generalisation techniques (adopted from Raposo, 2017)

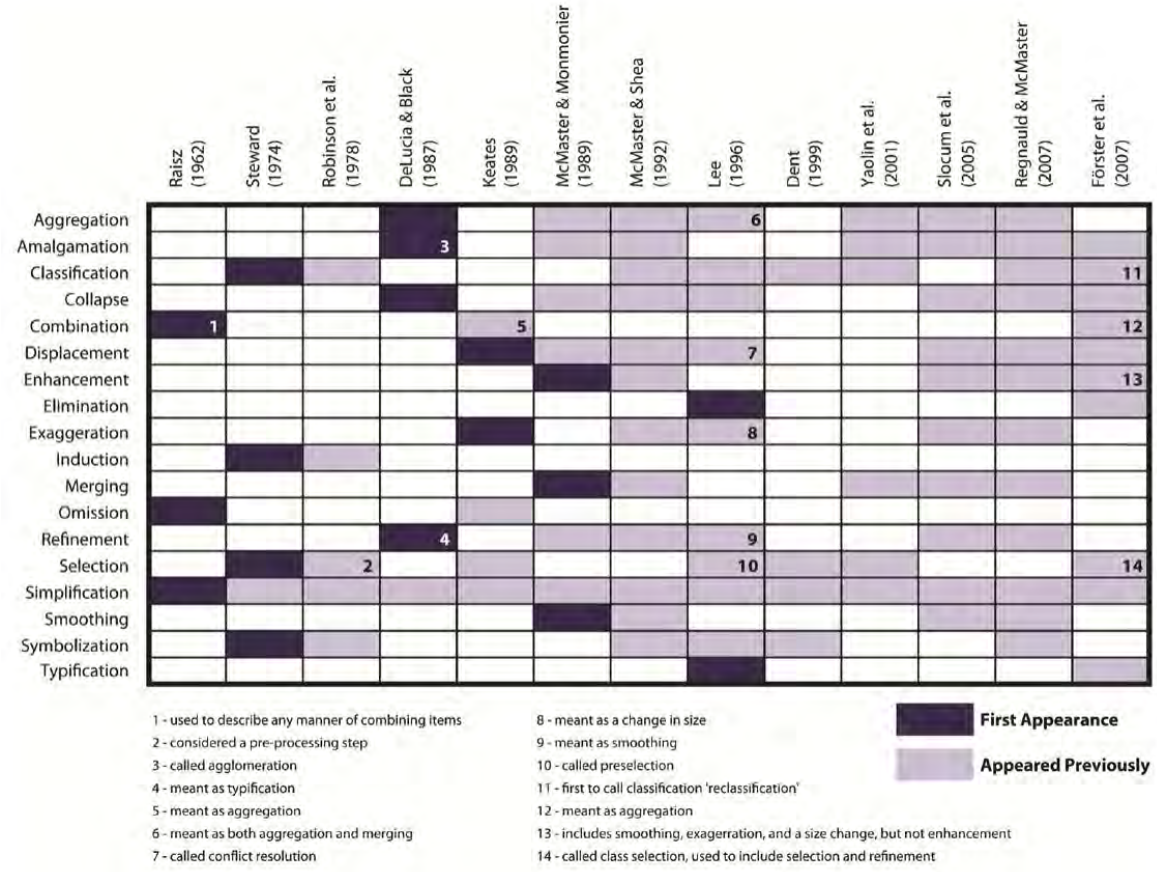

Figure 2.6: A comparison of cartographic generalisation techniques (adopted from Roth et al., 2011, p.35)

Following this line of thought – the combination of interaction, which Robinson et al. (2017) describes as an '*essential mechanism by which users can navigate, search, filter and compare*' and precision, that is spatial granularity – may help to overcome the dichotomy in current precision mapping. Particularly in precision agriculture, where precision maps have found common usage to reveal intra-field variability regarding crop yield, soil properties, but also plant infections, the process of spatial abstraction is limited to classification techniques from image processing either focussing on key wavelengths or the entire spectrum (Lowe et al., 2017). Classification of the imagery is necessary for information extraction and not only restricted to image processing, but also understood as a generalisation technique adopted in cartography (Fig. 2.7). Nevertheless, a classified high-resolution image does not equal a map yet, particularly, when the amount of detail restrains maintaining the visual overview or observing patterns within a map (Fig. 2.8).

From a cartographic perspective, Wahabzada et al. (2015) have conducted a very fruitful implementation of cartographic abstraction to plant disease detection focussing on the temporal dynamics of disease development. By using metro maps, where tram lines indicate the development of selected diseases, which uses a combination of visual variables such as colour, orientation and spacing to communicate the disease development, where stops along the tram line indicating changes to the plant caused by the disease or the visual per-

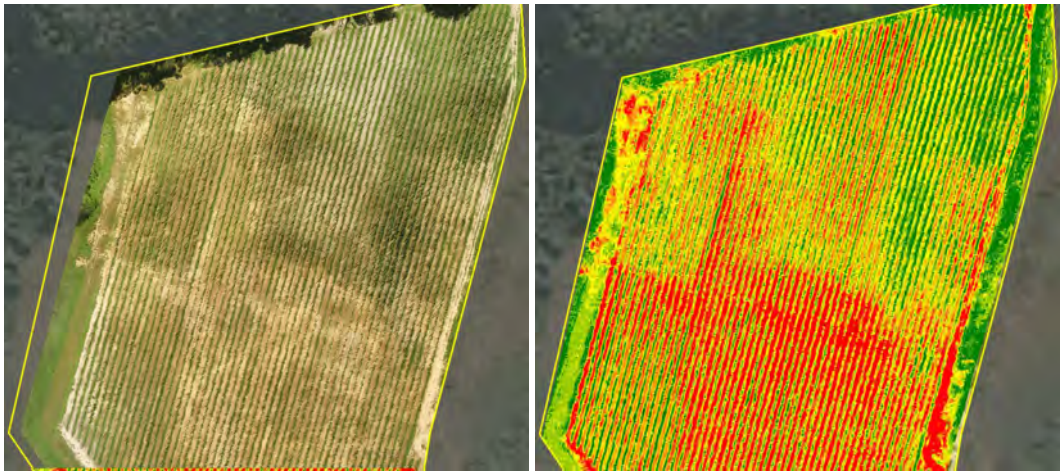

Figure 2.7: An example of an aerial, high-resolution orthophoto taken with an UAV and the derived NDVI classification (adopted from Pix4D)

ception of symptoms. In another study on plant phenotyping, Wahabzada et al. (2016) again use hyperspectral data like already in the aforementioned study, whereas the focus is not on schematic generalisation where the geographic reference is simply lost, but on the combination of hyperspectral information with labelling. Disease dynamics undergo a process of 'wordification', where words are used to express disease development and their respective symptoms are used as labels.

In terms of precision farming, Řezník et al. (2020) have identified already the need for applying cartographic techniques to precision maps. They, however, argue from a different point of view for integrating cartography into agriculture, as they focus on veracity in precision maps. Veracity, which is one of the '*4 Vs*' of Geospatial Big Data (Volume, Velocity, Variety, Veracity) (Robinson et al., 2017), is considered as most persistent issue in agro-environmental science together with variety, according to Lokers et al. (2016). Subsequently, this is taken as a justification by Řezník et al. (2020) to address bias within the collected field data and implement visual variables for highlighting uncertainty within the precision map. This can be considered definitely a step towards cartographic precision mapping, but the argumentation laid out by Řezník et al. (2020) does not include spatial scaling and thus adapting the spatial resolution of the 'raw' data depicted in the precision maps. This might be considered at least as equally important if not to be prioritised, as an overview of the general spatial pattern needs to be presented to the map user, thereafter more detail can be offered, following Shneiderman's (1996) visualisation mantra '*overview first, zoom and filter, then details on demand*'.

In cartography, great attention has been given to the development of an integrated design for representing the same geographic topic at varying resolutions and respective map scales, which is also known as multi-scale or multiscale mapping (for example Spaccapietra et al., 2000). Multiscale mapping is not the same as generalisation (Roth et al., 2011). The latter can be described as a design decision made on a single scale (Brewer & Buttenfield, 2009), whereas multiscale mapping is the compound of map design decisions across all supported scales (Roth et al., 2011). Hence, mapping at multiple scales involves generalisation across supported map scales aiming at maintaining map legibility. This in turn, implies that map

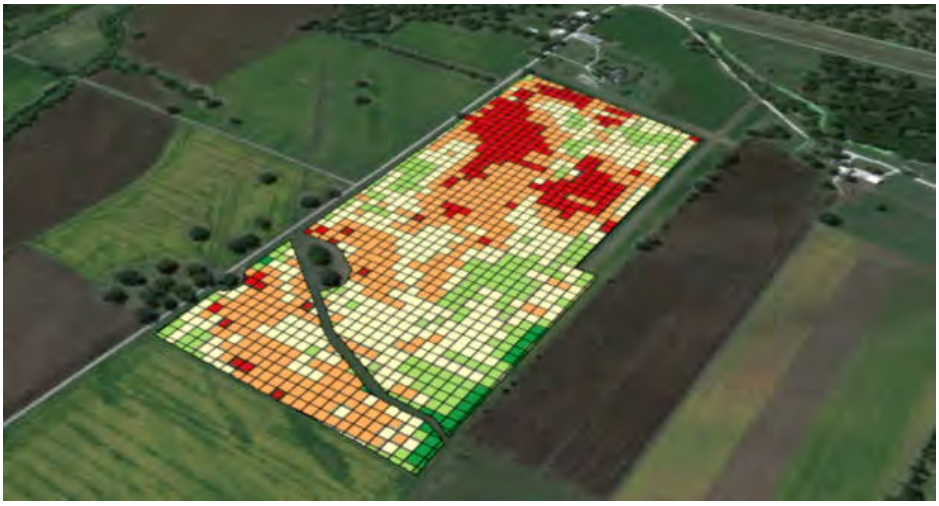

Figure 2.8: A precision map example using a regular grid for spatial aggregation (adopted from farmmanagement.pro)

precision or granularity needs to be adapted according to mapping scale. It is therefore essential to select, extracted and generalise features within the process of precision map making.

Roth et al. (2011) have identified at least three cartographic research and development efforts, where multiscale mapping is of relevance: (1) Multiple Representation Databases; (2) National Mapping Agencies; and (3) Web Mapping Services. Web-based mapping applications utilize remote web servers to deliver maps to the users. They are considered as service oriented cartography (Trakas, 2012). Deploying web mapping services also for precision farming seems very advantageous, as a use case from New Zealand demonstrates. Here, a complete GIS architecture (from the ESRI software suit) was installed to support spatial decision making regarding fertilising demands to increase field crop yields. This architecture relies on geospatial sensing systems that collect and transmit field data, satellite or aerial imagery for including orthophotos within the geospatial analysis. Eventually, fertilizer application data is transformed into a series of colour coded 'snail-trails' overlaid on the map (ESRI, 2006).

There are several other commercial web mapping services, web-based portals or mobile applications for precision mapping, that specialised on UAV-imagery for example Pix4Dfields[1], DroneDeploy for Agriculture[2] or PrecisionAnalytics Agriculture[3] amidst the vast ecosystem of precision agricultural software and services. In contrast, there are also open-source and free software solutions, the most prominent in the field being OpenDroneMap[4].

A Spatial Data Infrastructure (SDI) is not quite comparable to the above applications as it extends the concept of a user application by several more components that offer information on data quality in form of metadata as well as web mapping services that can be accessed within some of the above user applications. A major advantage of SDIs is that they facilit-

[1] https://www.pix4d.com/product/pix4dfields
[2] https://www.dronedeploy.com/solutions/agriculture/
[3] https://www.precisionhawk.com/precisionanalytics-agriculture
[4] https://www.opendronemap.org/

ate the exchange and sharing of geospatial data as well as services among stakeholders (Hjelmager et al., 2008). Open SDI have emerged (Vancauwenberghe & Valečkaitė, 2018), in the spirit of the freedom of access to information and its provision as a service to the public. An open SDI is rooted in the principles of open data and knowledge, thus making spatial data available to anyone without any restrictions to rights of access or use (Coetzee et al., 2020). Nevertheless, a SDI might also reserve certain access rights to administrators or developers who are in the process of sharing data, where further development is needed prior to publication. Furthermore, Hjelmager et al. (2008) identified that by organising spatial data across disciplines and organisations, SDIs meet the need to create multi-participant, decision-supported environments in order to address the issues of sustainable development and improving quality of life.

This is also true for spatial decision-making in terms of plant disease spread. A SDI enables visualising varying spatial dimensions of plant diseases and pests that compromise on crop yield and can be seen as a medium to address sustainable agriculture. Herein, plant diseases can be visualised across multiple scales, ranging from small-scale, cross-border maps to national or regional scales and eventually on a very large scale, such as at the level of a single orchard. The SDI-supported precision map would allow the identification and detection of plant diseases at a very high level of detail, which needs to be considered as a multiscale map. Subsequently, this thesis argues for cartographic generalisation of high-resolution imagery particularly used as a mapping basis in precision agriculture, without compromising on the precision of the original data set, as the whole precision map can be understood as a multi-scaled, layered map, where map interactivity like zooming allows presentation of further detail.

This proposal of a cartographic framework for precision mapping shall be applied in an experimental set-up on the plant disease AP serving as a case study in South Tyrol. Before continuing with the methodological scope of this thesis, it is necessary to be familiar with the disease in order to make the best use of the findings from the spectral analysis, which in the end sets the foundation for the mapping of AP.

2.4. Overview of Apple Proliferation Research

Figure 2.9: Shrinking of fruit size due to AP infection (adopted from Janik et al., 2020, p.17)

Phytoplasmas are considered important insect-transmitted pathogenic agents responsible for a breadth of plant diseases worldwide that entail large economic impact (Christensen et al., 2005; Weintraub and Beanland, 2006). They are bacteria without cell walls and their minimal genome makes them *'the simplest known natural self-replicating life-form, on the border between living cellular organisms and viruses'* (Christensen et al., 2005, p.527). Commonly transmitted by phloem-sucking insects, phytoplasma cause a wide variety of symptoms, flower alterations, stunting and a general decline in infected plants (Christensen et al., 2005). Amongst the most economically severe phytoplasmal diseases is AP (also referred to as *'apple witches' brooms'*). The cell wall-less bacterium *Candidatus Phytoplasma mali (Ca. P. mali)* causes AP and reduces fruit size, weight and quality in affected apple trees (Janik et al., 2020) (Fig. 2.9). AP has been recorded in several European Regions such as Austria, Belgium, Bosnia and Herzegovina, Bulgaria, Croatia, Czech Republic, Finland, France, Germany, Hungary, Italy, Norway, Poland, Romania, Serbia, Slovenia, Spain, Switzerland, the Netherlands and Turkey (Tedeschi et al., 2013). Hence, *Ca. P. mali* is listed as a quarantine organism in many countries and must be absent in planting material (Janik et al., 2020).

Particularly in both Italian provinces Trentino and South Tirol, where one can find large areas of apple cultivation, recurrent outbreaks of AP have been recorded. In the Province of Trentino, Rui (1950) reported first on AP in the 1950s but it was only to Bovey (1963) to investigate its epidemiological character linking the disease to specific vector insects, that spurred a progressive spread in the area (Amici et al., 1972). It is important to note that despite the intensive apple cultivation in the region of Trento and South Tyrol, AP has been detected not only in commercial orchards but is also present in low-intensity orchards, where infected trees are actually considered more of as a hub of infection (Seemüller et al., 1998).

Unfortunately, there is currently no curative treatment for this disease. Hence, a range of preventive measures exists to limit the disease spread with the foremost strategy being

(a) Witches Broom

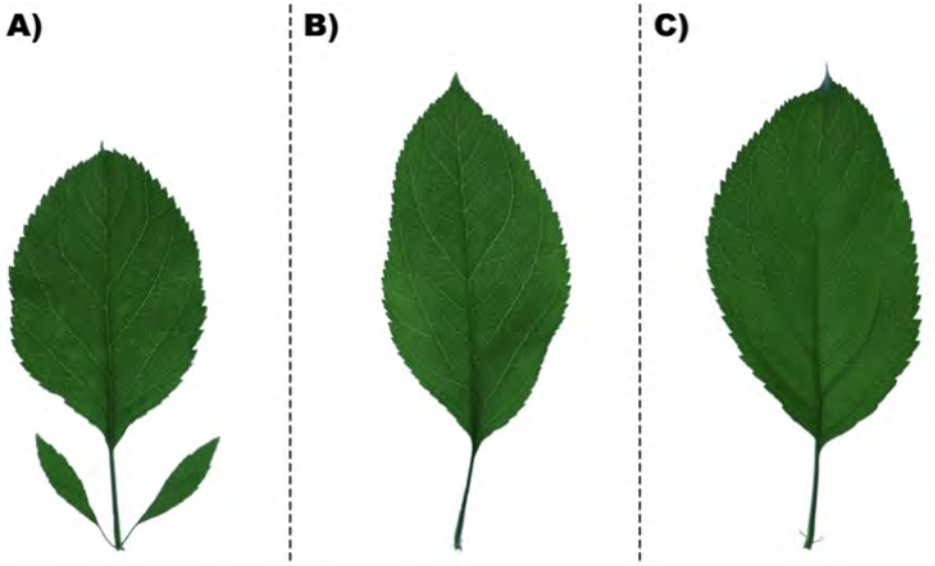

(b) Enlarged and dentate stipules

Figure 2.10: AP specific symptoms (adopted from Janik et al., 2020, p.15; Barthel et al., 2021, p.3)

insecticide treatment as means of vector control, followed by uprooting of infested trees as well as the use of certified uninfected planting material (Janik et al., 2020).

These management measures have proven effective in limiting disease outbreaks and spread in Northern Italy in the last decade (Janik et al., 2020), which can also be attributed to stronger political stewardship. Following the adoption of a Ministry decree in 2006 (Ministero delle Politiche Agricole e Florestali, 2006), control measures against AP were obligatory and a sanitation programme was implemented. These prescribed regular inspections for the presence of typical symptoms and subsequent removal of infested plants. More precisely, in the event of more than 25% infection in an orchard, the whole cultivation had to be uprooted. Additionally, growers received grants to subsidise uprooting of orchards older than 20 years or with more than 20% of infested trees, which ultimately promoted the adoption of recommended control measures. As a consequence, infection rates decreased due to mandatory uprooting of infected trees and prescription of chemical control measures

Figure 2.11: Leaf reddening as a typical asymptomatic symptom of AP (adopted from Janik et al., 2020, p.17)

against the insect vectors.

Currently, surveys are still being carried out and treatments against insect vectors prescribed in both regions (Janik et al., 2020; Tedeschi et al., 2013). Reliable recognition of infected trees, and hence, the ability to identify specific AP symptoms is decisive in infected plant removal and therefore an indispensable skill of any fruit grower in affected regions (Janik et al., 2020). Infection induces a broad range of symptoms in wild and commercial Malus species (Bovey, 1963; Blattny et al., 1963; Kartte and Seemüller, 1988) but symptom expression can vary enormously (Schmid, 1975). Here, it is essential to distinguish between AP specific and non-specific symptoms, where specificity means, as already touched upon, the unambiguous relation of symptoms to a particular disease, in this case an AP infection. The following have been identified as AP specific symptoms: the formation of witches' brooms, hence AP's alternative denotation, which is an *'abnormal bush like cluster of dwarfed weak shoots'* as well as an *'enlarged and dentate stipules'* (Janik et al., 2020, p.15), whereas the latter symptom is not easy to diagnose on a tree (Jarausch, 2007) (Fig. 2.10).

An early leaf reddening is the most visible and evident of the non-specific symptoms, which are those that cannot be clearly linked to an AP infection (Bovey, 1963) (Fig. 2.11). The degree of colouring can vary between cultivars and over time due to climatic conditions and is additionally characterised by a papery leaf texture (Mattedi, Forno et al., 2008). An early leaf reddening, however, can also be induced by mechanical tree damages, fungal infections or certain physiological conditions (Schmid, 1975). Furthermore, Mattedi, Forno et al. (2008) observed, in case of Gala apples, a pre-harvest chlorosis, which is the yellow colouring or bleaching of the leaf (Britannica [Britannica], n.d.-a), can be a hint for an AP infection. Schmid (1975) considers an earlier bud break in springtime as an indication for AP infected trees, which is rather difficult to recognize as a symptom, as it can only occur in a short time interval. Zawadzka (1976) has also observed stunted branches and rosette formation of apical leaves due to AP, which can emerge during summer, and new shoots from axillary buds of the old wood. Kartte and Seemüller (1988) describe late blossoming (or late flowering) as a non-specific AP symptom. Moreover, non-specific but economically important symptoms induced by AP, are the shrinkage in fruit size, their loss in taste and colour as well as the growth of a long stem (Blattny et al., 1963; Zawadzka, 1976; Schmidt et al., 2009;

Seemüller et al., 2010), making these fruits less marketable and resulting in outstanding revenue (Herzog et al., 2012). According to Jarausch (2007) most symptoms are developed in autumn, when the number of trees with specific symptoms has nearly doubled in comparison to springtime, thus arguing for the best period for visual symptom assessment being during harvest. However, symptoms can also co-occur and symptom expression is irregular (Carraro et al., 2004), which is why an iterative symptom assessment throughout the vegetation period is recommended, also considering that certain symptoms are observable only in specific time periods (Janik et al., 2020).

Further understanding and research is necessary to shed light onto differential symptom development, which is a complex interplay of differences in pathogen strains, sensitivity of apple types, phytoplasmal colonisation behaviour of the aerial parts of the tree, environmental factors and certain plant-physiological conditions (Seemüller, Schaper et al., 1984; Carraro et al., 2004; Seemüller and Schneider, 2007; Herzog et al., 2010; Baric et al., 2010). Adding to the complexity of detecting AP-specific and non-specific symptoms, symptomless trees can be infected as well. This is mainly because symptom expression can be affected by the physiological state of the tree, the phase of infection, climatic conditions and other factors (Janik et al., 2020). In most cases, AP symptoms are expressed within one-and-a-half to two years after infection, whereas prolonged latency periods of four years have also been reported (Unterthurner & Baric, 2011). What is referred to as *latency* period describes the time span from the AP infection to the development of visible symptoms in the plant (Janik et al., 2020). Visual inspections are therefore not sufficient to recognize the entirety of infected but asymptomatic plant material (Janik et al., 2020).

Similarly complex and not detectable though mere visual inspection is the phenomenon termed *recovery*, which according to (Osler et al., 2000), is the spontaneous remission of symptoms in field grown apple trees infested by *Ca. P. mali*. Osler et al. (2000) found that 71% of AP symptomatic trees of the cultivar *'Florina'* recovered within 10 years. This plant disease state may occur either transiently or permanently in infected trees (Seemüller, Schaper et al., 1984; Osler et al., 2000; Carraro et al., 2004). Despite the cessation of symptoms, recovered trees have not literally recovered from the disease but from typical symptoms, as bacteria persist in the roots, that can recolonize the canopy spontaneously and induce symptoms again (Carraro et al., 2004). However, after a period of dormancy characterised by the absence of symptoms, the tree may become symptomatic again and phytoplasma can be detected in the aerial parts of the tree (Osler et al., 2000; Carraro et al., 2004; Seemüller, Schaper et al., 1984; 2010). Consequently, visual assessment is very restricted and not reliable in identifying AP infected trees but PCR are commonly used to prove the presence of phytoplasma. Usually, root material of the respective tree is taken as the basis for analysis (Janik et al., 2020). The use of PCR methods require specific lab equipment and must be performed by trained personnel.

Apart from the reliable detection of AP through PCR analysis, there is also a clear consent regarding the *Ca. P. mali* transmission. Several forms of transmission have been recorded. One not uncommon way of transmitting *Ca. P. mali* is by natural root bridges, also referred to as grafting, or by dodder (Janik et al., 2020). Several tree species have shown interconnected root systems (Tarroux et al., 2014), which also seems to be very common with apple trees (Ciccotti et al., 2007). Root anastomosis, which is the technical term for this phenomenon, has been reported in more than 150 species and allows a tree community to improve its nutrient's absorption, increase root system longevity, strengthen tree stability

(a) *Cacopsylla melanoneura* (b) *Cacopsylla picta*

Figure 2.12: AP-transmitting insect vectors (adopted from Janik et al., 2020, p.41)

and mitigate competition between trees (Bormann, 1966; Epstein, 1978). On the other hand, epidemiological studies show that root bridges also serve inevitably as a medium in the spread of AP, particularly in medium-aged and old-aged apple orchards (Baric et al., 2007). Furthermore, remains of old roots left behind in the soil were tested positive for *Ca. P. mali* even after 5 – 6 years subsequent to uprooting (Mattedi, Ciccotti et al., 2008).

Without any doubt though, insects are the main drivers behind phytoplasmal spread, whereas transmission of phytoplasma is highly vector-specific, which means that they are transmitted by only one or a few vectors (Christensen et al., 2005). AP is mainly transmitted by two psyllids, also known as jumping plant lice (Britannica, n.d.-c), *Cacopsylla picta (C. picta)* (Förster 1848) and *Cacopsylla melanoneura (C. melanoneura)* (Förster 1848)(*C. picta*: Frisinghelli et al., 2000; Jarausch et al., 2003; Carraro et al., 2008; *C. melanoneura*: Tedeschi and Alma, 2004) (Fig. 2.12). Additionally, the leafhopper *Fieberiella florii (F. florii)* (Stål 1864) has been demonstrated to transmit *Ca. P. mali* (Krczal et al., 1988; Tedeschi and Alma, 2006). All of them are phloem-sucking insects, which tap the phloem, which can simply be described as food conducting plant tissue (Britannica, n.d.-d). When feeding on the plants' sap, the phytoplasma can then be transmitted through the saliva of an infested insect to the phloem (Christensen et al., 2005). The phytoplasma spreads systematically in the plant using the continuous sieve tube system and will eventually remain a parasitic occupant of the phloem. Phytoplasmas are pleiomorphic (*pleiomorphism* being the ability to take on several shapes and forms (Britannica, n.d.-e) and can pass freely through sieve pores due to their small size. Hence, they might be merely swept along with the *'assimilate flow from leaves to sugar consuming plant organs like systemic viruses'* (Christensen et al., 2005, p.531). Throughout the whole year *Ca. P. mali* is present in the infected apple tree (Baric et al., 2010), and more specifically in the root system (Schaper and Seemüller, 1982; Seemüller, Kunze et al., 1984; Baric et al., 2010) as constant phloem renewal allows the phytoplasma to survive there during winter (Schaper & Seemüller, 1982). In the course of the year though, phytoplasma concentrations vary in the aerial parts of the tree (Schaper and Seemüller, 1984; 1984; Seemüller, Kunze et al., 1984; Loi et al., 2002; Pedrazzoli et al., 2008; Baric et al., 2010), as recolonisation of the canopy by *Ca. P. mali* starts in late spring/early summer, peaks in late summer and lasts until December.

Phytoplasmas interact with their plant hosts on different levels, as they move through the sieve pores, interfere with physiological and biochemical processes in plants and block the phloem transport by obstructing the sieve tubes (Kartte and Seemüller, 1991; Lepka et al., 1999). Cell metabolism of *Ca. P. mali* relies, as any phytoplasma, on their plant host for their own nutrient uptake (Janik et al., 2020). Although the sugars in the phloem are a potential food source (Christensen et al., 2005), phytoplasma do not have the necessary toolset, such as enzymes to break down the sugars and make them available for glycolysis (Christensen et al., 2005); simply explained as the biochemical process of converting available glucose into cell available energy known as Adenosine triphosphate (ATP) (Britannica, n.d.-b). Not being able to make use of the available fructose or glucose but only sucrose, which, however, is not in the phloem, phytoplasma disrupt the plants metabolite between sieve elements and companion cells (Christensen et al., 2005). The collapse of sieve elements is considered as the primary effect of phytoplasma on plant's metabolism, which might be linked to available compounds provided by companion cells that might be an important food source for phytoplasma (Christensen et al., 2005).

Lepka et al. (1999) have demonstrated that AP infection induced impairment of carbohydrate transport (translocation) to sink tissue, which was correlated to the development of growth inhibition (stunting) and accumulation of carbohydrates in the source tissue. The increase of sucrose but also starch, total saccharides and amino acids was observed to go along with the decrease of glucose and fructose (Giorno et al., 2013), chlorophyll content and the amount of soluble proteins in AP infected plant tissue (Mittelberger et al., 2017; Bertamini et al., 2002). The former, the build-up of carbohydrates in source leaves, is considered to trigger feedback through inhibiting photosynthesis causing leaf degreening (chlorosis) (Negro et al., 2020; Lepka et al., 1999). Impaired photosynthesis is considered as secondary effect of phytoplasma on the plant metabolism which is related to inhibition of phloem transport (Christensen et al., 2005; Negro et al., 2020). Negro et al. (2020) showed at the example of pathogen infestation of the grape cultivar Bois noir, quantities of chlorophyll b, total chlorophylls (*a+b*) and carotenoids, were considerably less in September (at a later disease stage but not significantly different in the middle disease stage - July). This means, that biochemical concentrations are affected not only differently but also according to the disease stage or severity.

Infection with *Ca. P. mali* may trigger plant's defence reactions, which may lead to the increased production of different defence proteins (Negro et al., 2020). Particularly, phenolic and flavonoid compounds increase in infected plant tissues, which are both associated with the strengthening of the plant's resistance towards pathogens and in turn seem to alter hydrogen peroxide production in the infected plants (Negro et al., 2020). Hydrogen peroxide is considered to counteract symptom development also in AP infected plants (Mittelberger et al., 2017).

In order to design an AP tailored precision map, it is inevitable to be aware of the *Ca. P. mali* and what changes and symptoms it may cause in the apple plant. Hence, the above outline on past research on AP which goes beyond the cartographic domain is nonetheless fundamental for the analysis, classification and interpretation of the remotely sensed data.

2.5. Summary

The main research ideas evolving from the preceding literature review are based on the motivation of developing an early detection of AP which is caused by the phytoplasma *Ca. P. mali*. With the resurgence of witches' brooms in recent years, Janik et al. (2020) have highlighted the importance for a systematic and interdisciplinary approach to deepen knowledge about the disease, phytoplasma and plant host interaction and possible reasons for its spatial clustering in certain regions. It is therefore necessary to understand the interaction of the phytoplasma with the plant host, what biochemical and physiological changes are caused and that an infected tree can also be asymptomatic which poses a challenge to in-field, eye-based visual identification (Janik et al., 2020).

The use of hyperspectral data can provide insight and be used as an indicator for infected plants, as plant physiology can be monitored outside the visible electromagnetic spectrum (Lowe et al., 2017).Hence, various studies have investigated the use of hyperspectral data for remote sensing of plant diseases (Albetis et al., 2017; Al-Saddik et al., 2018; Mahlein et al., 2013; Mahlein, 2016; Rumpf et al., 2010), aiming at an early identification of the diseases plants allowing an early intervention and implementation of pest control strategies, such as the removal of infected plant at an early stage in the growing season to prevent it of becoming a source for further infection.

In order to support spatial decision making in plant disease control, precision maps can be considered as a powerful tool in communicating plant disease spread visually to the end-user. Originally precision maps have been used in precision agriculture which relies on the use of sensing systems for the collection of environmental data that in turn are used for spatial decision making for agricultural practices. Especially, that precision maps are generally based on high-resolution imagery which in themselves already represent a form of Geospatial Big Data, it is necessary to extract relevant, high-resolution geoinformation that can then be communicated visually to the end-user (Sishodia et al., 2020). Common precision maps, however, do not follow a cartographic understanding of presenting the essential spatial information, but instead offer high-detail imagery to the end user.

This thesis therefore argues for the implementation of cartographic generalisation within the precision map making, which may aid in detecting spatial patterns that can be clearly communicated to the map user. Cartographer Arthur Robinson and his colleagues (1995, p.42) formulate that *'the act of generalization gives the map its raison d 'être'*. A precision map needs to undergo a process of generalisation, as it is a cartographic product. The above quote by Robinson et al. (1995) was primarily concerned with static maps at the time, where a constant display is given, but the notion of generalisation is also applicable for digital interactive maps. Interactive maps allow an overview of the abstracted or more generalised spatial information, before offering further spatial detail, which follows Shneiderman's famous visualisation mantra 1996 for interactive visualisations – a map essentially being a form of visualisation – and is described as follows: *'overview first, zoom and filter, then details on demand'*. Consequently, combining interactivity with cartographic generalisation may aid in representing high-resolution imagery at multiple scales in what one can then coin a precision map. Multi-scale mapping which is the application of cartographic generalisation at different zoom levels may help to bridge the inner conflict of a precision map between displaying precise geoinformation based on high-resolution remote sensing and the abstraction of real-world phenomena or objects that is intrinsic to map-making. An integrated multiscale

design may aid decision making in respect to plant disease control. As a cartographic tool, precision mapping, can to be used for minimizing crop losses due to plant diseases and therefore pose the technological potential for promoting sustainable agriculture.

3 Methodology

Although there are several already existing studies dealing with the detection and mapping of plant diseases (Albetis et al., 2017; Al-Saddik et al., 2018; Mahlein et al., 2013; Mahlein, 2016; Rumpf et al., 2010), there is no existing methodology for the detection and visualisation of AP. Thus, the thesis is considered as experimental research focussing on the development of a data-driven methodology covering the entire data life cycle: starting with an in-field detection of AP infection; follow-on multivariate data processing and analysis of multi- and hyperspectral data; setting the basis for the fusion of multi-modal data obtained at varying scales; and finally the implementation of a precision map, made accessible as open data.

The methodological set-up underlying the thesis is oriented towards a data-centric workflow presented in the visualisation pipeline. The latter being a theoretically as well as practically long-prevailing methodological concept, firstly described by Haber and McNabb (1990) as a creation of visualisation through a procedure of transformations.

Each data handling step within the work flow is seen as a transformation of its original, raw character to processed, increasingly abstracted representations. The original concept has

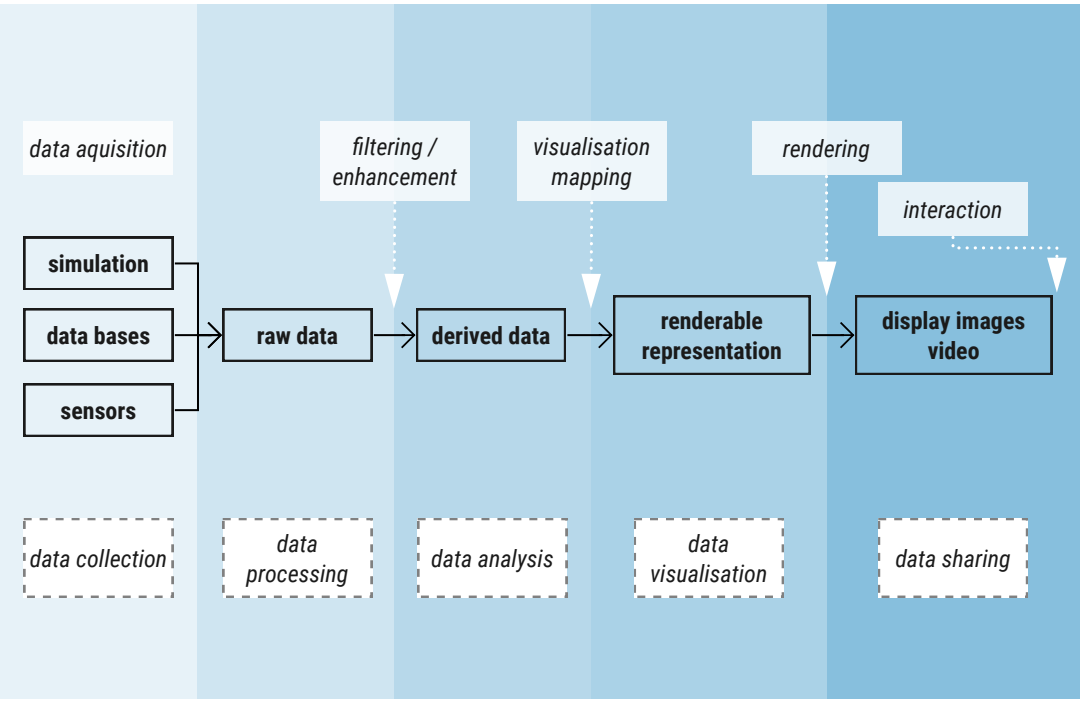

Figure 3.1: Visualisation Pipeline Scheme (based on Haber and McNabb, 1990)

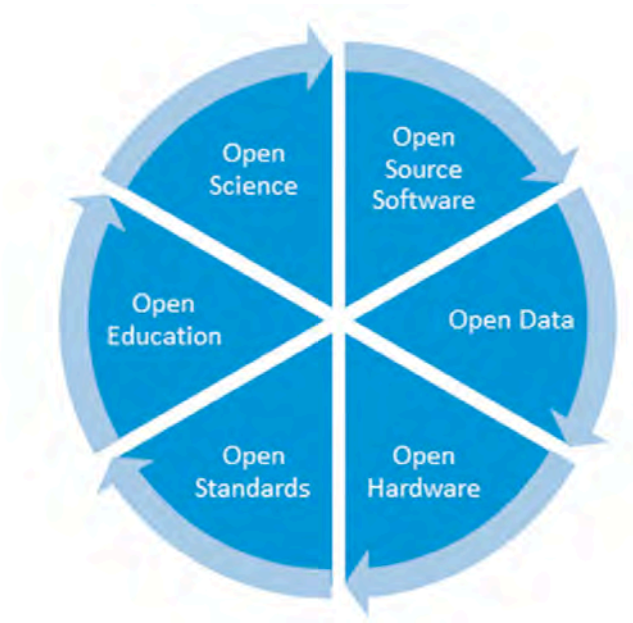

Figure 3.2: Components of Openness (adopted from Coetzee et al., 2020, p.2)

evolved since its first formulation and found its adoption in software packages that have automatised this workflow to present the final visualisation to the user or integrating interactivity in the visual exploration or visual analytics (Card et al., 1999; for example). Hence, the concept covers nearly all aspects of the data life cycle, ranging from the collection of raw data to its visualisation and data sharing. The archival of data and respective visualisations is not addressed in this methodological framework at hand as it exceeds the scope of this thesis. However, attributing the raw data with its respective metadata is crucial when contributing to open data in the geospatial domain. Providing contextual information on data quality and purpose, not only creates a transparent and reproducible work process but allows others to adopt the data for their needs (Bossomaier & Hope, 2015).

In achieving this, the methodological framework is set around the idea of open science, which is defined as '*making scientific research and its dissemination accessible to all levels of the society*' (Coetzee et al., 2020, p.2). The term openness is understood here as typically referring to '*transparency, to free and unrestricted access to information, and to inclusive consensus-based decision-making*' (Brovelli et al., 2019, p.1). Embracing this belief in open science means that openness runs through the entire data life cycle and ideally is reflected in every working step, as its concept and practice are intrinsically anchored in applying knowledge (Coetzee et al., 2020).

Thus, science, as the process of building knowledge (Coetzee et al., 2020), is considered as open science, if the produced knowledge is '*open if anyone is free to access, use, modify, and share it - subject, at most, to measures that preserve provenance and openness*' (Open Knowledge Foundation, n.d.). Another prerequisite with digital Open Scientific Geospatial Data are the foundational principles of *FAIR* data, aiming at a sustainable use of digital resources, increasing the data value in being reused by humans or even machines (Coetzee et al., 2020) and ensuring that the data are **F**indable, **A**ccessible, **I**nteroperable, and **R**eusable (Wilkinson et al., 2016). Although FAIR data does not require the data to be open (Laurie

et al., 2012), the principles of both, openness and FAIR, should be viewed as complementary in data science, particularly once public funding is involved for publishing resources, those '*need to be as open as possible and only as closed as necessary*' (European Comission, 2018, p.10).

To live up to the presented understanding of open science, the choice of technology sustains openness, and thus, open-source (geospatial) soft- and hardware form the fundamental pillars (Coetzee et al., 2020). However, for the sake of scale and scope of the thesis as well as the project's capacities, the choice for open-source (geospatial) soft- and hardware had to be weighed up against what was technically possible and timely feasible. Therefore, the use of commercially licenced soft- and hardware was indispensable, as some of the measurements instruments come with their own software suite or other commercial software are considered as state of the art in their domain and application. Nevertheless, the use of open-source software packages was preferred, especially those offered through the OSGeo software ecosystem, which projects are considered as the foundation of open-source geospatial software and services that are designed for every geospatial application (Coetzee et al., 2020), all covering the aforementioned stages in the visualisation pipeline. Thus, the work packages defined in the development of the thesis are closely coupled to each procedure outlined in the visualisation pipeline covering the *collection of raw data*, *data processing*, *data analysis*, *data visualisation*, and *map creation* as well as the *sharing of the data* in the form of a precision map. In the following sections, these steps adopted within the workflow shall be described in more detail.

3.1. Data Collection

As previously mentioned, the methodological focus is on the development of a robust in-field identification of AP infected plants on an orchard. On-site measurements, therefore, constitute the first step in the visualisation workflow – the data collection. Unlike sampling under laboratory conditions, in-field data collection is subject to the prevailing weather conditions on the day of the field campaign as well as the daily management activities when sampling on an agriculturally cultivated site, such as an orchard. Hence, careful and in-advance planning of the field campaign is a necessity as the quality of collected data can be compromised by unfavourable weather conditions, such as clouds causing shadows for example, which can create illumination differences within a scene of an aerial image taken of the Earth's surface. Non-invasive technical sensing of plant diseases, either using remote or proximal sensor systems, can provide highly detailed information on the infection status and even severity (Oerke et al., 2014).

For the purpose of this thesis, a multi-modal data collection strategy was employed, which includes the use of several sensing platforms covering different scales. Firstly, taking a ground-based proximal sensing approach on the *leaf level*, a hand-held device, such as a spectroradiometer, gives information about the spectral signatures of infected and uninfected leaves. The leaf spectral signature constitutes the reflection of light by the leave from which leaf biochemical and -physical composition, and ultimately the infection state, can be induced. Additionally, the geographic position of each sampled tree is determined with a GNSS signal receiving system. In order to validate the results from this non-invasive sensing technique, root samples of the respective trees are taken once early in the phenological stage to test for the presence of *Ca. P. mali*. After measuring the leaf spectral signatures,

the respective leaves are used as samples for follow-on laboratory analysis as well. A PCR and laboratory spectroscopic analysis provide further insight into the infection status of the leave and respective tree. Hence, the laboratory findings serve as ground truth of the apple proliferation invested or uninfected plants. Secondly, following an airborne proximal sensing procedure on the *orchard level*, multispectral and hyperspectral cameras mounted on an UAV deliver high-resolution imagery covering the orchard's extend. Prior software-based flight planning allows control and optimisation of flight parameters (such as duration, speed, elevation, amongst others), and it specifies the approximate number of images taken to ensure minimum over- and sidelap for seamless follow-on image stitching.

3.2. Data Processing

Leaf Level

Prior to the spectral data analysis of the leaf signatures, pre-processing is required of the raw data that was collected with the field-spectroradiometer. Spectral data processing typically starts with the correction for atmospheric effects as well as the calibration of target scans with respective references before the actual data wrangling. Regarding the atmospheric correction of leaf spectral signatures, the atmospheric effect on the spectral signatures can be considered as very minimal and even negligible. The adopted ground sensing approach with the spectroradiometer implies close contact between the lens and the single leaf, literally not leaving a lot of space for air to influence the recorded reflectance values. Seemingly atmospheric correction does not seem relevant for the ground sensing approach with a spectroradiometer. In case of this study, calibration of the spectroradiometer is done automatically already prior to recording leaf spectral signatures and therefore only requires taking reference scans before each batch of leaf scans for a single tree. More detail on this will be presented in the following chapter though. Theoretically, a base line correction can be applied, if collected spectral signatures show a vertical shift along the y-axis (reflectance). This shift can be explained through the black background of the spectralon which was recorded during the target scan and thus impacts the trend of the spectral signature. Hence, it is advisable to cover the entire foreoptic lens prior to sampling unless the area of the black background is known and can then be accounted for in the baseline correction. Thereafter, leaf spectral signatures are resampled to an evenly spaced spectral response of 1 nm high spectral resolution, which involves interpolation of the spectral data. Once the original data has been resampled, the spectral signatures are filtered, removing outlier measurements that could have an impact on follow-on data analysis. Depending on the software and working packages deployed, the follow-on data analysis requires a further transformation of the data format to be used for statistical analysis and plotting.

Orchard Level

Pre-processing of the UAV imagery deviates from that of spectral signatures collected with the spectroradiometer as it is slightly more complex and involves several working steps. However, calibration is equally important and is also required for the cameras mounted on the UAV either prior to or after the data collection, depending on the camera. Once the images are orthorectified as orthomosaiced, the images are radiometrically corrected. The former relies on the SfM principle, which requires the identification of tie points within the overlapping scenes of neighbouring images. Tie points are used to align the images to each other, which includes supplementary orientation parameters (interior orientation, ex-

terior orientation and aerial triangulation) for photogrammetrical bundle block adjustment (Szabó et al., 2017). Due to the low flying altitude of the UAV, possible atmospheric absorption features are considered to be negligible again; hence atmospheric correction is also not applied to the proximally sensed imagery. Certainly, the atmosphere has a specific impact (e.g. water droplets) on the spectral reflectance of the earth's surface recorded at the sensors, but the influence is considered to be fairly low under sunny and cloud-free weather conditions.

Nevertheless, the recorded images need to be georeferenced to align spatially. Hence, the coordinates from the Ground Control Points (GCPs) are used as reference points for translating the images in the respective coordinate system. Once the imagery is georeferenced, a DEM can be computed using the multispectral images as a basis. The digital elevation model typically consists of a Digital Surface Model (DSM) and a Digital Terrain Model (DTM), and their difference is equal to the Canopy Height Model (CHM). The latter represents the heights of the detected tree canopies, which serve as input for the tree canopy delineation. Ideally, individual tree canopies can be delineated and segmented from the CHM using inverse watershed algorithms, where the highest points or local maxima in the tree crown model are used as seeding points for the watershed algorithm (Barnes et al., 2017, for instance). However, this ideal procedure for an object (i.e. tree) oriented classification on the basis of the CHM had to be compromised which shall be elaborated in the following chapter in more detail. Thus, as an alternative to the single tree classification and introducing further cartographic abstraction, a regular grid structure allows binning of the hyperspectral information in the data analysis.

3.3. Data Analysis

Leaf Level

The processed leaf spectral signatures can be regarded as a multivariate data set because one leaf spectral signature is composed of reflectance values respective for each recorded wavelength within the detection window of the spectroradiometer. Consequently, one leaf spectral signature consists of hundreds or even thousands of wavelengths (to be thought of as a variables) and the corresponding reflectance values. This shear number of variables for a single measurement makes this data set high-dimensional. Dimensionality, which is understood here as the number of variables – a variable representing one dimension of the data – is an essential characteristic in the hyperspectral data structure.

Hence, within the scope of this thesis, the data analysis aims at the extraction of spectral information from the collected data in order to differentiate AP infected from uninfected leaves on the orchard based on their spectral reflectance behaviour – their spectral signatures. In order to pinpoint spectral changes between these two classes or physiological states of the leaves, it would be ideal to narrow down the whole data set to a smaller number of spectral bands where the greatest changes can be observed and compose VI that serve as the first indication for general plant stress. The wavelength or waveband selection of hyperspectral data requires data dimensionality-reduction techniques. These aim at reducing the number of wavelengths (i.e. dimensions) of high-dimensional data to a set of a few wavelengths by either variable selection, when specific variables, in our case, wavebands are selected, or feature extraction, which is the creation of composite variables by (linear or non-linear) projection methods (Izenman, 2008). Both approaches imply information loss,

funnelling the entire data to essential and relevant information for further analysis and interpretation. However, spectral wavelengths are highly inter-correlated, which means that a potential change in plant's health status will most likely not affect a single band only, but impose alterations across the spectral signature, which means a lot of redundancy in the spectral signal (Wegmann et al., 2016). Nonetheless, the recorded reflection will probably show greater changes in some bands than in others (Izenman, 2008), which can be considered basically as noise for the spectral analysis. Thus, dimensionality reduction aims at identifying bands that inhibit essential information. Consequently, the change in amplitude of the spectral signatures is considered as relevant information for the spectral differentiation between infected and uninfected leaves within the methodological framework of this study. In other words, wavelengths, which show the highest difference or variance between the reflectance values of infected and uninfected leaves, are of interest for the variable selection or feature extraction.

As one of the most prominent projection methods for feature extraction not only for hyperspectral data, is the PCA (Wegmann et al., 2016), which was introduced as a dimensionality reduction technique by (Hotelling, 1933). The PCA computes new dimensions by orthogonally projecting a set of correlated variables, ranking the projections in decreasing sequence based on their variance (Izenman, 2008). Based on the predefined settings of the PCA, ten to 20 dimensions are usually computed, where one dimension is a linear composition of the eigenvectors of the variables respective to their share in total variance within the data set. Hence, the first PC is the newly computed dimension with the greatest variance amongst the variables, whereas each variable within this newly computed dimension contributes differently by their loadings to the orientation of that dimension (Kucheryavskiy, 2020). Therefore, the 20^{th} PC will show least variance amongst the set of PCs as it inhibits least variance amongst the variables. Variance is therefore used here as a statistical variable property to deduce relevant information from a reduced data set. Anyhow, it is not the variance per se that is of interest but the separability of the two classification groups (infected vs. uninfected) and therefore identifying which variables or which dimensions are best suitable for separating these two groups in feature space.

Orchard Level

The findings from the dimensionality reduction of the hyperspectral data on the leaves level can then be incorporated into the follow-on image analysis of the multi-and hyperspectral imagery, in respect to composing vegetation indices and applying classification algorithms to delineate the infected from the uninfected trees. Scaling is the keyword when transferring the results obtained from the leaf spectral analysis and applying them to another level of analysis. Zarco-Tejada et al. (2001) have already described various approaches in scaling their findings from the spectral analysis on the leaf level to the canopy level, whereas their particular focus in their study back then was on the relationship between leaf pigments and reflectance values. For this study, variables' loadings contributing to the respective PC are considered as an important criteria from the leaf level to be included in the orchard level. High loadings (or, in other words, greater contribution to the newly formed PC) are considered as an indicator for more significant variance within recorded reflectance values. Hence, a larger variance may imply better separability between infected and uninfected leaves, which is why these wavebands are selected for the composition of vegetation indices.

However, the vegetation indices are yet to be considered as disease unspecific. Thus, a re-

producible, disease-specific classification of the hyperspectral imagery would be ideal for delineating AP infected from uninfected trees. As already mentioned in the literature review, machine learning algorithms are widely used in image classification and also in plant disease identification and detection from imagery. Ideally, when applying machine learning classification techniques, it is advisable to test and experiment with several algorithms, as each classification algorithm performs differently well on various plant diseases. Therefore, there is no machine learning approach that '*does it all*' or what Wegmann et al. (2016) describe as 'no-free-lunch theorem'.

For a supervised classification, training and validation data sets are required for the algorithm to separate two or more classes and evaluate the classification performance. The idea is to use the trees that are also sampled with the in-field spectroradiometer as training data or input for the machine learning classification in order to (a) scale the findings from the leaf level of the exact same tree to the canopy level, and (b) the infection status is known prior (ground truth provided by a priori laboratory analysis at LRC. Ground validated GPS measurements shall help to identify the exact trees in the aerial imagery. Additionally, the vegetation indices may be used as a further indication for delineating the training data as plant stress can be identified within the canopy.

3.4. Data Visualisation and Map Design

Leaf Level

The resampled leaf spectral signatures are plotted in line graphs to visually compare the curvatures of the uninfected and the AP infected leaves. Firstly, all leaf measurements of a single tree (10–12 samples) are plotted in one diagram in order to understand the intra-tree variability. Thereafter, the leaf spectral signatures are averaged to a mean leaf spectral signature. These are also visually plotted as line graphs for visual comparison with other infected and uninfected trees. The averaged leaf spectral signatures cannot be strictly speaking treated equally as respective tree canopy spectral signatures but as mere leaf averages of the respective tree. Averaging the spectral mean leaf signature allows capturing a certain pattern across the electromagnetic spectrum for each tree's respective leaves. Finally, these tree respective leaf means are aggregated once more by averaging in respect to infection status to obtain an AP infected and uninfected mean leaf spectral signature.

Furthermore, PCs are also visualised in several ways. A so-called scree plot displays each PC's relative share in total variance found within the dataset in descending order, consequently beginning with the first PC where the greatest variance is found in the dataset, which decreases sharply to the last computed PC. More importantly though is the plotting of PCs against each other. This allows making use of the maximum variances along with the PCs in order to increase visual separability between the infected and uninfected trees.

Regarding the visual display and differentiation between the two infection statuses in the plots, colour hue is the only colour variable to represent qualitative data suitably (White, 2017), or in other words the two categories (binary classification) *infected* and *uninfected*. The choice of colour hue, though, is not trivial, as colour invokes certain associations, but at the same time, is an essential visual variable that can effectively convey information visually. Additionally, it is advisable to bear in mind a colour-blind safe choice of hues to avoid confusion of the two plant infection categories.

Orchard Level

The development of an interactive web map allows implementing a multi-scale designed precision map. For this purpose, the map user interface shall consist of several thematic layers displayed in (a) a spatially aggregated format and (b) its original spatial resolution acquired by the camera sensors. The thematic map layer represents different aspects of the spatial information on the orchard, including an orthophoto, multi- and hyperspectral vegetation indices and the AP map layer, which is the classified imagery regarding AP infection using a machine learning classification. These map layers shall be displayed at a high zoom level or large map scale in full detail. Whereas, when accessing the map, the user shall firstly be presented with aggregated spatial information of the respective thematic layers to have a general overview of the orchard.

Ideally, the tree canopy shapes can be extracted as polygonal outlines from the CHM in order to implement a spatial aggregation and object-based classification. Alternatively, the classified spatial information can be aggregated cell-wise using a grid structure which is then colour coded according to predefined classes. This procedure is comparable to a tessellation approach, where regular polygons (equilateral triangles, squares, and hexagons) can be used to tessellate (or aggregate) cells without overlapping (Carr et al., 1992). Unlike tessellation, though, which covers the entire map pane, the regular grid structure is applied only to the tree rows, where a single grid cell is used as a graphical primitive to abstract the tree canopy shape. Although tessellation foresees the mapping of frequency or occurrence of real-world phenomena (represented as vector points), graphical primitives can also be used to apply zonal statistics, such as the average or the majority, to the classified raster images to obtain an aggregated value within the respective bounds.

Again colour is used as a visual variable (including hue and value [lightness]) to represent data classes. Here one needs to distinguish between the visual representation of vegetation indices, on the one hand, which adopt a sequential colour scheme and therefore colour value (lightness) needs to be successively adapted between classes and the binary image classification for AP infection, on the other hand, where a qualitative colour scheme is more suitable, and consequently the colour hue is crucial.

Commonly, map user interfaces offer additional components or map elements, such as navigation buttons on the side for panning and zooming within the web map; a display of scale or scale bar; an overview of (active) layers; and a legend. When selecting interactively map features, a window will pop-up at the side offering further details on the feature regarding information stored in the attribute table or exact pixel values on demand.

3.5. Data Sharing

The web-based precision map is not a single application but is part of an orchestra of soft- and hardware that form a SDI. The architecture of a SDI can be generally stratified into an user interface (which includes the map user interface), an application layer, which serves the data for the web application, a data layer that hosts or stores the data and a metadata catalogue which provides essentially information about the data that is being used within the mapping application. A SDI therefore needs to be understood as a complex system comprised of several components (soft- and hardware alike) with the aim to facilitate and coordinate spatial data exchange amongst stakeholders (Hjelmager et al., 2008). Web map-

ping services can be offered through a SDI which supports the idea of openness as well as open and FAIR data access.

Particularly for academia and scientists, SDIs can promote open scientific data, where research findings are shared to be reused, provide incentives for verification or promote new findings (Coetzee et al., 2020). Furthermore, as this research is understood as an experimental study on precision mapping of AP, a SDI enables the storing of the relatively large data volume of the high-resolution imagery and, at the same time offering accessibility to the findings. Additionally, the use of open geospatial software (for instance, the OSGeo ecosystem) and implementation of open standards (i.e. publicly developed and available specifications for hardware, software, or data) (Open Geospatial Consortium [OGC], n.d.; International Organisation for Standards et al. [ISO et al.], 2018) underlines the idea of openness. Therefore the development of an AP specific precision map in the scope of this thesis can be considered as open science.

As mentioned briefly already, the use of metadata is essential when guaranteeing a standard conform dissemination of the precision map as a mapping service. Metadata provide essential information about a dataset, regarding its content (what it is about), means of collection (When, where and how the data was acquired?), authorship (Who produced the data?), and its structure (Bossomaier & Hope, 2015).

4 Case Study: Apple Proliferation in South Tyrol

Study Site

The orchard, that was taken as a case study for this thesis and is specifically used for scientific studies on AP at the LRC, is situated in the Upper Adige Valley between Meran and Bolzano, in the Italian province of South Tyrol. To be precise, the orchard is located at 11°1939' E, 46°642' N and around 745 m of elevation close by the Fragsburg Castle on the west-facing slope of the Tschögglberg (western mountain fringe of the Sarntal Alps) in the Etschtal. It is an exceptional site for the study of AP as infected trees may be kept in place on the orchard for further scientific investigation and thus do not face uprooting by Italian law which is followed as soon as an apple tree is identified as infected (Ministero delle Politiche Agricole e Florestali, 2006). The orchard itself is split into two parts. Relevant for this study is the northern part which, unlike the southern half, is not treated with pesticides to prevent the spread of AP and, therefore, consists of infected and uninfected trees. The apple variety grown on the orchard is called Golden Delicious.

Climate

The prevailing moderate, continental climate in South Tyrol ensures a yearly average temperature of 12,4°C in Bolzano (266 m) (Tappeiner et al., 2020). Generally, the seasons are defined by cool to cold winters and warm to hot summers, typically with little rainfall, especially in the broad main valleys of South Tyrol. The average annual precipitation is between 500 mm in Schlanders in the Vinschgau, northwest of Meran, and 1100 mm in the area between Passeier and Brenner. In July and August, maximum precipitation is reached. Profiting from the inner-Alpine location and the resulting mass warming effect, South Tyrol registers a high number of hours of sunshine, creating favourable apple and wine-growing conditions. Even in higher altitudes just over 1000 m above sea level, it is possible to cultivate these. Additionally, temperature differences of up to 20°C between day and night

Figure 4.1: View from the Orchard over the Frabsburg Castle, Meran and the Etschtal

Figure 4.2: Drip and Overhead Irrigation Systems (adopted from Zebisch et al., 2018, p.70)

provide good ripening conditions for grapes and apples (Tappeiner et al., 2020).

Background - Agricultural Context

Fruit growing and viticulture have an essential share in South Tyrolean agriculture and achieve together 60% of the agricultural value added (Institut für Wirtschaftsforschung, 2016). Particularly the district of Überetsch-Unterland, in the valley floor between Bolzano and Merano, in the Vinschgau and the middle Eisack Valley, specialised fruit and wine farms cultivate about 11% of the agricultural land (Tappeiner et al., 2020). The favourable growing conditions as well as increased mechanisation and industrialisation of the fruit and wine growing sector have pushed harvest volumes to rise sharply since 1990 by an average of around 1.8% per year, resulting in an increase of over 58% over 27 years (Tappeiner et al., 2020). The economic importance of fruit growing industry and viticulture for the region can be easily understood from this historical development. With the agricultural intensification, the fruit and wine cultivation also expanded in terms of elevation, reaching altitudes up to around 1000 m in the Etsch- and Eisack Valleys (Tappeiner et al., 2020). Spraying of plant protection products, like pesticides, fungicides, or herbicides, are common practice in extensive apple orchards, such as the use of black hail nets (to protect the fruits during growing and ripening stages from hail as well as acting as filters to diminish the risks of sunburn) (Zebisch et al., 2018).

Also, in terms of water use, irrigation in the fruit growing sector is considered as one of the most intensive in South Tyrol, compared to wine or grassland farming (Tappeiner et al., 2020). Especially deep south-facing cultivation areas, like the entire Vinschgau region in general, have always depended on additional irrigation (Tappeiner et al., 2020). Overhead irrigation or foliage sprinkling systems are widely deployed in fruit growing, as they can also be used for frost protection. However, steering towards a more sustainable agriculture, conscious and regulated water use for irrigation is inevitable and has lead to a continuously increasing share of drip irrigation over the past ten years (Tappeiner et al., 2020). Instead of sprinkling water over a large area consuming large quantities, drip irrigation systems are considered to be more efficient in irrigating the apple trees, especially with water shortages in summer months (Tappeiner et al., 2020). This drip irrigation is one example of precision agriculture.

Technological innovations that implement farming measures on a small scale or locally according to demand contribute to more sustainable agriculture. Following the vision of ag-

riculture 4.0, which summarises the latest technological developments in the agricultural sector, precision and digital farming form an integral part. This idea spans from the aforementioned improvements in irrigation to advances in fertilisation, crop protection, livestock management and optimising bureaucratic processes through the use of sensors, automated monitoring systems and UAVs (Tappeiner et al., 2020).

This thesis aims at contributing to this vision of sustainable agriculture through developing a methodology for precision mapping of plant disease detection at the example of AP by adopting a proximal and ground sensing approach (Fig. 4.3).

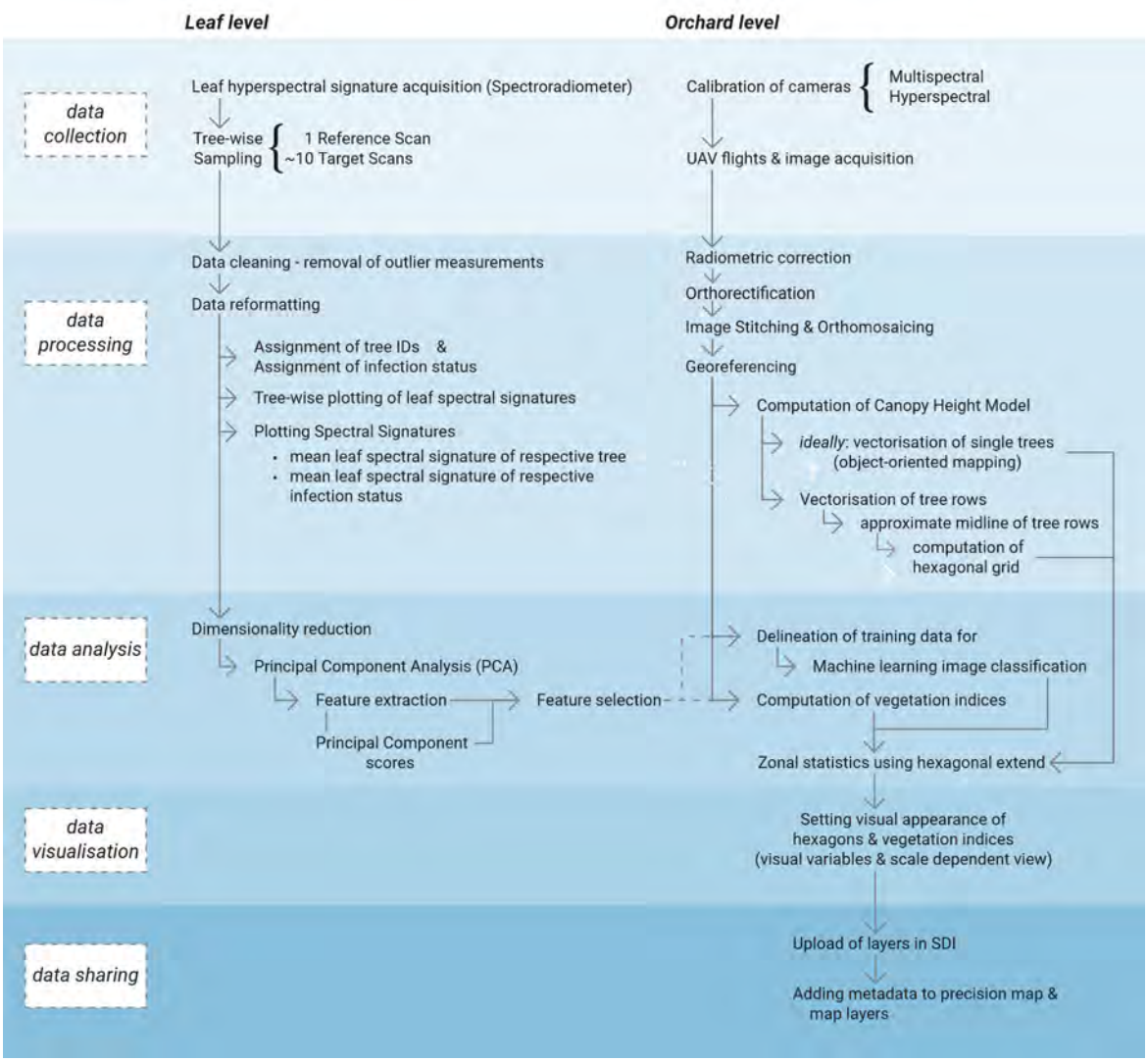

Figure 4.3: Schema of the adopted workflow

4.1. Data Collection

Within the scope of this thesis, the data collection was structured in four field campaigns covering several phenological growth stages from April (inflorescence emergence - *stage 5*) through to apple fruit development in August (*stage 7*), according to the BBCH-Scale (Meier, 2001) (Table 4.1).

Field campaign	Date	Penological stage description (BBCH-Scale)
1	06.04.2021	inflorescence emergence (phenological stage **56**), green buds, still closed single petals begin to separate from each other
2	18.05.2021	fruit fall after flowering (**71**)
3	23.06.2021	between T-stage and fruit about half final size (**74/75**)
4	21.07.2021	fruit about 70% final size (**77**)

Table 4.1: Overview of field campaigns and the corresponding phenological stage according to the BBCH-Scale

The first field campaign was conducted in an experimental and explorative manner in order to test the sampling procedure and analyse first spectroradiometric measurements obtained and potentially improve the overall sampling procedure for subsequent fieldwork.

Leaf level

Similar to Al-Saddik et al. (2018), a field-portable spectroradiometer (SVC HR-1024i, SVC, Poughkeepsie, New York, USA) was deployed for spectral reflectance measurements of leaf surfaces (Fig. 4.4). SVC's HR-1024i offers a detection window of wavelengths ranging from 350 nm to 2500 nm (SVC, 2012), covering parts of the Ultraviolet (UV) (UV-A: 315–400 nm), VIS (400-700nm), NIR (700–1100 nm) and parts of the SWIR (1100–1350 nm, 1400–1800 nm, 2000–2500 nm) electromagnetic wavelength spectra (Schowengerdt, 2006). Furthermore, it is equipped with three diffraction grating spectrometers with one silicon (with 512 discrete detectors) and two InGaAs diode arrays (each having 256 discrete detectors) that provide the capability to read 1024 spectral bands (SVC, 2012). The spectral resolution of the spectroradiometer is defined as fwhm which also varies across the detection window (SVC, 2012):

$\leq$ 3.5 nm fwhm between 350–1000 nm

$\leq$ 9.5 nm fwhm between 1000–1850 nm

$\leq$ 6.5 nm fwhm between 1850–2500 nm

Leaf spectral signatures were obtained using SVC's LC-RP PRO, a pistol-like hand-held extension, which is connected via a foreoptic sleeve and a fibre optic light guide to the spectroradiometer that is carried in a backpack for conducting fieldwork (Fig. 4.5). The leaf clip accessory is supplied with power through the spectroradiometer's LI-Ion batteries, when fully charged allowing over three hours of operation according to SVC (2012), and the collected data is transferred back from the LC-RP PRO through a signal cable. A measurement is taken, also referred to as a target scan, after having performed a scan of the white reference spectralon plate, a reflectance disk that is used for the reference scan. The disk is attached at

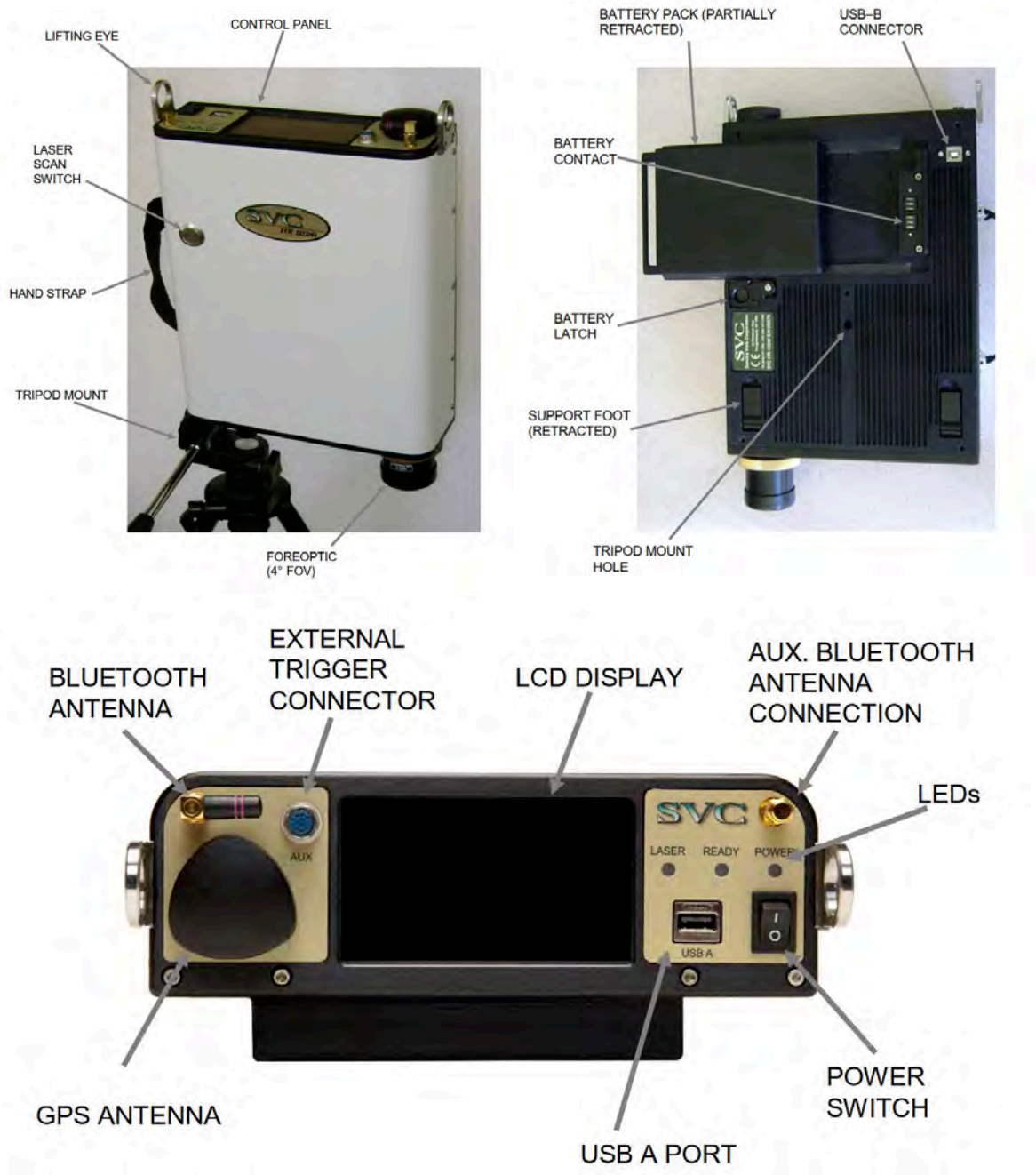

Figure 4.4: Set-up of the SVC-HR-1024i spectroradiometer (adopted from SVC, 2012, p.7ff.)

the back of the sample plate holder of the leaf clip. A measurement is conducted by placing a leaf between the sample plate holder's dark plate as a background and the probe window, covering the entire leaf clip's field of view (FOV) (Fig. 4.6). While taking the target scan, the probe should be held steady in order to avoid abrupt changes in the sampled leaf area that, in turn, can affect the recording of the spectral reflectance (SVC, 2012). A scan time

Figure 4.5: Leaf spectra Sampling using the hand-held spectroradiometer on the orchard

of five seconds was chosen during which the leaf is exposed to the leaf clip's artificial light source. It is worth mentioning that prior to sampling, the 'low' light setting needs to be selected when sampling vegetative material. The 'high' light setting is selected when sampling harder or rougher surfaces, such as rocks or soil, and would, therefore, burn the sampled vegetation. A single percent reflectance measurement is provided by the acquisition software, taking the scan of the white disk reference surface radiance (in $\mathrm{W\,cm^{-2}\,nm^{-1}\,sr^{-1}}$ – watt per square-centimetre per nanometre per steradian) and calculating the ratio of the target scan to that reference (SVC, 2012). Following the recommendation by SVC (2012), a new reference measurement was taken at the beginning of a new set of scans – a set of scan being around ten leaves of a single tree – and also when the instrument was turned off and back on again during sampling. Deviating from the originally defined sampling strategy of

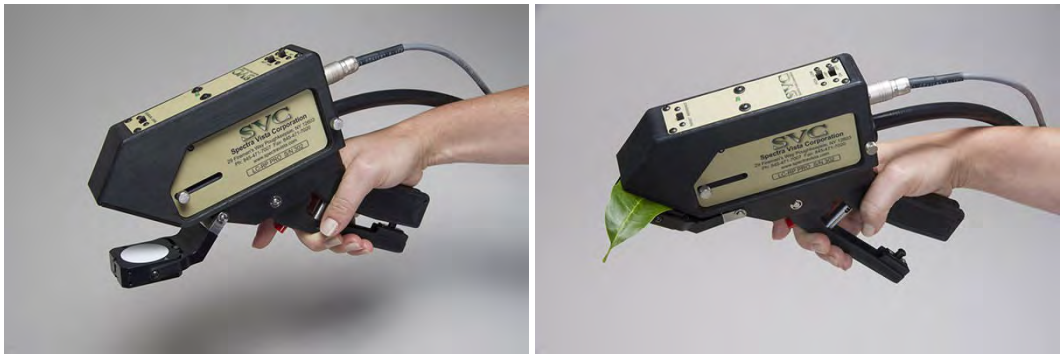

Figure 4.6: SVC's LC-RP PRO(adopted from Spectra Vista Corporation, 2021)

Figure 4.7: RTK ground station receiver

collecting spectral data from 20 infected and 20 uninfected trees, around 20-23 trees were sampled in total during each field campaign. The selection of apple trees for spectroradiometric sampling was subject to the long-term monitoring and studying of certain trees on the orchard by LRC. Consequently, the infection status of each sampled apple tree was validated by testing respective root samples in the laboratory taken from the first field campaign. Thus, the spectroscopic and PCR laboratory analysis of the root material, as well as additionally sampled leaves that were taken after each spectroradiometric measurement, served as ground truth. Hence, the tree's infection status was known prior to sampling. Under the guidance of colleagues from LRC's Department for Functional Genomics, leaves were 'randomly' selected for in-field spectroradiometric sampling. However, absolute randomness cannot be assumed due to two main reasons: firstly, the sampling design stipulated leaf measurements to be taken from the same side (which faced east) in between apple rows to remain somehow consistent during the sampling procedure. And secondly, sampling itself was limited to the reaching area restricted by the arm's length and that of the power cable supplying the leaf clip. Additionally, the selection of sample leaves was biased by preferring rather older leaves over younger leaves, as these are considered more representative for the entire tree canopy.

It is worth mentioning that the weather conditions were fairly stable during the sampling activities. However, outdoor temperatures varied from the first (beginning of April) to the fourth (mid-July) field campaign as well as throughout the day, with typically rising temperatures towards midday and the afternoon. The SVC HR-1024i's internal temperature sensor also recorded a difference in temperature of around 30°C during the last field campaign in July (circa 22°C with beginning of sampling activities from a cold start at 9 o'clock in the morning and around 50°C after the last leaf sample at 3 o'clock in the afternoon). The meas-

urements with the spectroradiometer were usually taken between 9 o'clock in the morning till noon and from 2-5 o'clock in the afternoon. All measurements were completed within around 6-8 hours.

The geographic position of each sampled tree was obtained using the Leica GS14 GNSS RTK Base & Rover Receiver Set (Leica Geosystems AG, Heerbrugg, Switzerland)(Fig. 4.7).

Orchard level

In addition, an airborne proximal sensing strategy was adopted by deploying an UAV equipped with two cameras. Prior to take-off, it is necessary to plan the flight missions according to the mapping interest and the area to be mapped. For instance, one should be aware of the extend of the area of interest and be able to set a flight altitude for appropriate coverage. What kind of product is needed and which camera or sensor system is suitable for the survey? How are the camera's mounted (e.g. using a gimbal) and what are the camera's specifications? And not to forget to mention the take-off and landing conditions in the field (Szabó et al., 2017). Hence, taking into consideration the high sensor payload and consequent load on the UAV's batteries, two consecutive flights with an approximate flight duration of eight minutes were performed during each field campaign for safety reasons. The open-source and free firmware MikroKopter-Tool, or short Kopter-Tool (Version 2.20b, HiSystems GmbH, Moormerland, Germany)[1], allows flight pattern computation prior to take-off. Such a pattern can be a regular grid or zig-zag flight pattern covering the whole aerial extent of the orchard.

Figure 4.8: Soleon Octocopter mounted with the MicaSense Red Edge and the Rikola hyperspectral camera

[1] https://wiki.mikrokopter.de/MikroKopterTool

The prior flight control software use planning algorithms to improve accuracy (Li et al., 2016) and allows setting the flight parameters in advance to the UAV launch. Thus, flight altitude and speed were specified prior as 45 m above ground ideally and 2 m/s, respectively. Every 5 seconds, images are taken, ensuring approximately 60-80% of longitudinal and transversal overlap of image strips for follow-on image stitching. Georeferencing is done with three to four GCPs which are pre-marked artificial features (Szabó et al., 2017). These are placed on the ground prior to the flight mission in a way that clearly appear in the recorded scene of the orchard. Their respective locations are also recorded in a known reference system.

During surveying, the UAV's flight controller unit (FCU) follows the predefined waypoints and flight route autonomously, additionally handling speed and manoeuvring. Equipped with further positional sensors, such as a GPS/GNSS sensor, a magnetometer and/or an inertial measurement unit (IMU), actual flight parameters (e.g. attitude, accelerations, and altitude) are recorded and controlled during the flight in order to follow the predefined flight route as close as possible. However, the FCU permits pilot intervention through a remote controller, as the pilot needs to have the UAV in their FOV throughout the entire flight.

The CSS's octocopter (Soleon GmbH - SRL, Varna, Italy) (Fig. 4.8) was deployed for airborne imaging, which is a lightweight multicopter made out of a carbon and plastic construction, equipped with six 15" carbon propellers (Soleon GmbH, n.d.). Unlike the spectroradiometer, the UAV's motors and propellers are powered by lithium-polymer (Li-Po) batteries. At the UAV's underside, the PSC1 Rikola hyperspectral camera (Rikola Ltd., Finnland) and the MicaSense RedEdge (MicaSense, Seattle, WA, USA) multispectral camera were mounted on a 2d-axis gimbal for aligning both cameras to nadir view. By and large, a gimbal is a stabilizing mount that automatically corrects for weak flight turbulences and holds the camera or sensor in the intended orientation (Szabó et al., 2017). Both cameras achieve a Ground Sampling Distance (GSD) of 5 cm, which is the distance between centres of two adjacent pixels or, in other words,the spatial resolution of the imagery.

Figure 4.9: MicaSense RedEdge multispectral camera (adopted from MicaSense, 2021)

From the MicaSense RedEdge five spectral bands were obtained covering the following bandwidths:

Multispectral band	Centre wavelength in nm	Bandwidth in nm
Blue	475	32
Green	560	27
Red	668	14
Red edge	717	12
Near-Infrared	842	57

Table 4.2: Recorded Wavelengths and respective bandwidths of the MicaSense RedEdge multispectral camera

The Rikola hyperspectral camera was measuring radiance in the following bands and their respective fwhm:

Wavelength in nm	fwhm in nm	Wavelength in nm	fwhm in nm
506.285	9.84	716.158	11.92
521.498	14.62	731.318	10.53
536.468	11.51	746.096	10.27
551.474	10.06	761.157	15.64
566.249	9.76	776.245	13.97
581.498	14.01	791.462	12.81
596.211	12.53	806.339	14.67
611.086	17.53	820.873	15.0
625.943	16.4	835.804	21.04
645.258	12.74	850.597	25.85
656.031	12.85	866.602	24.49
671.165	16.08	881.009	20.16
686.279	15.14	896.406	22.87
701.45	11.25		

Table 4.3: Recorded Wavelengths and respective fwhm of the Rikola hyperspectral camera

Figure 4.10: PSC1 Rikola hyperspectral camera (adopted from Patria Magazine, 2017)

However, what was not considered prior to the second field campaign was the hanging-up of black hail nets above and across the apple tree rows on the orchard. This being a very common practice in South Tyrol, as summer showers in the alpine environment can pose a severe risk to apple fruits. Summer rainfall can rapidly turn into hailstones due to sudden cooling at high altitudes in a montane environment. Consequently, irradiance measurements were taken using the SVC-HR-1024i spectroradiometer once more, but in combination with SVC Direct Connect Full Sky Irradiance Sphere (SVC, Poughkeepsie, New York, USA) attached at the foreoptic port on the front of the instrument. Two solid sphere halves form the 3.3 inch (≈84 cm) diameter spherical integrating chamber, enclosed in a robust metal housing, mated with solid high-density spectralon PTFE, having one inlet and one exit port (SVC, 2016). Two irradiance measurements were taken with the spectroradiometer mounted on a tripod between the apple tree rows directly beneath the black hail net and the other just outside the hail net.

Figure 4.11: SVC Direct Connect Full Sky Irradiance Sphere (left) and the SVC-HR-1024i spectroradiometer equipped with the Sphere (right) (adopted from SVC, 2012)

4.2. Data Processing

Leaf level
The collected leaf spectral signatures are stored in the SVC specific Signature (SIG) file format, which is a text file containing a header with the measurement's respective metadata (for example, measurement ID, scan duration, geographic coordinates, time, units, battery status, instrument temperature, etc.) followed by the spectral information (SVC, 2012). The .sig-file lists for every recorded wavelength (in nanometres) the respective radiance values (in $W\,cm^{-2}\,nm^{-1}\,sr^{-1}$) of the target as well as reference scan and ultimately the respective reflectance (in percent) (SVC, 2012).

The proprietary PC Data Acquisition Software that comes with SVC's HR-1024i spectroradiometer was used to calibrate and resampling the leaf spectral signatures. Reflectance scans were taken of the white reference disk during data collection prior to every batch of tree-specific leaf measurements. These reference measurements are compared to the respective values of the internally stored White Plate Reflectance Data File, which is a two-column text file, containing the wavelengths in nanometres and respective reflectance values (SVC, 2012). Based on this calibration, the leaf radiance and reflectance values are corrected retrospectively.

As mentioned in the methodology already, a baseline correction can be conducted, if a vertical shift along the reflectance-axis can be seen from plotting the leaf spectral signatures. This is due to the exposition of the black spectralon background during leaf sampling. Only part of the foreoptic lens is covered by the leaf and the overall reflectance measured is reduced due to light absorption features of the black disk. Not knowing the exact area of the black background that was exposed during a spectral measurement makes it difficult to quantify the black spectralon background's absorption. Consequently, leaf spectral signatures were not baseline corrected during data processing. This absorption effect of the black disk was most significant in the first field campaign when the sampling technique was still to be refined. For the subsequent field campaigns greater attention was paid to the leaf sampling, ensuring that the spectroradiometer's lens was entirely covered by the sampled leaf.

After radiometric correction, leaf spectral signatures were resampled using the PC Data Acquisition Software to 1 nm intervals through spline interpolation. Hence, each measurement's spectrum ranges from 350 nm to 2500 nm at 1 nm increments.

Once the radiometric resolution was enhanced, the follow-on data wrangling, plotting and data analysis was conducted with R (R Core Team, 2021) in the RStudio IDE (RStudio Team, 2021). For data wrangling, R was favoured over the commercial software provided by SVC, as it is one of the leading open-source data science languages in the domain of remote sensing and geospatial sciences (Coetzee et al., 2020), allowing the plugging-in of several different packages. The 'spectrolab' package (Meireles et al., 2017) for instance was used for reading the reflectance values from the sig file formats to be processed in the RStudio environment. The 'dplyr' (Wickham et al., 2021) and 'magrittr' packages (Bache & Wickham, 2020) were used for data cleaning and formatting and 'ggplot2' (Wickham, 2016) for producing plots of leaf spectral signatures, both packages being part of the 'tidyverse' R-package (Wickham et al., 2019).

A tree data set usually consists of ten leaf measurements per tree, with a few cases also

eleven or twelve leaf measurements. All tree data sets were plotted in a single graph and visually inspected for potential measurements deviating from the 'common' trend. A more reproducible approach using a statistical selector would have been favoured over this fairly subjective selection of leaf measurements through visual interpretation. However, not knowing the natural variability within the tree spectra, filtering for outliers in a tree dataset might be considered a legitimate approach to reduce the influence of seemingly different leaf spectral signatures that do not follow the same distribution of the other measurements. A higher number of target scans per tree (at least 30) would have been a statistically reasonable number for computing an averaged tree specific leaf spectral signature that could have been used for filtering, e.g. selecting all spectral signatures within a certain tolerance or variance from the tree mean signature.

Orchard Level

Subsequent to the UAV flight(s), the camera sensors and the derived multi- and hyperspectral images need to be calibrated and corrected respectively, thereafter the imagery is stitched to orthomosaics and georeferenced during the processing stage prior to image analysis.

Radiometric calibration/correction is necessary for both types of camera sensors and imagery, multispectral as well as hyperspectral data. However, the MicaSense RedEdge camera requires radiometric calibration prior to the flight mission, using a white reference, which is scanned before take-off in the field. The imagery from the Rikola hyperspectral camera, on the other hand, requires radiometric correction afterwards. Coloured tarps (black and white as theoretical limits, as well as grey) were laid out in the orchard (Fig. 4.12) and recorded within the scene, which are then used for radiometric correction.

The obtained multi- and hyperspectral images were radiometrically corrected using the cameras' metadata files to transfer the pixel values (or also called digital number (DN)) into radiance values. Spectral radiance being the amount of energy radiated from an area, energy values ranging from 0 to 1. The multispectral images have a radiometric resolution of 8 bit (256 DN) and the hyperspectral images of 12 bit (4096 DN). Radiometric correction of the images was performed with the proprietary ENVI software package based on IDL[2], which are both considered still as state of the art in remote sensing.

Atmospheric correction of the imagery was not considered to be necessary, as the UAV-derived imagery taken at the low altitude is not as affected by atmospheric absorption as for instance, remotely sensed satellite imagery (Hernández-López et al., 2012).

Theoretically, the multi- and hyperspectral images would need to be corrected for the black hail net, which spans above the apple tree rows and acts as a filter to the incoming solar irradiance and, consequently, impacts the recorded reflectance from the apple trees (Fig. 4.13). Practically speaking, this is considered as a fairly complex task, exceeding the scope of the thesis, as it would require further segmentation of the apple rows to apply the radiometric correction to compensate for the filtering effect of the black hail nets. Also, this filtering effect is not spatially equal within the recorded scene due to a multitude of factors. Firstly, the hail net undulates across the rows, being higher at the hail net concrete poles and hanging in-between tree rows. Thus, the black net cannot be treated as a plain surface across the covered area with homogeneous reflectance properties.

[2] https://www.l3harrisgeospatial.com/Software-Technology/ENVI

Figure 4.12: White, grey and black tarps used in the field for calibrating the Rikola camera

Secondly, this undulating character means that solar irradiance enters the hail net not spatially equally, as incidence angles vary across space. Same is true for the outgoing radiance from the trees.

Consecutive to the image correction, the recorded images are photogrammetrically stitched together for each respective band. Single images are collected at around 5 second intervals, resulting in a total of around 96–160 images per spectral band. The very-user friendly Pix4D software, again considered as state of the art in the field of photogrammetry, particularly for processing UAV imagery was used for orthorectification and orthomosaicing (or image stitching). Thereafter the UAV images were projected to the European Terrestrial Reference System 1989 / Universal Transverse Mercator (UTM) zone 32 N coordinate system (EPSG-code: 25833). Pixel values were converted to relative surface reflectance values in each band.

Tie points which are corresponding points in the overlapping areas of neighbouring images were identified in order to photogrammetrically merge the images to a mosaic covering the extend of the orchard in nadir view. Images are simultaneously orthorectified according to the images' orientation parameters.

The orientation parameters are obtained through the UAV log-file which is a GPX-file that stores the GPS-coordinates of the image camera position at a point in time during the flight, which corresponds to the time stamp allocated to each image taken. With the open source tool Geosetter[3] the metadata from the GPX log-file can be transferred to the respective image using their respectively shared timestamp.

[3] https://geosetter.de/en/main-en/

Figure 4.13: Black hail net hanging across the apple tree rows on the orchard

Thereafter, once each spectral band has been mosaicked and orthorectified, the processed images are georeferenced using 6–9 GCPs, that have been recorded with the Leica GNSS Receiver and their coordinates read out from the log-files with the software LEICA Geo Office 4.0 (Leica Geosystems AG, Heerbrugg, Switzerland)[4]. Using the Georeferencing tool in the open source and free GIS, QGIS (Version 3.18.2-Zürich, QGIS Development Team [QGIS], 2021), the GCPs were used to translate and spatially align the imagery as good as possible.

So far, the images have been processed band-wise, which eventually enables the composition of multispectral RGB true-colour orthoimages from the MicaSense Red Edge camera as well as hyperspectral VIs.

As mentioned previously in the methodology, an object-oriented classification was initially aimed at, as the high-resolution imagery would have granted an accurate delineation of the tree canopy. However, the black hail net not only functions as a radiance filter but also modifies the DEM of the apple orchard. Both DSM and DTM were obtained through the SfM principle from the multispectral imagery in order to derive the CHM. A lot of noise has been introduced into the imagery due to the small plastic clips that hold together the net, the concrete posts that hold the whole construction, and the black net itself, acting as a thin blanket above the tree crowns. As the hail net is not a plain surface, the camera sensors either detect the black net or the radiance from the tree canopy or vegetated ground below.

This, in turn, makes it increasingly difficult to apply an inverse watershed algorithm to the local maxima of the CHM to delineate the individual tree crowns (Fig. 4.14). Local maxima should theoretically reflect the highest points in the tree canopy, but instead, many features from the hail net structure are picked up (concrete poles and net clips). Despite manually filtering and removing those false local maxima, the remaining true local maxima do not serve as seeding points as the neighbouring pixels are a mixture of vegetations response or signals obtained from the hail net reflectance. As a result, this theoretically ideal approach could not be adopted for the follow-on analysis.

[4] https://leica-geo-office.software.informer.com/4.0/

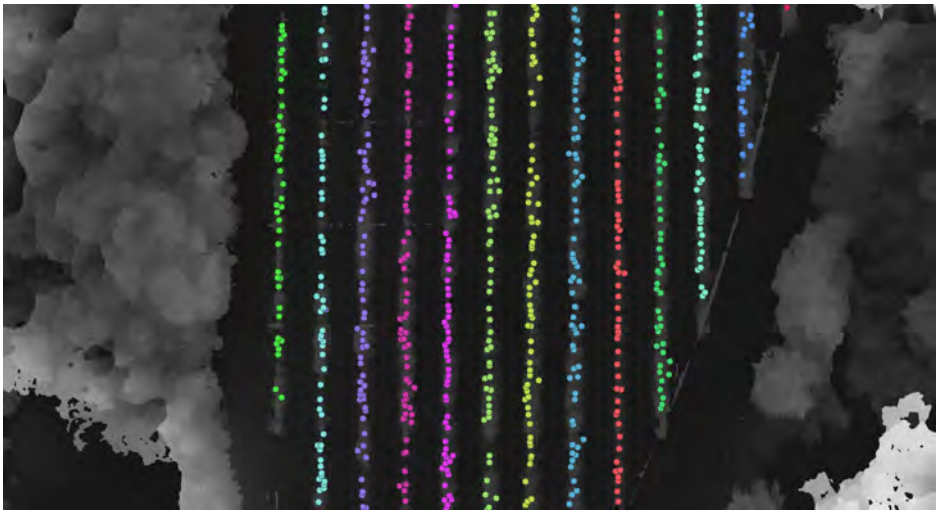

(a) Manually cleaned local maxima from the CHM colour-coded according to the tree row

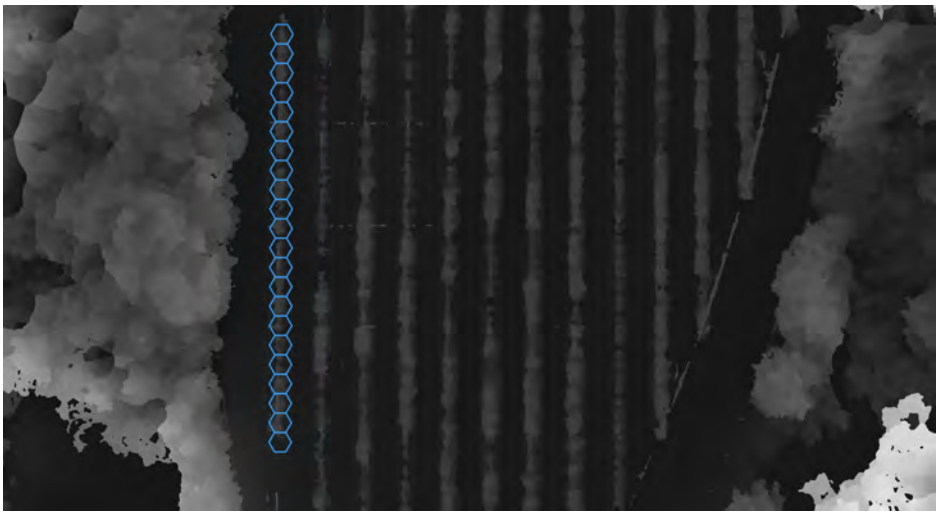

(b) Exemplary hexagonal grid structure for one tree row laid over the CHM

(c) Exemplary hexagonal grid structure for one tree row laid over the orthophoto

Figure 4.14: Illustration of the adopted working procedure to derive a hexagonal grid structure

Alternatively, the CHM was used to extract canopy tree heights ranging between 2–4 m in order to obtain the apple tree rows on the orchards. Again this segmentation contained some noise as the concrete poles holding the hail net, the net itself and the hail net clips were also within this height range. Thereafter, the binary raster image was vectorised using the GDAL 'Polygonize'-tool offered through QGIS[5]. Some of the noise was manually removed from the computed vector file to obtain the outlines of the tree rows, which served as a basis for computing the centreline of the tree row polygons. Once these lines were defined, a hexagonal grid structure was created with QGIS's 'Create Grid' vector processing tool[6]. One column of hexagonal cells running from north to south seem to be an adequate cartographic abstraction of the individual trees as well as the apple tree rows on the orchard. Commonly, tree plantings on an orchard follow standard regulations, which meant for the studied apple orchard that distances between tree rows are around 3.5 m (for orchard vehicles to drive through) and the distance between tree stems in a row around 1.2 m. The dimensions of a single hexagonal cell measure 1 m vertically and 1.155 m horizontally. The hexagonal shape was also preferred over a quadrilateral cell as it follows a more organic outline for abstracting the tree canopy rather than a pixel-like square.

During the image analysis and data visualisation the hexagonal grid structure will serve as a graphical primitive as well as a common classification reference for applying zonal statistics reflectance values. However, it is important to note that a single hexagonal grid cell is not filled entirely by the tree canopy, as also the trees on the orchard vary in size and shape. Consequently, a signal from the soil or also parts of the neighbouring tree might be represented within a hexagonal cell; thus one hexagonal cell does not equal to one orchard tree on a one-to-one basis.

4.3. Data Analysis

Leaf Level

The '*mdatools*' R-package (Kucheryavskiy, 2020) proved useful for the implementation of the PCA for dimensionality reduction and feature extraction. The PCA was applied to the three hyperspectral data sets collected with the spectroradiometer during the three last field campaigns. To be precise, several PCAs were conducted. Firstly, the entire dataset consisting of single leaf spectral signatures ($n \approx 230$) but also tree respective mean leaf spectral signatures ($n = 23$) were analysed. However, reflectance values in the UV spectral range were excluded $\leq$400 nm from the remaining spectral subset 401–2500 nm before each data set was analysed for PCs. Spectral reflectance in the UV range were not considered for the analysis as the spectral signals showed significant variation and, therefore, considered as noise that distorted the entire PCA. In another processing step, each data set was trimmed a second time in respect to the detection window of the Rikola hyperspectral camera 500–900 nm and PCA was applied once more.

[5] https://docs.qgis.org/testing/en/docs/user_manual/processing_algs/gdal/rasterconversion.html#gdalpolygonize

[6] https://docs.qgis.org/testing/en/docs/user_manual/processing_algs/qgis/vectorcreation.html#create-grid

Orchard Level

From the PCA on the leaf level, some spectral bands contribute according to their loading more than other wavelengths to the computation of new PCs. Hence, wavelengths' loadings were considered as a statistical indicator for more significant variance along the respective unit vectors, potentially allowing greater separability between infection classes. Consequently, VIs were chosen that are based on similar wavebands as revealed by the PCA as a first indication for plant stress that may be linked to AP infection. The bands used for the composition of VIs do not correspond exactly to those wavelengths found in the literature as particular, the hyperspectral camera was not programmed prior to the field campaigns to detect at exactly the same wavelengths found in the literature. Many VI can be found in the literature, all aiming at different biochemical or biophysical plant characteristics. The following VIs seemed relevant to this study, setting a particular focus on leaf pigments:

Vegetation Indice	Waveband composition	Description	Reference
Normalised difference vegetation index (NDVI)	$(R750-R705)\div(R750+R705)$	NDVI is a very typical index. Positive values suggest vegetated areas	Tucker, 1979; Tucker et al., 1981
Photochemical reflectance index (PRI)	$(R531-R570)\div(R531+R570)$	PRI index is a function of the reflectance at the 531 nm, this reflectance is related to xanthophyll. When the xanthophyll activity is high, the light use efficiency is low, meaning a possible stress occurred	Peñuelas et al., 1994.
Anthocyanin reflectance index 2 (ARI2)	$R800\cdot(1\div R550)-(1\div R700)$	ARI index is designed to estimate the stack of anthocyanin in senescing and stressed leaves	Gitelson et al., 2001
Gitelson and Merzyak 1 (GM1)	$R750\div R550$	GM1 and GM2 were created to measure the chlorophyll content in vegetation leaves	Gitelson et al., 1996; Gitelson and Merzlyak, 1997
Gitelson and Merzylak 2 (GM2)	$R750\div R700$		
Zarco-Tejada Miller (ZTM)	$R750\div R710$	ZTM is a Red edge index highly correlated to chlorophyll content. At the canopy level, it has the advantage of minimizing shadow effects	Zarco-Tejada et al., 2001; Underwood, 2003

Table 4.4: Overview of hyperspectral VIs (adopted from Al-Saddik et al., 2018)

The above listed VIs are disease unspecific as already mentioned which is why the implementation of a robust and reproducible machine learning approach for classifying the hyperspectral imagery for AP infected trees was initially set as a research goal (RO.3) (Table 4.4).

In order to experiment and at the same time not exceeding the scope of this study, the spectral analysis of the hyperspectral imagery was confined to the testing of a single machine learning algorithm for classifying AP infected trees. As already mentioned in the previous chapter, ideally several machine learning algorithms should be tested and evaluated according to their classification performance. This would, however, require a whole study for itself and exceeds the frame of this research.

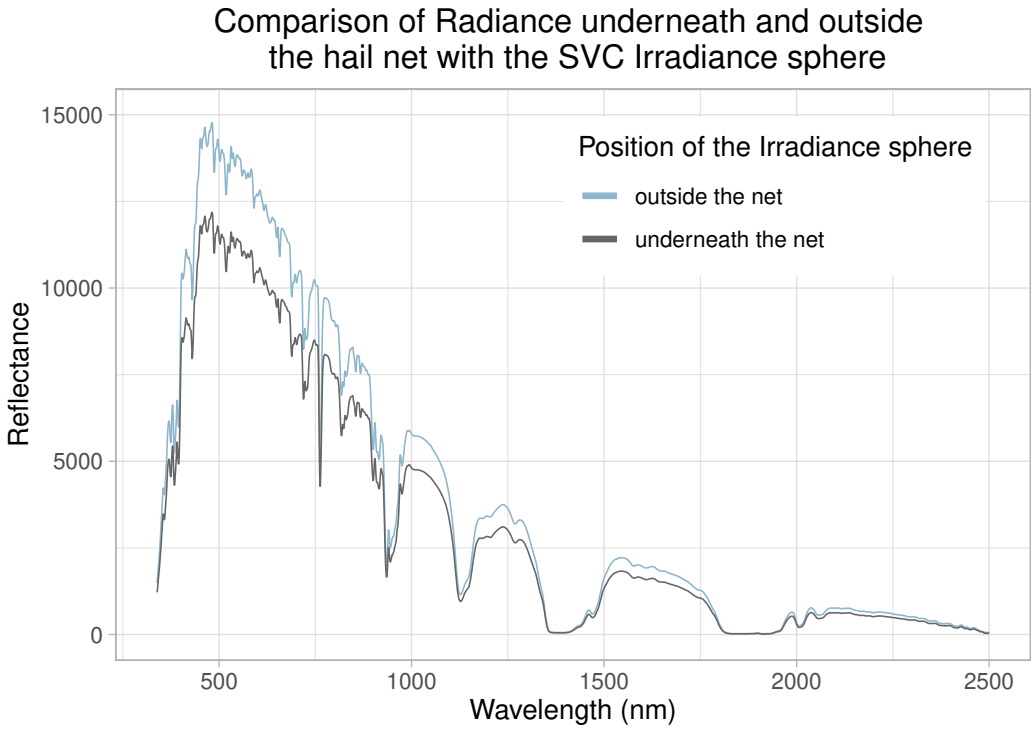

Figure 4.15: Comparison of Radiance underneath and outside the hail net with the SVC Irradiance sphere

In the end, a supervised classification was adopted as the trees, that were sampled with the spectroradiometer serve as training data for the image classification. A few studies have shown that the SVM is a robust algorithm for a supervised classification, relatively easy to implement and achieves good classification results of plant diseases even using on a small number of training data (Rumpf et al., 2010; Albetis et al., 2017; Al-Saddik et al., 2018). Al-Saddik et al. (2018) and Rumpf et al. (2010) achieved high classification accuracies using SVM which performed better than some other classification algorithms for identifying different plant diseases. According to Ben-Hur and Weston (2010), SVMs find the best separating hyperplane between classes according to the hyperplane with the maximal margin. A penalty is defined by a cost parameter for misclassifying objects which in turn introduce soft margins allowing objects to lie on the wrong side. Particularly, when classes are not fully separable, this may be suitable. Furthermore, SVMs use a kernel for non-linear decision boundaries needed in feature space, whereas amongst others the radial basis function kernel is commonly used.

Hence, the SVM seemed promising for testing a machine learning based image classification approach applied to the detection of AP infected trees. As it is a supervised classification, the GPS coordinates of the sampled trees set a starting point for the sampling of training and testing data from the hyperspectral imagery. Additionally, the computed vegetation indices were used as further indicators for potential plant stress in the canopy for delineating the input data. Two approaches were followed and tested to extract training data from the imagery. Firstly, the Semi-Automatic Classification Plugin (Congedo, 2021) was used in QGIS for selecting so-called regions of interest (ROIs). For selecting ROIs one

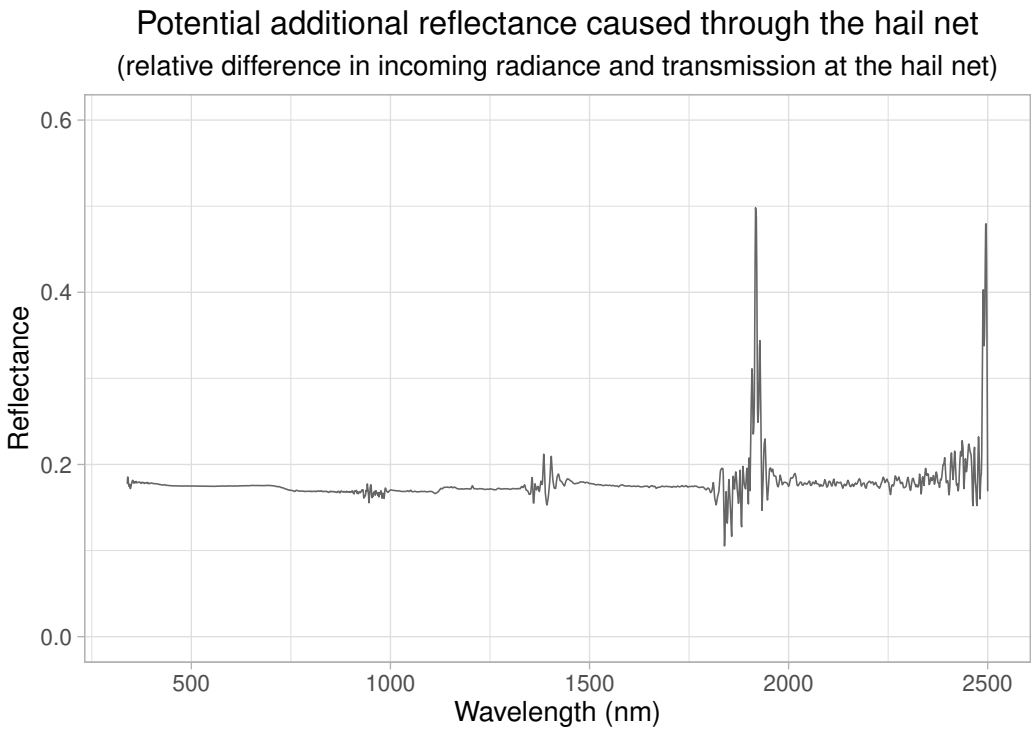

Figure 4.16: Potential additional reflectance caused through the hail net

can choose between pixel or area-based ROIs computation. The latter was chosen in this study, as the user can interactively select a pixel and according to an adjustable threshold. When selecting a pixel of interest, its DN is compared to those of adjacent pixels, which are also selected in respect to the threshold to form a larger polygon with similar spectral characteristics. And secondly, a polygon was simply drawn around the respective tree on top of the orthomosaic to provide the bounds of the training input to the SVM which was performed in QGIS using the SAGA-GIS module SVM Classification[7]. A binary classification was adopted with the attribution of the ROIs as either infected or uninfected, considering the latent trees also as infected.

Unfortunately, the testing of the SVM for AP classification of the hyperspectral imagery did not work out as expected. The effect of the black hail net spanning across the apple tree rows is considered to be the reason, as it impacts the spectral responses recorded at the sensor. According to the measurements taken with the irradiance sphere, there is a clear difference between the incoming solar irradiance and the radiance transmitting the hail net (Fig. 4.15). Consequently, a certain amount of incoming solar energy that does not pass through the hail net is converted into heat or is reflected at the net surface. This may also explain, why the hail nets in the region are also considered as a sunlight filter to protect the apple fruits from sunburn (Zebisch et al., 2018). The filtering effect of the hail net means for the taken UAV imagery that the collected reflectance values of the vegetation are distorted by the hail nets, which increases the recorded reflectance values.

In Figure 4.16 one can see the ratio of the radiance that does not pass the hail net to the

[7] http://www.saga-gis.org/saga_tool_doc/2.2.4/imagery_svm_0.html

overall incoming solar irradiance. Consequently, it can be said that the hail net potentially adds to the recorded reflectance across the entire detection window, whereas not uniformly. Particularly in the SWIR range, there is a greater variance. Although the effect of the hail net may seem to fluctuate less in the detection window of the Rikola hyperspectral camera 500–900 nm, this amplifying effect can not be accounted for easily. If the hail net would be a flat surface, the image may be radiometrically corrected for this effect. However, the hail net undulates between rows and thus seems more like a light-absorbing blanket.

Nonetheless, the cartographic idea of implementing a multi-scale mapping approach in precision mapping presents coarser spatial information at a smaller scale, and further detail at a larger scale was alternatively applied to the VIs. For this purpose, spatial data was aggregated to the hexagonal grid cells using the Zonal Statistics Raster tool[8] offered through QGIS.

4.4. Data Visualisation and Map Design

Leaf Level

As already outlined in the data processing stage, the R-package 'ggplot2' (Wickham, 2016) was used for plotting leaf spectral signatures as line graphs for visual comparison. It was already necessary to plot the obtained spectral signatures during the processing stage as a visual interpretation of the overall trend was the basis for including individual signatures for further analysis. As already touched upon, natural variability in tree respective leaf signatures was not known. Thus, a more reproducible statistical approach was challenging to implement, especially as the number of leaf scans per tree was limited to a comparable small sampling number of 10–12 samples. Once the outliers were removed, tree related sets of spectral signatures were individually plotted.

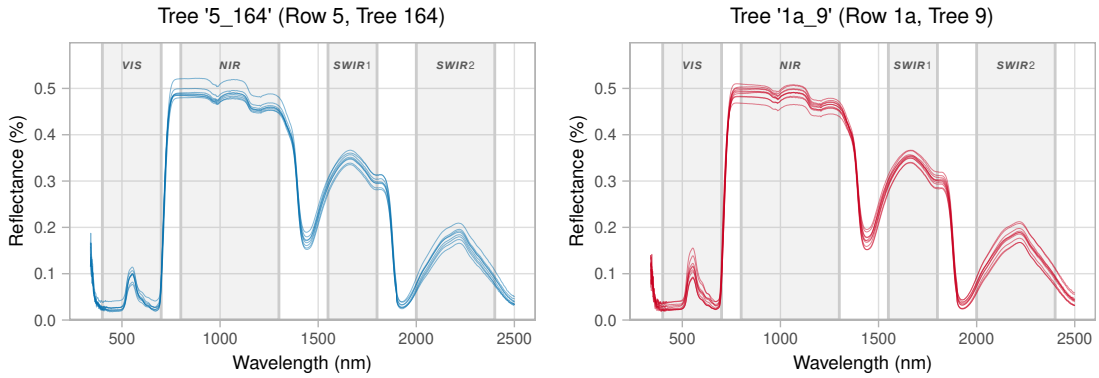

(a) Leaf spectral signatures of an uninfected..

(b) ..and of an AP infected tree

Figure 4.17: Comparison of Spectral Signatures of (a) an uninfected and (b) AP infected tree sampled in the second field campaign

In order to identify certain spectral ranges where AP infected and uninfected trees might deviate, leaf spectral signatures were averaged tree-wise to obtain a representative leaf signature for that specific tree. These signatures show that there is a certain inter-tree variab-

[8] https://docs.qgis.org/testing/en/docs/user_manual/processing_algs/qgis/rasteranalysis.html#qgiszonalstatisticsfb

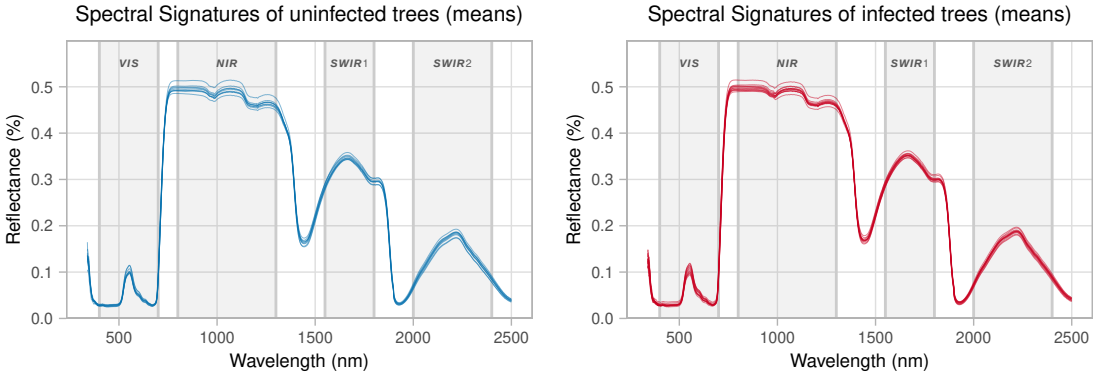

(a) Mean leaf spectral signatures of uninfected..

(b) ..and of AP infected trees

Figure 4.18: Comparison of mean spectral signatures of (a) uninfected and (b) AP infected trees sampled in the second field campaign

ility. This means that spectral signatures of the 'tree means' of the same infection status (infected and uninfected) not only vary but that they also overlap in certain ranges within the electromagnetic spectrum, where a clear separability cannot be visually observed.

Lastly, these 'tree' means were further averaged regarding their infection status to produce two spectral signatures representing infected and uninfected averaged leaf signatures, already accounting for intra and inter-tree variability.

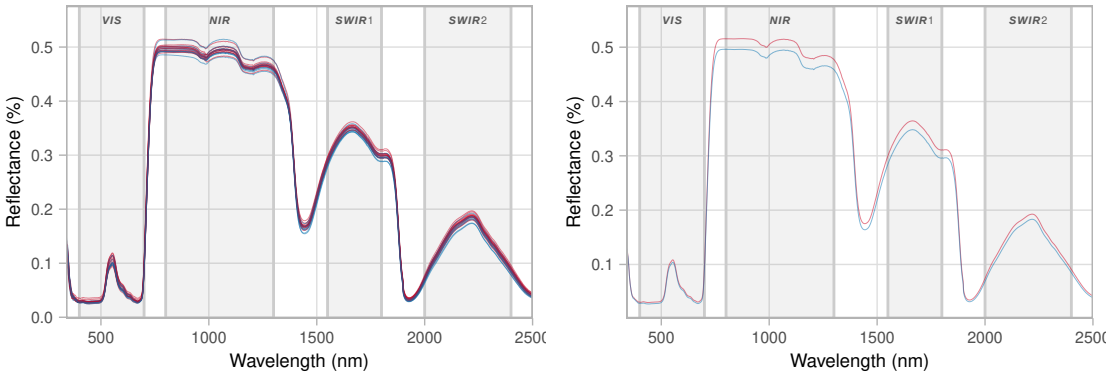

(a) All tree-wise averaged leaf spectral signatures

(b) Averaged leaf spectral signatures regarding infection status

Figure 4.19: Leaf spectral signatures averaged (a) tree-wise and (b) regarding infection status sampled from the second field campaign

In the PCA, scree plots were drawn to visualise the relative share in total variance exhibited by the PC. As can be clearly seen from the scree plots, the first PC has the accounts for the greatest variance of the leaf spectral signatures, which decreases rapidly with an increase in PCs. In search of best separability between the two spectral signature classes (infected/uninfected), computed PCs were plotted against each other to utilize their respective variance to increase the division between classes in feature space. The PCA was applied to all three datasets from the field campaigns covering 400–2500 nm of the electromagnetic

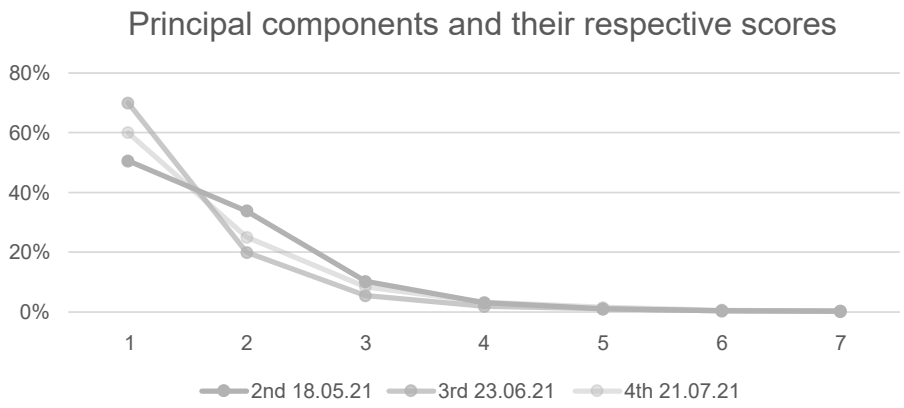

Figure 4.20: Scree plot of the PC's loadings regarding the entire hyperspectral range and from all field campaigns

spectrum and to a subset defined by the detection window of the hyperspectral camera (500–900 nm). Of particular interest was the detection window of the hyperspectral camera, as the PCs expected to indicate which wavebands may seem suitable for applying the SVM classification to detect AP infected trees.

In terms of visual display, a blue and red tone were chosen as colour hues to represent the two infection statuses or two categorical classes (uninfected and AP infected, respectively). The colour hues were adopted from the colour blind barrier-free colour pallet suggested by Okabe and Ito (2002). A blue colour hue was chosen over a green hue deliberately, as it is not only colour blind friendlier, but the latter might also invoke a false sense of a healthy plant, whereas this study only focusses on one particular disease. Thus, a more neutral colour hue was chosen to infer that there those samples are not AP infested. Latent trees which could have also been viewed as another class were, however, considered as AP infected for the purpose of the study.

Orchard Level

Eurac's EDP which is a geoportal maintained by the CSS provides the SDI with a map user interface based on the open source OpenLayers[9] library.

The precision map is intended as a slippy map, where the map user can interact with the map content by zooming and panning, which makes the map slip around[10].

Several basemaps are offered through OpenLayers and can be interactively selected as background information, such as a mosaic of satellite imagery or OpenStreetMap[11] layers.

Furthermore, the precision map consists of orthophotos of the orchard and several VIs at the original resolution of the multi- and hyperspectral cameras. The VIs were classified and accordingly colour coded, whereas in terms of colour choice, sequential colour schemes were adopted, intentionally moving away from the overused and partially shrill rainbow colour map (Moreland, 2016) or 'traffic light' colour sequence in common VIs.

[9] https://openlayers.org/
[10] https://wiki.openstreetmap.org/wiki/Slippy_Map
[11] https://www.openstreetmap.org/

Řezník et al. (2020) argued in their study, that mainly focussed on uncertainty mapping, for the adoption of exactly this easily understandable solution for new and inexperienced users (Drecki & Maciejewska, 2005), as a map reader can utilise everyday experience (traffic lights) easily to decode categories intuitively. Hence, according to Řezník et al. (2020) it facilitates map users to integrate their external knowledge into the map-based decision-making process. On the other hand, a sequential colour palette might seem more adequate to represent a continuous increase or decrease in value. Thus, colour value (lightness) may be used instead of adding additional chroma to a colour ramp. Consequently, change in colour value (lightness) may be perceptually closer to a change in class (McNeall, 2015).

For the intended map on AP which was supposed to be derived from the SVM classification of the hyperspectral imagery, the binary image classification (infected or uninfected) would be visually expressed rather by adopting a qualitative colour scheme. Again a blue (for uninfected) and a red tone (for AP infected) were used to express the infection status. However, due to the issues encountered with the black hail net and the consequent spectral distortions, which complicate the implementation of the SVM classification, the sampled trees were alternatively represented in the map through coloured hexagons depending on their infection status. This may indicated the idea of abstracting and scaling the information gathered on the leaf level to the orchard level by using single hexagonal cells to convey AP infection within the orchard, although restricted to the number of trees that were sampled with the spectroradiometer.

It would have been ideal to use the outlines of the tree canopy for an object-based classification which can be segmented theoretically from the CHM. A regular grid, however, assimilates already the tree row structure on an orchard. Single hexagonal grid-cells function as graphical primitives for the individual tree canopies, bearing in mind, though, that this relationship is not on a one-to-one basis, as a canopy of a neighbouring tree may also be within the same hexagon, as already mentioned. To demonstrate the cartographic idea of a multi-scale map design and introduce a scale dependent visualisation in precision mapping, generalisation was applied to VI as an alternative to the not successful SVM image classification.

For this purpose, the same colour scheme and classification that was used for the VIs was also applied to the hexagonal cells that represent coarser granularity. Each hexagon was attributed with the majority value that was obtained through the zonal statistics tool in QGIS regarding the extent that the graphical primitive covered.

To offer more details on demand, the intended map user can interactively select features to obtain further information, such as spectral values or ratios. In the case of the hexagons representing AP infected or uninfected trees, averaged leaf spectral signatures collected with the spectroradiometer are also available as additional information. Ideally, spline graphs could be used to visualise the spectral signatures of selected features on-demand in a separate panel within the user interface. This, unfortunately, is not supported with the spatial data structure of the attribute table of a shapefile. Thus, additional data formats, such as a data cube, seem promising for this purpose (as indicated in Fig. 2.5).

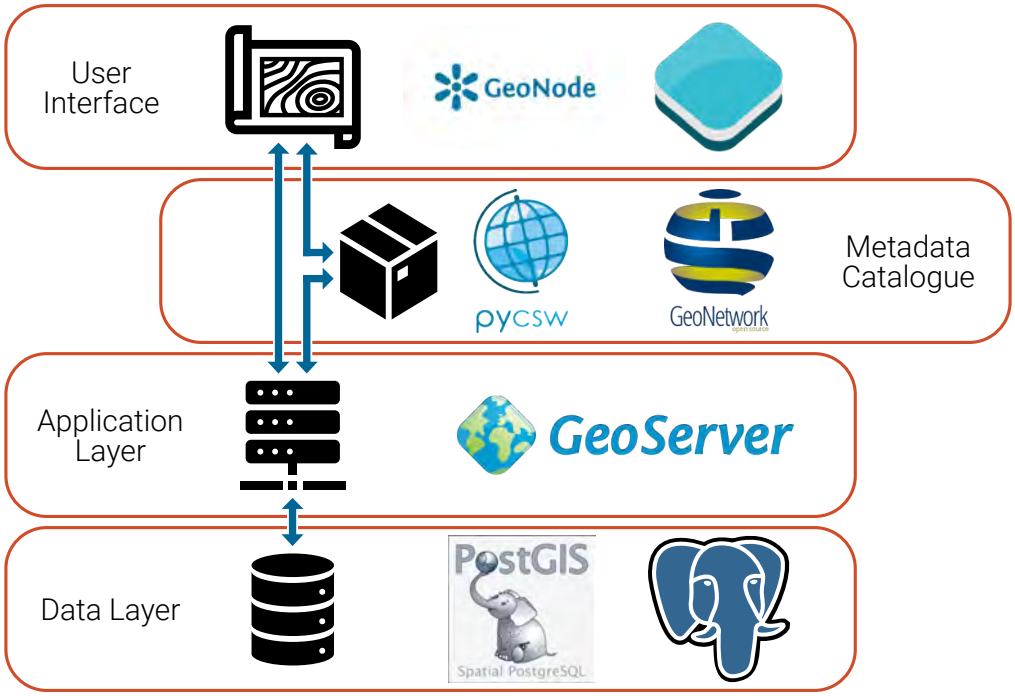

Figure 4.21: Spatial Data Schema used for the Implementation of the Precision map

4.5. Data Sharing

Eurac's CSS kindly offered their resources, amongst others the EDP[12] for developing and implementing the precision map. The EDP, in turn, is the user interface and therefore one layer within the SDI's set up (Fig. 4.21) used for implementing the precision map. One can consider the SDI at the CSS as an open SDI as it relies on open source and free hard- and software to offer open data access to the public. In particular, software from the OSGeo finds their implementation within the different layers of the SDI's architecture.

The user interface is internally at the CSS also referred to as 'maps' and allows publicly sharing research findings, engage and collaborate with project partners in ongoing work and create interactive maps. The EDP builds up on GeoNode[13], an open-source Content Management System (CMS) for geospatial data (GeoNode Development Team [Geonode], n.d.). As a web-based application and platform for deploying SDIs, GeoNode offers an easy-to-use interface and pulls together open-source software (Geonode, n.d.). Through GeoNode spatial data can also be uploaded to the Geoserver and already converts vector data into geospatial tables and retains raster data as GeoTIFFs. Additionally, all the layers are automatically re-projected to web Mercator for map display, which allows the use of basemaps, like Open Street Map or Google Satellite (Geonode, n.d.). Map visualization, for instance is done through OpenLayers[14] which can be embedded into GeoNode.

[12] https://maps.eurac.edu/
[13] https://geonode.org//
[14] https://openlayers.org/

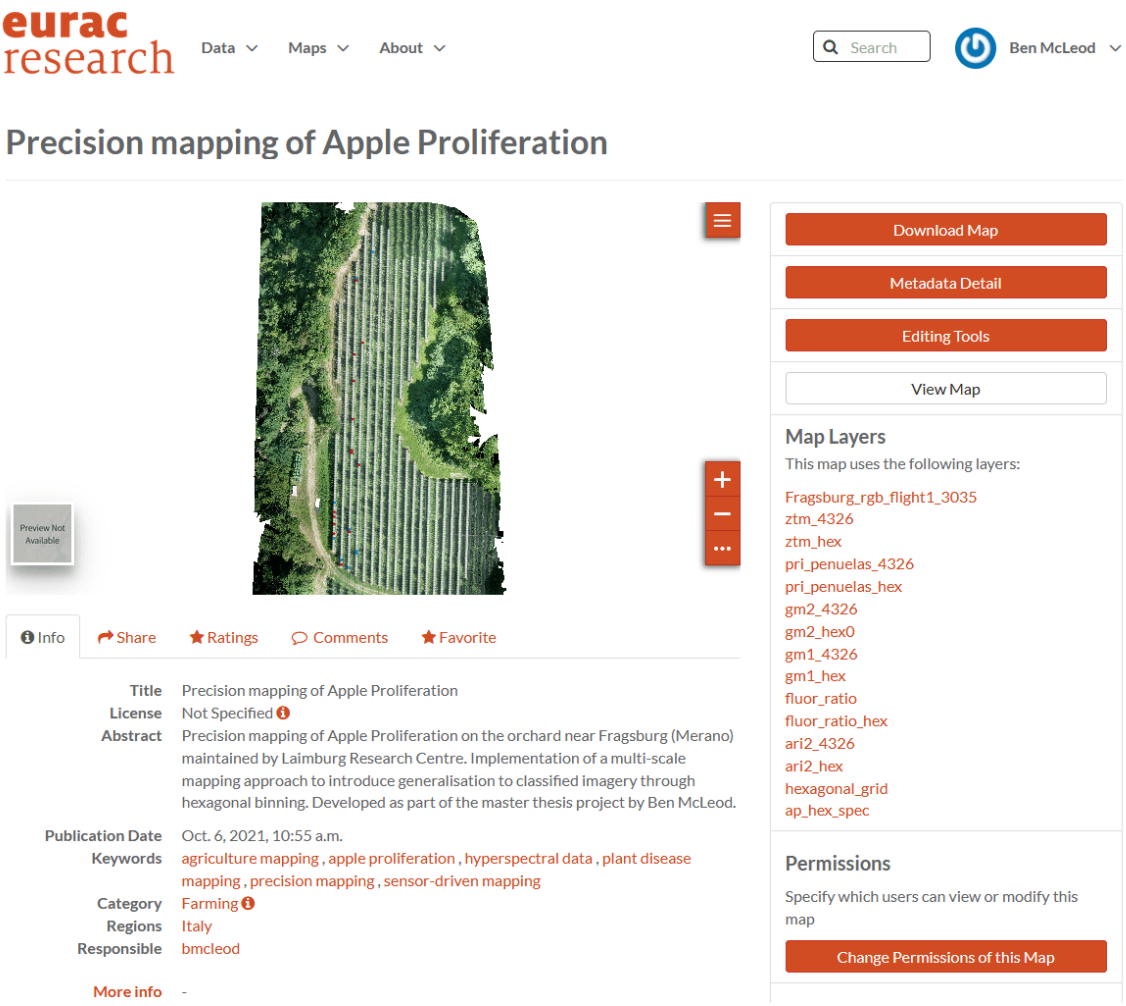

Figure 4.22: Map entry in the EDP

In addition to the user interface (Fig. 4.22), the SDI consists of a metadata catalogue, an application layer and a data layer. The latter uses PostgreSQL[15] as open-source database management system with the PostGIS[16] extension for storing and managing geospatial data on Eurac's servers.

On the application layer, GeoServer[17], an open-source, Java-based server, is deployed for hosting the geospatial data from the spatial database to the GeoNode web application.

The metadata catalogue composes of two catalogue applications to manage spatially referenced resources: pycsw[18] as well as GeoNetwork[19]. The former is automatically linked to GeoNode already, whereas GeoNetwork is installed as a stand-alone system and therefore requires additional handling of entries.

[15] https://www.postgresql.org/
[16] https://postgis.net/
[17] http://geoserver.org/
[18] https://pycsw.org/
[19] https://geonetwork-opensource.org/

All above components of the SDI architecture comply to open standards defined by the Open Geospatial Consortium (OGC) which allows interoperability of the different software components and underlines the idea of openness and FAIR principles adopted for the implementation of the precision map as a service-oriented web map.

5 Results

Synthesising the findings from the work implemented in this thesis, it is important to place the results into scientific context outlined in the literature review and relate these to the initially defined research objectives.

5.1. RO/RQ-1

The first research objective and the respective question set at the beginning of this thesis read as follows:

RO.1 Develop a cartographic understanding and definition for a precision map.

RQ.1 How can a precision map be defined from a cartographic understanding?

The prior literature review clearly shows that the term precision mapping is used interdisciplinarily and enjoys wide application. As a result, different understandings of precision mapping have developed depending on the map maker and their underlying intentions. This may also be linked to the close terminological overlapping of precision and resolution, which are partially confused and therefore misleadingly used interchangeably. Precision refers to spatial granularity at which distinctions can be made by a sensor (Raposo, 2017). Resolution, however, refers to the degree of detail to which a phenomenon is detected or represented (Raposo, 2017). Indeed, both terms are seemingly closely related but it is important to make this differentiation in order to understand the inherent conflict at which precision mapping sees itself. The literature review suggests that the map intentions and themes are very broad and different, although all of them claim to produce precision maps, whereas reference units vary from the sub-district level, to 5x5 km^2 and decimetres. Hence, geographical and ultimately map scale varies hugely between the thematic map examples, which implies that precision and resolution are both variables in an interplay with scale and need to be adapted accordingly. Raposo (2017) again defines scale as a '*measure of relative size, of objects or representations*'. Particularly in cartography, cartographic scale is correlated to resolution (Raposo, 2017), which means that the balance between scale and detail needs to be considered in the map-making process, e.g. showing less spatial detail at a smaller map scale than at a larger scale. Scale depended map-making relies on cartographic generalisation, which aims at the reduction of the complexity in a map by reducing the detail and maintaining the essential spatial information (Weibel, 1997; Raposo, 2017). However, in contemporary precision mapping, classified high-resolution imagery is mistakenly understood as synonymous with a map. Therefore, it is important to stress that spatial resolution is considered foremost in precision applications but can only set the basis for the final map, as scale-depending map generalisation is inevitable, such as spatial aggregation or displacement (amongst other generalisation techniques) scaled representations of the original data. Consequently, in light of providing a definition, a precision map shall be herewith proposed as being a

'*sensor-driven, interactive, thematic map that offers different degrees of granularity at multiple-scales*'.

5.2. RO/RQ-2

The initial idea of precision mapping derived from the need to visualise intra-field variability in precision agriculture (Thenkabail et al., 2018). Precision mapping has since established itself as a method adopted in agricultural spatial decision making regarding plant or crop monitoring, which primarily includes yield estimation, application of fertilizers but also plant disease monitoring, amongst others (Thenkabail et al., 2018). The latter is of great importance, as plant diseases and pests compromise on crop yields (Oerke, 2006; Savary et al., 2012, for example). Remote sensing of vegetative surfaces follows a non-destructive approach for an early plant disease identification (Lowe et al., 2017). In order to reduce crop losses due to plant disease, it is important to understand the specific disease and relate plant pathology to spectral analysis. Hence, changes within the plant caused by the disease can be related to a change in spectral characteristics, referred to as the spectral signature. This way, the analysis of spectral signatures helps to differentiate between infected and uninfected plants. The methodological approach adopted for the scope of this thesis aims at combining multi-modal data, which were collected at different scales. The underlying intention is the upscaling of the findings from the spectral analysis of the hyperspectral data to UAV image classification used for designing a plant disease precision map, at the example of AP. For this purpose, the second research objective and respective questions defined previously, recapitulate as follows:

RO.2 Identify relevant spectral bands (SB's) and vegetation indices (VI's) that meaningfully discriminate between leaves infected from AP vs. uninfected leaves (binary and multi-class discrimination).

RQ.2 Which meaningful spectral bands from the hyperspectral range and which vegetation indices (VI) can be identified, or computed, respectfully, from the spectral signature of a diseased leaf..
(a) to reflect changes caused through AP?
(b) to therefore be an indicator for the presence of AP?
(c) to ultimately be used to distinguish between healthy and diseased leaves [binary classification]?
(d) additionally: to distinguish degree of disease severity from healthy leaf [multi-class classification]?

As already mentioned, a binary classification of the hyperspectral data was the focus of the study, distinguishing between the two infection statuses *infected* and *uninfected*. A multi-class classification regarding plant disease severity or including uncertainty regarding the likelihood of an infection would be possible approaches but, in the end, exceeded the scope of this experimental analysis.

At this stage it is also necessary to retrospectively differentiate between 'healthy' and 'uninfected' as they are used interchangeably in some literature. Consequently, there was a lack of awareness in respect to this difference at the time of defining the research objectives. As only one particular plant disease is analysed for, already knowing from the laboratory findings from the LRC that some plants are already infected by AP, categorising the uninfected trees as healthy would ignore other potential biotic or abiotic plant stress.

In a first attempt at identifying potential spectral differences, spectral signatures were plot-

ted and both infection groups visually compared. Thus, the leaf spectral signatures that had been obtained with the spectroradiometer were grouped regarding infection status and averaged according to the respective tree (Fig. 5.1).

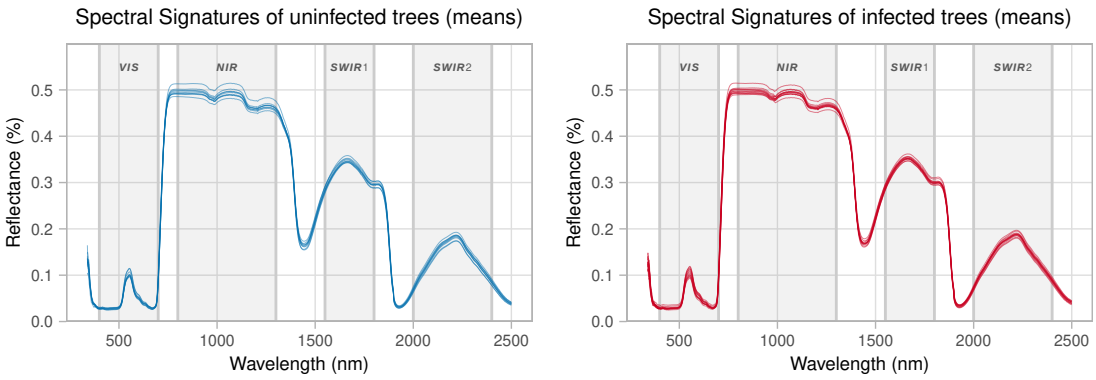

(a) 2nd field campaign (May)

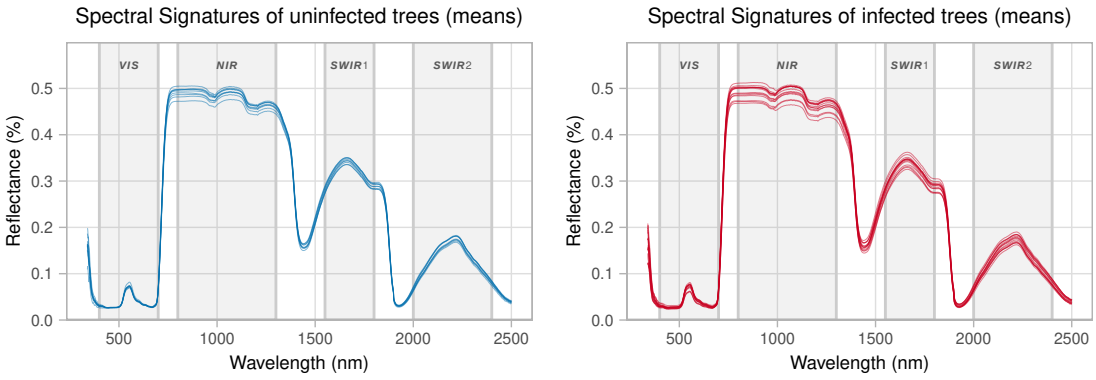

(b) 3rd field campaign (June)

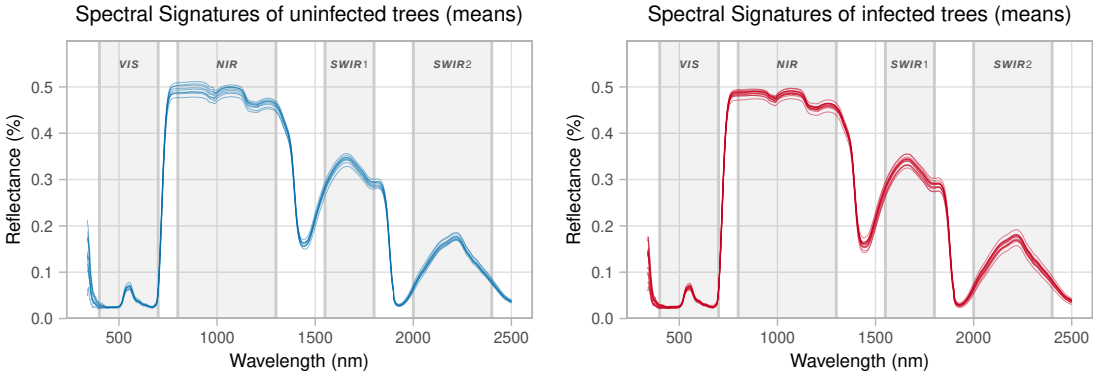

(c) 4th field campaign (July)

Figure 5.1: Uninfected (blue) and infected (red) tree respective mean leaf spectral signatures of all field campaigns

The 'tree' spectral signature of both infection groups do not substantially vary in shape and, when overlaying both groups (Fig. 5.2), it becomes even more difficult to detect spectral difference.

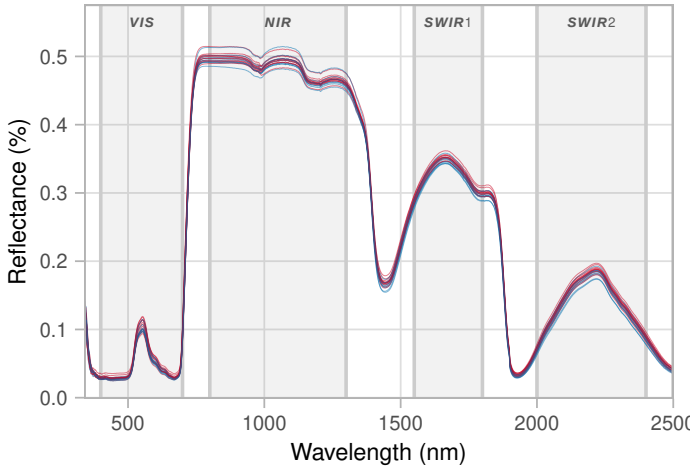

(a) 2nd field campaign (May)

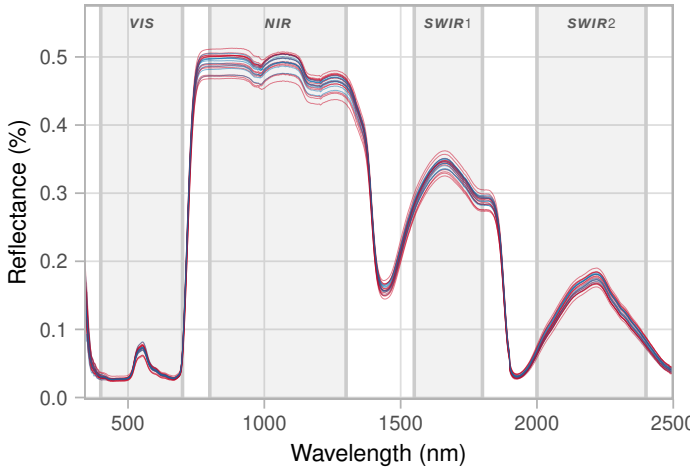

(b) 3rd field campaign (June)

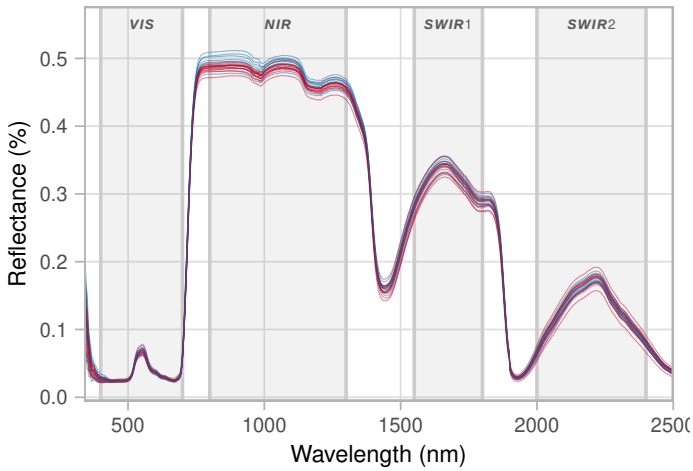

(c) 4th field campaign (July)

Figure 5.2: Overlay of uninfected (blue) and infected (red) tree respective mean leaf spectral signatures of all field campaigns

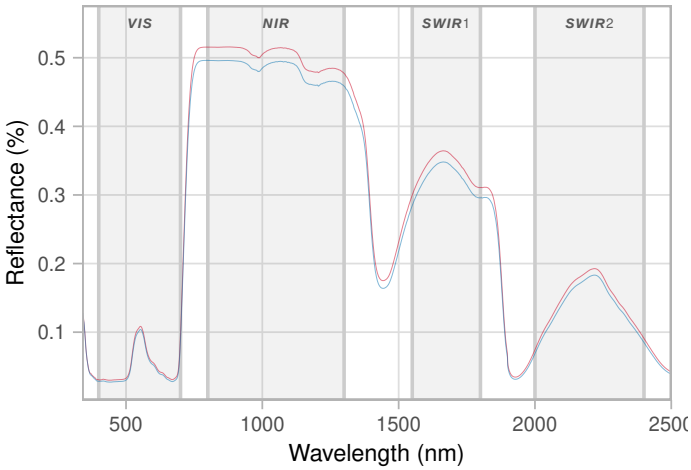

(a) 2nd field campaign (May)

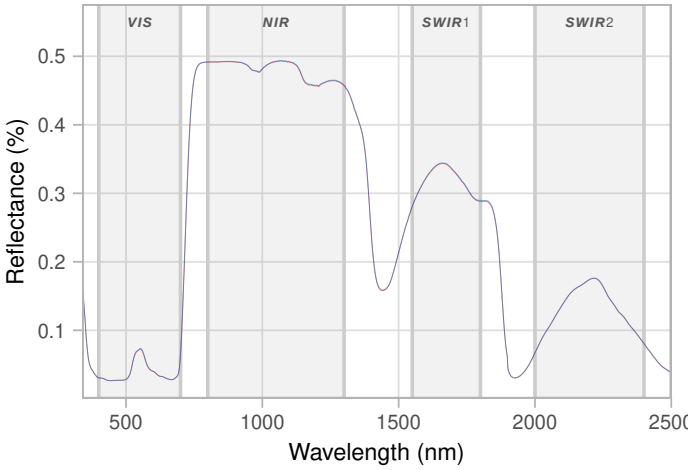

(b) 3rd field campaign (June)

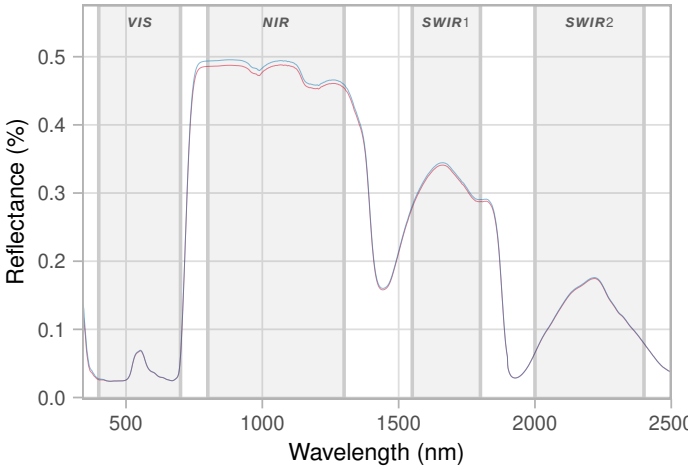

(c) 4th field campaign (July)

Figure 5.3: Mean leaf spectral signatures by infection status

To reduce the visual clatter of the individual 'tree' spectral signatures, one can group the curves by infection status to obtain two averaged spectral curves (Fig. 5.3). What can be seen from the line graphs is that spectral differences between the two groups are easier to distinguish at an earlier phenological stage (despite very low visual expression of symptoms which become visually more expressive in September/October). Spectral differences seemed to be larger in May as both means are visibly more separable. In June and July, it becomes even more difficult to distinguish between these two groups as they are nearly identical. It is difficult to give a plausible explanation for the assimilation of the spectral signatures with progression in phenological stage but it might be linked to the outdoor temperature. This is rather speculative but might be a reasonable argument as with an increase in outdoor temperature the leaf temperature increases as well, ultimately affecting the leaf's water household. In combination with water stress on the plants (due to high temperatures), the leaf may deploy self-protection mechanisms such as the closure of the stomata (which is an opening of the leaf to transpire water which is a byproduct during photosynthesis) (Pastenes et al., 2004).

In order to pinpoint which spectral bands may indicate the presence of AP, PCs may be a good indication as these exhibit variance within the dataset. Consequently, tree means were used rather than single leaf measurements to investigate spectral separability between uninfected and AP infected trees. Table 5.1 gives an overview of the first five principal components (that make up more than 98% of the total variance within the dataset according to Fig. 4.20) and their respective 10–15 spectral wavebands with the greatest loadings. These waveband ranges are characterised by high loadings for the respective wavelengths, as the variance between the two infection statuses were comparatively large.

Furthermore, it is necessary to have a look also at the spectral bands within the detection window of the hyperspectral camera as ultimately the image bands are within the range 500–900 nm (Table 5.2).

When comparing both tabular overviews regarding the PCs' respective spectral bands, it is clearly noticeable that the spectral wavebands do not match. The main reason being the different coverages of the electromagnetic spectrum used for the analysis, as the subset focuses on a far smaller spectrum. Additionally, which is perhaps more important though, is that in the PCA of the entire dataset, the first and second PCs are outside of the spectrum

Entire Dataset (400–25000 nm)			
Field Campaign	2nd	3rd	4th
Month	May	June	July
PC1	1850–1859	1788–1799	1839–1847
PC2	1077–1105	1077–1086	1079–1085
PC3	645–654	645–655	630–645
PC4	554–563	702–711	426–435
PC5	1884–1890 1393–1398	400–413	683–690

Table 5.1: Tabular Overview of the PCs for the entire dataset and their respective 10–15 spectral bands with greatest loadings

Rikola Detection Window (500–900 nm)			
Field Campaign	2nd	3rd	4th
Month	May	June	July
PC1	731–743	731–743	734–746
PC2	889–910	522–531	504–516
PC3	716–727	674–686	710–722
PC4	680–690	684–706	682–694
PC5	517–526	639–652	694–706

Table 5.2: Tabular Overview of the PCs and their respective 10–15 spectral bands with greatest loadings within the subset covering the hyperspectral camera's detection window

from 500–900 nm covered by the subset. In the PCA on the dataset collected from May spectral bands show more significant variance mainly in the SWIR, primarily corresponding to changes in structural leaf components. Furthermore, wavebands ranging from around 645–655 nm and at around 685–710 nm also appear often amongst the PCs for the entire dataset. The latter range in the electromagnetic spectrum was also prominent in the composition, especially of the fourth PC of the subset. Especially the range between 731–746 nm seemed to show greater variance as the spectral wavelengths within this range contributed most to the first PC due to their high loadings. However, what both analysis show are the temporal dynamics throughout the phenological stages. One can see from the Figures 5.4 and 5.5 that the magnitude of variance within the spectral bands changes over the growing season and, thus, the composition of PCs changes. This means, that the wavebands with the highest loadings for a particular PC do not necessarily remain amongst the ten wavelengths with greatest loadings for the respective PC of a dataset from another phenological stage.

For the subsequent image analysis, it is important to understand which image ratios may entail the best separability between the two infection classes that could potentially be also used in the composition of VIs. Therefore, PCs and their respective scores, that are the coordinates of projected data points in principal component space (Kucheryavskiy, 2020) were plotted against each other. For this purpose, the first five PCs from the data subset were used as more than 98% of the total variance is concentrated here. It was found that the two classes can actually be visually separated in principal component space, whereas the combination of PCs varies again in order to achieve good visual separability. For the second field campaign in May the combination of PC 4 with PC 1 allowed a good visual separability, whereas for the third and fourth field campaigns (in June and July, respectively) it was the combination of PC 5 and PC 1 (Fig. 5.6).

Regarding the feature selection for the narrowband VIs, the wavelengths with highest loadings for the respective PCs roughly correspond to the Rikola hyperspectral camera's wavebands 10, 13 and 16. Especially, the latter two were used for computing a Fluorescence ratio (690 nm / 735 nm)[1]. The narrowband VI referred to in the previous chapter (Table 4.4) – NDVI (705 nm), PRI, ARI2, GM1, GM2 and ZTM – were also computed, trying to come as close as possible to the ideal wavelengths (Table 5.3).

[1] https://www.indexdatabase.de/db/i-single.php?id=313

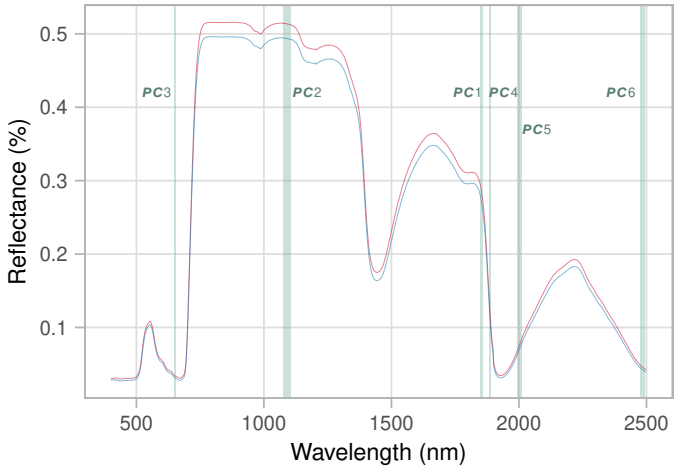

(a) 2nd field campaign (May)

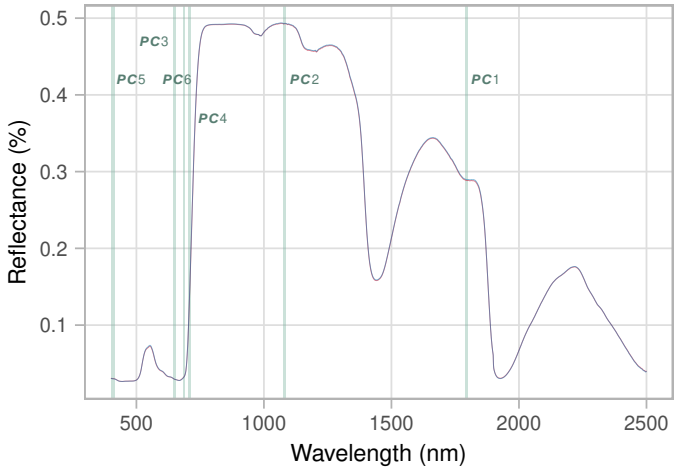

(b) 3rd field campaign (June)

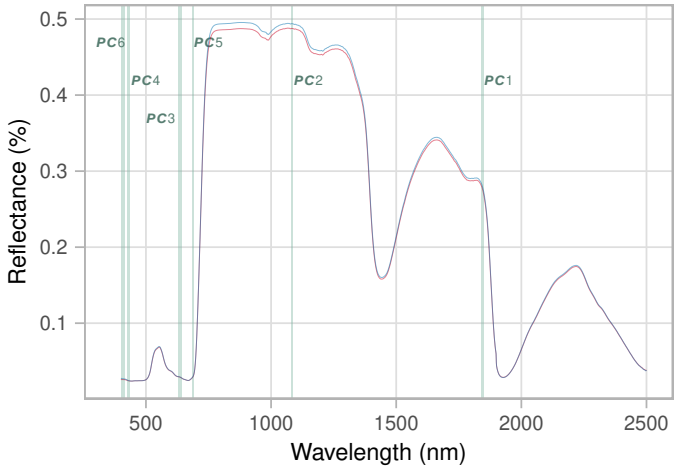

(c) 4th field campaign (July)

Figure 5.4: Mean leaf spectral signatures by infection status and highlighted relevant spectral bands from the PCA

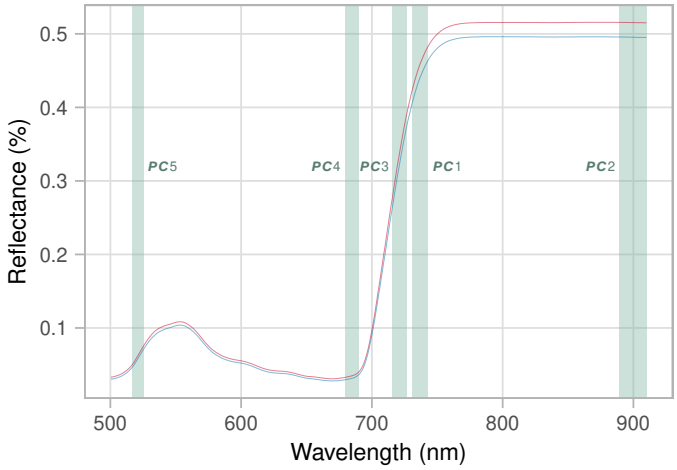

(a) 2nd field campaign (May)

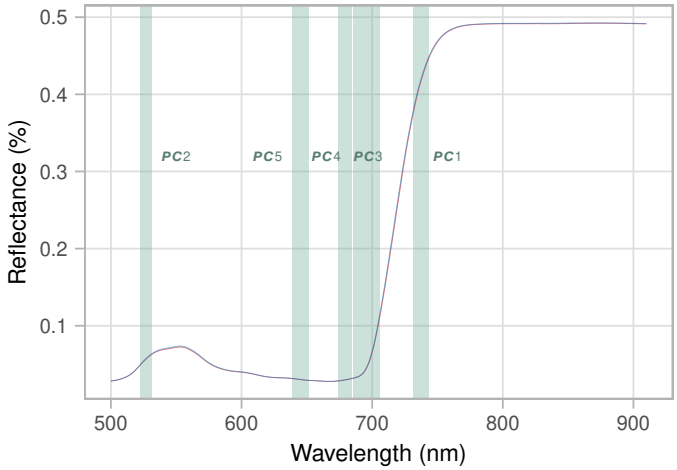

(b) 3rd field campaign (June)

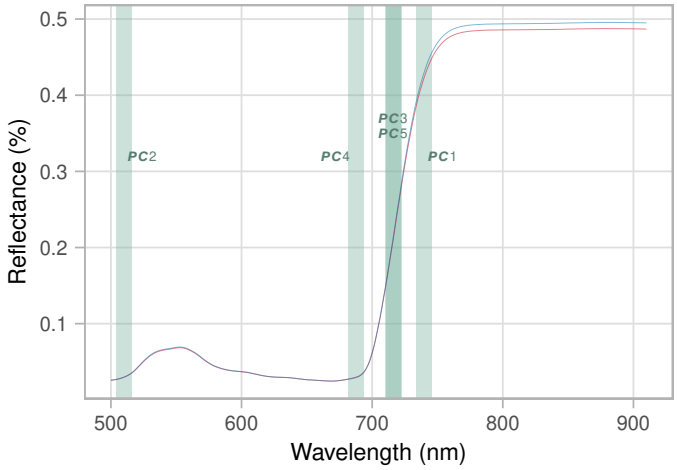

(c) 4th field campaign (July)

Figure 5.5: Mean leaf spectral signatures by infection status and highlighted spectral wavebands from the PCA within the detection window of the hyperspectral camera

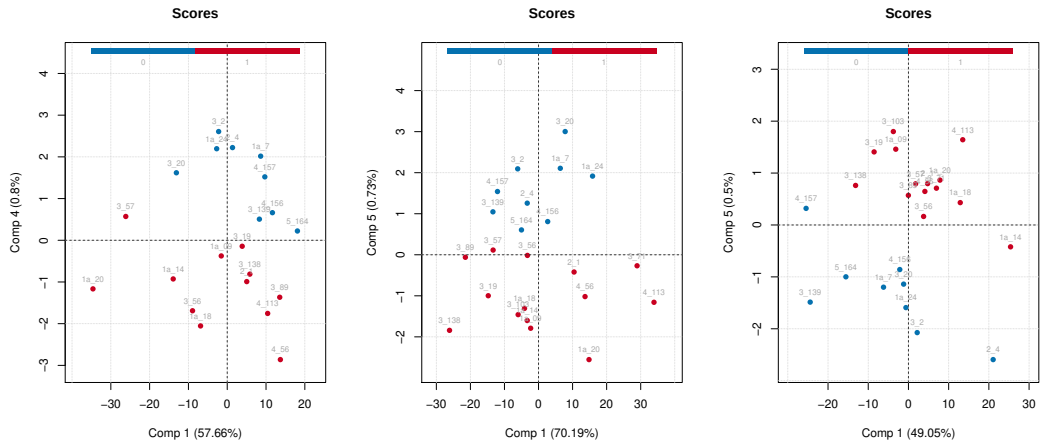

(a) 2nd field campaign (May) (b) 3rd field campaign (June) (c) 4th field campaign (July)

Figure 5.6: PCA - Score plots for good visual separability of infection groups

Unfortunately, the bands from the hyperspectral camera do not correspond to the ideal wavebands needed for the VI. Consequently, it is a challenge to reproduce exactly the same ratios and therefore highlight spectral differences to the same extend as what has been described in the scientific literature. As a result, it remains difficult to judge and quantify VI classification performance.

Additionally, the spectral ratios also suffer from the influence of the black hail net causing spectral distortions in all bands which adds to the difficulty in quantifying classification performance.

Based on visual interpretation, though, the ZTM seemed a good indicator for slight nuances in chlorophyll content between infected and uninfected trees. This would definitely need to be evaluated quantitatively, how well the ZTM corresponds to areas classified as AP infected.

Rikola Waveband	Wavelength (in nm)	fwhm (in nm)	Ideal wavelength used for VI (in nm)	2nd campaign	3rd campaign	4th campaign
1	506.285	9.84				PC2
2	521.498	14.62		PC5	PC2	PC2
3	536.468	11.51	531		PC2	
4	551.474	10.06	550			
5	566.249	9.76	570			
6	581.498	14.01				
7	596.211	12.53				
8	611.086	17.53				
9	625.943	16.4				
10	645.258	12.74			**PC5**	
11	656.031	12.85				
12	671.165	16.08			PC3	
13	686.279	15.14		**PC4**	PC3/4	PC4
14	701.45	11.25	700		PC4	
15	716.158	11.92	710	PC3		**PC5**
16	731.318	10.53		**PC1**	**PC1**	**PC1**
17	746.096	10.27	750			**PC1**
18	761.157	15.64				
19	776.245	13.97				
20	791.462	12.81				
21	806.339	14.67	800			
22	820.873	15.0				
23	835.804	21.04				
24	850.597	25.85				
25	866.602	24.49				
26	881.009	20.16		PC2		
27	896.406	22.87		PC2		

Table 5.3: Tabular overview of matching Rikola wavelengths and PCs' wavelengths for VI composition

5.3. RO/RQ-3

Research objective 3 and the respective question were formulated as follows:

RO.3 Implement a robust and reproducible image classification procedure based on a machine learning approach specifically for the identification of AP on varying levels of detail (at the leaf, tree, and orchard level).

RQ.3 Which machine learning approach produces a robust multi-/ hyperspectral image classification for identifying and classifying AP on different scales (leaf, tree and orchard)?

Unfortunately, this research objective was not met in the scope of this research and the respective question remains unanswered. Prior to the commencement of the field collection, one was not aware of the orchard practices during the fruit growing season which in the region of South Tyrol commonly includes the use of a black hail net. As has been shown through the irradiance sphere the black hail net adds to increased reflectance, thus making

it impossible to capture the spectral signatures from the leaf surfaces that are needed for a supervised classification method. As can be seen from the orthophotos in the precision map, a lot of noise is being introduced to the image including blurring effects.

This shows, in retrospect, that this research goal was highly dependent on controls out of the author's reach of influence. This may also demonstrate that working under field conditions with a real-life dataset seems more challenging than working under laboratory conditions as there are some unknown controls that can have an impact on the research. Nonetheless, the findings from the principal component analysis of the hyperspectral dataset collected with the spectroradiometer serve as a starting point for follow on research and classification of in-field collected UAV imagery for AP identification and detection.

5.4. RO/RQ-4

Despite not being able to use the UAV imagery to apply a machine learning classification for the detection of AP, research objective 4 was not compromised and aims at the following:

RO.4 Establish a mapping technique to produce precision maps dedicated to AP on different levels of detail.

RQ.4 How can multi-scale data be effectively visualised on various granularity levels?

When reading the research question carefully, the focus is rather on the map making itself, allowing a certain flexibility and independence from the outcome of the image classification regarding AP. Of course, it would have been ideal to present a precision map on AP. However, the cartographic methodology developed in this thesis is considered at least as equally important, if not even higher. As already touched upon this aspect throughout the course of this thesis, contemporary precision mapping sees itself in a dichotomy between offering thematically classified, high-resolution imagery and the claim to be a map which justifies its *raison d'être* through cartographic generalisation of real-world objects. Thus, the design of a map concept for precision mapping is at the core of this research objective.

Following Shneiderman's (1996) visualisation mantra '*overview first, zoom and filter, then details on demand*', an interactive, multi-scale web map was implemented to allow layering of the classified high-detail imagery and generalised map features. Multi-scale mapping involves cartographic generalisation, which can be several generalisation techniques applied jointly to spatial information across supported scales (Roth et al., 2011). Cartographic generalisation techniques that were employed for map design include the segmentation of tree rows from the grassy alleys between tree rows, classification of the hyperspectral images, and ultimately applying a form of tessellation using the hexagon as regular graphical primitive to assimilate the tree canopy abstractly and aggregate pixel values within. The latter is similar to the concept of hexagonal binning, whereas, instead of using the density of typically vector point data, a statistical value was calculated from the pixel values within the respective hexagon.

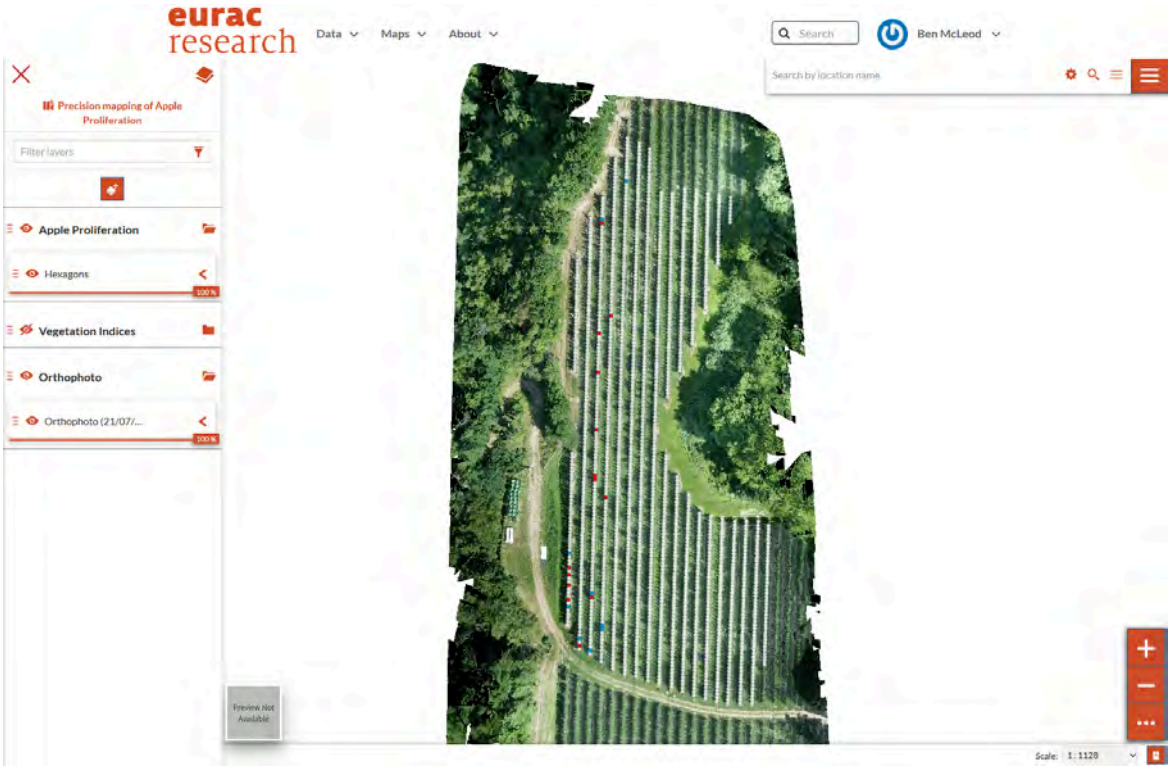

Figure 5.7: Overview of the precision map and the contained layer groups: Apple Proliferation, Vegetation Indices and Orthophotos

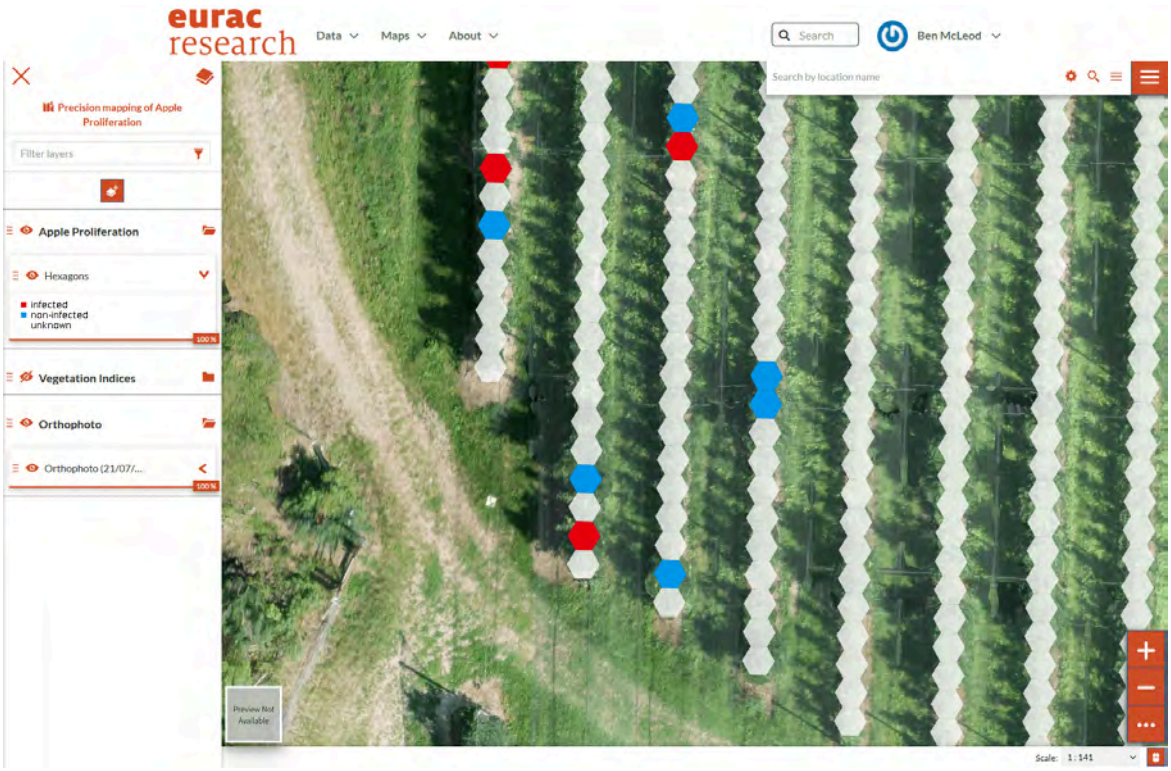

Figure 5.8: Spread of apple proliferation diseased trees visually abstracted as hexagonal cells

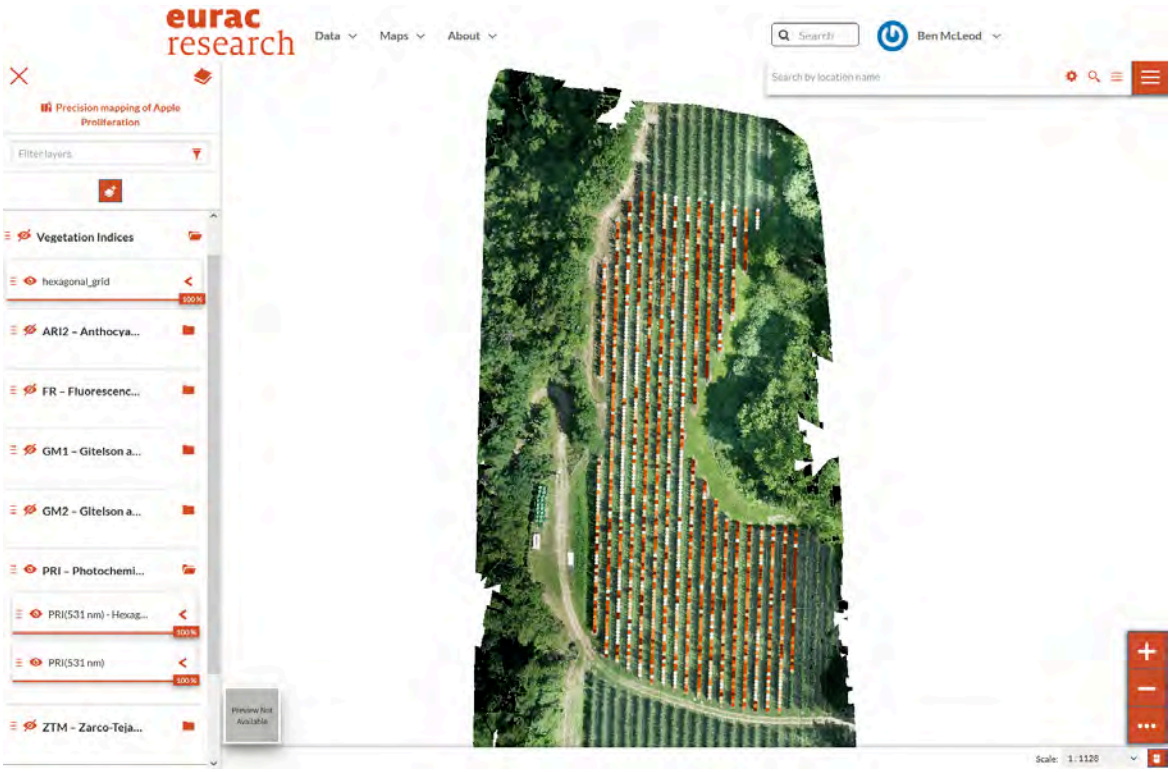

Figure 5.9: Hexagonal abstraction of PRI vegetation index layer – at small scale

Figure 5.10: Hexagonal abstraction of PRI vegetation index layer – zoomed in

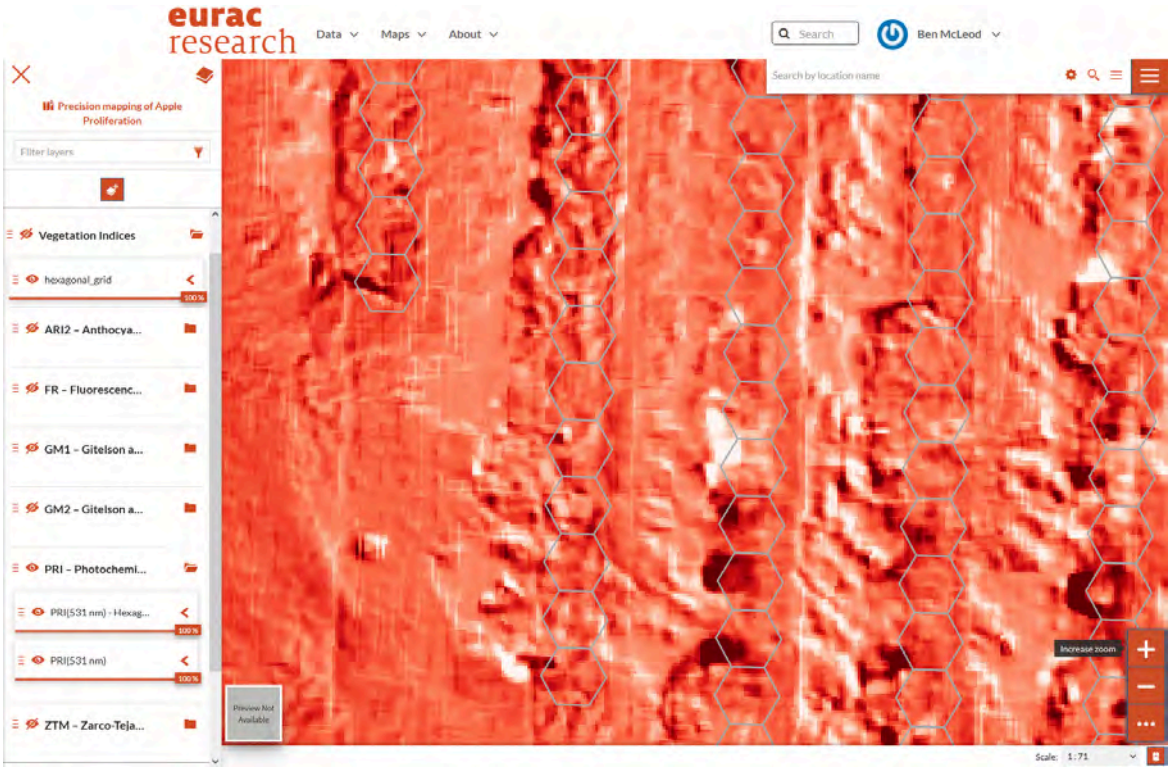

Figure 5.11: Full resolution of PRI vegetation index layer – at large scale

6 Discussion

6.1. Contextualising the Spectral Analysis

Spectral analysis of leaf reflectances constitutes a non-destructive approach to uncover phytoplasma-host interaction, as changes in spectral bands are closely linked to biochemical and biophysical alterations which can be inferred to impacts caused by phytoplasma. The findings from PCA indicate that spectral variance between AP infected and uninfected trees is not in a single wavelength or spectral range but that there are differences across several wavebands in the VIS, NIR and SWIR spectra. It can be argued that the reasons for the spectral differences are twofold. On the one side, it can be assumed that phytoplasma assimilates a wide range of nutrients and organic compounds from the host cells (Janik et al., 2020). As a result of phytoplasma infestation, the host metabolism is impacted, which is partially expressed through symptoms that indicate a disturbance of hormone balance, disorders in the phloem function and/or altered content of the phloem sap (Lee et al., 2000). On the other side, Curran (1989) points out that chemical compositions are highly interconnected. Thus, a high correlation between reflectance and chemical concentration in one waveband may not be reasoned by single chemical bonds but a strong intercorrelation between several chemicals. As an example Curran (1989) refers to the starch concentration being often correlated with reflectance at around 660 nm, as starch concentration is correlated with chlorophyll concentration, the latter strongly absorbing in this spectral region.

Particularly in the VIS electromagnetic spectrum, photochemical pigments, such as chlorophylls, carotenoids and anthocyanins, account for strong light absorption (Blackburn, 1998; Peñuelas and Filella, 1998). According to Blackburn (2006), those wavelengths with high absorption are sensitive to lower pigment concentrations. In other words, it is assumed that wavelengths where high pigment concentrations result in high absorption are more sensitive to low pigment concentrations. Consequently, spectral differences between uninfected and infected plants, are expected to be more apparent in these wavelengths, as photochemical pigment concentration is lowered as a reaction to phytoplasma infestation.

For instance, Chlorophyll a+b absorption bands are said to be correlated to the wavelengths at 430 and 450 nm and at 700 and 630 nm, respectively (Blackburn, 1998; Sims and Gamon, 2002). Additionally, Peñuelas and Filella (1998) suggests that chlorophyll concentrations can be derived at 675 nm (where maximum absorption occurs and thus sensitive to reflectances even at very low concentrations) and at 550 nm (where reflectance sensitivity is higher for medium-to-high chlorophyll concentrations). Blackburn (1998) also argues for optimal individual wavebands for pigment estimation at 680 nm for chlorophyll a, 635 nm for chlorophyll b, and 470 nm for the carotenoids. Peñuelas and Filella (1998) suggest 430 to 445 nm wavelengths for carotenoids to be used for physiological reflectance indices. Anthocyanin absorption is supposed to be pronounced at 550 nm wavelength (Gitelson et al., 2001). When looking at the spectral wavebands that contributed with their high loadings to the composition of PC, one can see that PCA highlighted some of these wavebands, which are typically characterised by high photochemical pigment concentrations (Table 6.1).

The colouration of the above table cells is to be understood as an indication that these

Entire Dataset (400–2500 nm)			
Field Campaign	2nd	3rd	4th
Month	May	June	July
PC1	1850–1859	1788–1799	1839–1847
PC2	1077–1105	1077–1086	1079–1085
PC3	645–654	645–655	630–645
PC4	554–563	702–711	426–435
PC5	1884–1890	400–413	683–690
	1393–1398		
Rikola Detection Window (500–900 nm)			
PC1	731–743	731–743	734–746
PC2	889–910	522–531	504–516
PC3	716–727	674–686	710–722
PC4	680–690	684–706	682–694
PC5	517–526	639–652	694–706
	Legend:	chlorophyll a	chlorophyll b

Table 6.1: Relation of photochemical wavebands (chlorophyll a and chlorophyll b) to spectral bands from PCA

ranges of spectral wavelengths pick up differences in the respective photochemical pigments. It is to be read with a certain caution, as this study did not evaluate the chemical concentrations of the pigments in the leaves to clearly relate the concentrations to the difference in spectra between AP infected and uninfected trees. However, other studies on phytoplasma-induced plant disease have found similar spectral patterns, relating the spectral bands to impacts and thus the presence of phytoplasma in leaves. Negro et al. (2020) found out in their study on the plant disease *Bois Noir* that the chlorophyll content and partially the carotenoid decreased in infested leaves due to the phytoplasma. More specifically on AP, Barthel et al. (2021) proves a downregulation of chlorophyll in infested leaves. As a result of chlorophyll reduction, photosynthetic activity decreases as well (Bertamini et al., 2003), which is also indicated by the PCA in this study. Specifically, in the data subset covering the spectra of the hyperspectral camera detection window, the first PC relates to spectral bands that indicate chlorophyll fluorescence, which closely relates to photosynthetic activity. The spectral range at around 735 nm is the end of rapid change in slope in the red edge area and, therefore, a sensitive range to vegetation stress and dynamics[1]. According to Lichtenthaler and Rinderle (1988), the chlorophyll fluorescence intensity has its maxima near 690 and 735 nm. Therefore, an increase in the ratio 690/735 nm increases as leaf chlorophyll content begins to decrease.

Contrary to the drop in chlorophyll content in phytoplasma infected leaves, contents of soluble sugars, starch, and total saccharides significantly increased (Negro et al., 2020; Barthel et al., 2021).

[1] https://www.indexdatabase.de/db/i-single.php?id=537

Al-Saddik et al. (2018) discovered in their study on *Flavescence dorée* that with a rise in infestation level, the spectral signature increased in the VIS region, whereas it decreased in the NIR region.

Additionally, Barthel et al. (2021) linked in their spectroscopic analysis of AP infected leaves a strong relation between AP infection to differences in cellulose content. Phytoplasmas are considered to affect cellulose which is one of the most abundant structural carbohydrates in plants (McFarlane et al., 2014), strengthens the cell wall, and acts as a protective layer against water loss (Sieber et al., 2000). Downregulation of cellulose synthesis weakens the cell walls and facilitates phytoplasma entry (Kalluri et al., 2016).

Particularly, the first PC of the entire dataset indicates greatest spectral differences between uninfected and AP infected leaves in the NIR and SWIR. Especially the bands around 1820 nm correlated to cellulose as well as 1780 nm, which is also related to sugar. The second PCs are potentially more related to changes in oils or lignin in infected leaves. According to Curran (1989), the plant contained oils correlated well to 1040 nm and lignin to 1120 nm. For example, Negro et al. (2020) found out that in *Bois noir*-positive leaves lignin content decreased.

Furthermore, Negro et al. (2020) observed that anthocyanin and carotenoid concentration also decreased through phytoplasma infestation. The PCA did not indicate though spectral bands that correlated to the anthocyanin and carotenoid concentration that would indicate the spectral difference between the two infection statuses. However, this means that those expected changes may still occur but where perhaps smaller compared to the changes in cellulose or chlorophyll content. Additionally, changes in anthocyanin and carotenoid concentrations may also be more evident at a later phenological stage, when the discolouring is more pronounced in September and October.

6.2. Hyperspectral Imaging for AP Detection

Generally, spectral analysis enables identifying spectral differences in leaf spectral signatures of diseased plants, which can be related to phytoplasma-induced changes. Hence, spectral analysis lays the foundation for developing an early and reproducible in-field detection, follow-on image classification, and, lastly, the mapping of plant diseases, such as AP.

Commonly, biological tests have been used that allow laboratory and even in-field analysis of leave samples to test for the presence of phytoplasma(Al-Saddik et al., 2018). However, biological testing in the laboratory has its limitations, as it implies labour and time-intensive sample preparation (collection and extraction) and therefore adopts a 'destructive' or invasive approach by plucking leaves as sampling data. In-field testing methods definitely enable real-time results at the sampling cite but seem both impractical and expensive in larger fields (Al-Saddik et al., 2018). Despite having revolutionised the identification and quantification of pathogens, they are considered as incapable of detecting early stages of disease development.

Hence, there is a keen interest in the agricultural sector to replace this manual process with more automated and sensitive approaches (Lowe et al., 2017). Remote sensing has therefore proved itself useful at assessing the physiological state of a plant in respect to plant stress and disease manifestation (Peñuelas and Filella, 1998; Wegmann et al., 2016).

Generally, phytoplasma infestation causes a reduction in the concentration of photosynthetic pigments, which leads to a reduction of the photosynthetic activity (Peñuelas & Filella, 1998). However, broadband multispectral imagery is less suitable for remote sensing of phytoplasma-related impact on photochemical pigment composition in diseased plants. Narrowband hyperspectral data can provide higher spectral resolution to analyse single wavelengths (Blackburn, 2006).

Subsequently, hyperspectral data bears the potential to design disease-specific spectral ratios (or VI) and can also be used for machine learning model training to facilitate image-based identification of diseased plants. The development of a AP-specific VI based on hyperspectral data seems very promising, as spectral ratios are fairly easy to compute (Yao et al., 2018) and would allow a fast understanding of the spatial variability of the disease from a disease monitoring point of view. A machine learning based model would prove very beneficial in terms of upscaling the classification algorithm to and applying the information gained from hyperspectral data also to other orchards for disease detection. Both, the development of a AP-specific VI and machine learning classifications are considered as paths for future research.

6.3. Precision Mapping

Due to recent technological advancements, UAVs have not only become a presence in everyday life (Klauser & Pedrozo, 2015) but also find popular use for agricultural applications, such as for precision agriculture.

Despite being targeted for the mass market, UAV-based mapping for taking aerial imagery still remains subject to accessibility, affordability, and ultimately, feasibility. In terms of making UAVs more accessible, the aim is to increase the efficiency of UAV-based mapping at the lowest possible cost, where *cost* refers to the overall effort (financial, technical, bureaucratic) borne to successfully deploy UAVs in the field (Casagrande & Gusto, 2017). Hence the feasibility, or viability of UAV-based precision mapping in the field, largely depends on the field deployability. The latter largely depends on (a) the make-up of the UAV allowing immediate availability, use, portability and extensibility; (b) the operator's ease in setting up and flying the UAV on-site; and (c) regulatory and technical aspects, such as the qualification for pilots (flying licence), required authorisation for performing flights and validation for the respective UAV (Casagrande & Gusto, 2017). It is important to be aware of these aspects, as a drone can also become an unpredictable cause of damage in case of failure or interference with the flight control system. The potential danger of a UAV is implied by its weight, payload, material and the surrounding environment, which is why certain regulations are involved in the flying of UAVs ensuring human and environmental safety.

Legitimately, the question arises whether UAV-based precision mapping is an adequate tool for plant disease monitoring? Particularly, when looking at the financial costs UAVs imply and when dealing with plant diseases, especially the challenge in dealing with the dimensionality and complexity of hyperspectral aerial imagery (Albetis et al., 2017). In a recent article published by the German newspaper ZEIT ONLINE, the author made a thought-provoking comment regarding the use of UAVs for sustainable agriculture, especially in regions that do suffer immensely from crop losses but where the people, that are living of the land, not even access to electricity (Grefe, 2021). On the other hand, Nebiker et al. (2016) argues that high-resolution aerial images may replace ground inspections of farmlands in the near fu-

ture. Notably, small UAVs have become popular as they show great potential for acquiring reliable and detailed bi- and tridimensional data, which are essential in spatial reconstruction and mapping (Casagrande, 2017).

Furthermore, precision approaches would result in the reduction of pesticides and herbicides usage, with subsequent beneficial impact for the environment, ecosystem services, grower finances and the end consumer (Lowe et al., 2017). Deploying remote sensing techniques for plant disease identification could also improve our knowledge of the amount of pest- and pathogen-induced damage, and thus prevent excessive use of chemical controls (Peñuelas et al., 1994).

Klauser and Pedrozo (2015) argue that a deep reflection on the increased use of UAVs and the arising political implications is increasingly urgent, though. Sandbrook (2015), for instance, describes UAVs as relatively affordable, safe and powerful tools, whereas their use compatible with the regulations and their overall perception are not obvious. The social implications of using UAVs are not fully understood but one can assume that a negative social perception could severely affect their use and should be carefully avoided. A negative perception may possibly be rooted in the origins of UAVs as they derived from military ancestors (Birtchnell and Gibson, 2015 cited by Casagrande and Gusto, 2017). Hence, the word *drone* is consciously avoided throughout the course of the thesis to differentiate and not cause false misperceptions in the underlying intentions of using UAVs.

Moreover, Tsouvalis et al. (2000) address in their study the farmer's experience and perception of precision farming techniques for yield mapping in the English counties of Lincolnshire and Suffolk, at a time when this technology was newly introduced in agriculture. Although it becomes fairly clear in the course of the argumentation that the authors adopt a certain stance in supporting the local farmers by victimizing them, one needs to be aware of competing knowledge cultures, especially when technological-based knowledge, gains an institutionalised stance overruling farmer's knowledge. Despite Tsouvalis et al. (2000) very dual portrayal of farmer's participation – basically none, apart from a few exceptions, where farmers were more technology oriented – in precision mapping processes, the author emphasizes the suppression of already exiting farmer's knowledge by scientific knowledge imposed, reinforcing the image of the otherness of non-scientific forms of understanding (Harvey, 1997 cited by Tsouvalis et al., 2000). As a consequence, farmers redefined their identities in response to technological change and rather taking a rejecting stance towards precision farming and viewing it as impractical. This sense of disapproval grew consequently when the farmers felt to be more dependent on technicians in order to implement the technologies. One of the farmers was saying that '*if you have to rely on this technology you're not a good farmer*', clearly referring to decision-making increasingly being based on virtual representations of reality. Furthermore, and of immense importance from a cartographic point of view, is the challenge in interpreting the yield maps that were produced for the farmers back then. In order to design effective precision maps, user needs and requirements need to be assessed, and the map content visually displayed to the users' abilities.

Additionally, the map users, who are intended to be mainly the farmers themselves, should be ideally involved in the precision map-making process. In their study, Tsouvalis et al. (2000) got positive feedback when farmers were included in the process of knowledge sharing and the development of the technology tailored to their needs. Consequently, offering either a participatory approach or giving the farmers more stewardship in the precision map-

making process would win greater acceptance for the use of technological innovations in their daily spatial decision making in the field, instead of imposing a system that seems to be plausible from a scientific viewpoint.

According to Tsouvalis et al. (2000) map illiteracy seemed to be a major challenge, which is why cartography can bridge the gap between cognition of space and a meaningful visual representation of exactly the same place. Applying cartographic principles in precision map-making enables the reduction of spatial data to the most relevant information, which, in turn, reduces cognitive load, and, consequently, facilitates communicating the essential visually to the map user. Principally, the aspect of cartographic generalisation has, however, received very little attention in existing precision map making. The here proposed definition of a precision map being *sensor-driven, interactive, thematic map that offers different degrees of granularity at multiple scales* aims at highlighting the increased need for scale dependent map display. A multi-scale mapping implies the adoption of cartographic generalisation techniques at various supported scales (Roth et al., 2011), allowing the visual display of different spatial granularities. By applying cartographic generalisation, according to Robinson et al. (1995), the map maker takes the decision, how much detail to display at the chosen scale and finding a balance between reducing the amount of information and maintaining the essential geographical characteristics of the mapped phenomena.

In this thesis, an object-oriented classification was suggested to map the infection status of apple trees across the orchard. The hexagon was chosen to abstract the tree's canopy shape and use the graphical primitive to aggregate the classification results from the hyperspectral imagery. According to Carr et al. (1992), the hexagon has several advantages over using squares for binning a 2D surface – strictly speaking, hexagonal binning is slightly different from the approach followed in this thesis, though, as hexagonal binning plots density, rather than raster values. Nevertheless, hexagons are more similar to a circle than a square and may seem to resemble the canopy shape more naturally than a quadrilateral cell. However, using a hexagonal shape for abstracting trees, might not work for a farmer as the intended map user, though. This would need to be assessed in map use related studies.

According to Robinson et al. (2017), that is exactly the challenge, transforming 'raw' data into insights and meaningful information in the future, and not a possible lack of geospatial data. It is cartography though, so they argue, that can play an important role in overcoming this hurdle.

6.4. Agriculture 4.0 in South Tyrol

Adopting cartographic approaches in agriculture may also prove itself advantageous not only in the sense of cartographic generalisation but in the exchange and sharing of geospatial data and services among stakeholders, which is facilitated by SDIs (Hjelmager et al., 2008). According to Nebert (2004), a SDI comprises of policies, technologies, standards, and human resources needed for an effective collection, management, access, delivery and utilisation of geospatial data for a specific community. Rooted in the principles of open data and knowledge, an open SDI aims at making spatial data available to anyone without restrictions to rights of access or use (Coetzee et al., 2020). Following open standards, such as the provision of metadata, and by adopting FAIR principles, establishes greater transparency and strengthens the collaboration between stakeholders. Coupling a SDI with plant disease monitoring on a regional level may prove beneficial for an effective collaboration between

stakeholders from science, technology and local agriculture joining regional forces in tackling plant disease spread, and at the same time, bearing a huge participatory potential for local stewardship of farmers.

As the case study of AP in South Tyrol shows, phytoplasma is not restricted to administrative borders, which is why the use of a SDI for regional plant disease management would seem favourable for all involved stakeholders. This said, South Tyrol is also an exceptional example in terms of agriculture and the formation of unions. The agricultural area of South Tyrol totals 455,840 ha, which is almost 62% of the national territory, whereas only around 28% of the land (an area of around 209,232 ha) is used as cultivated land, meadows and pastures due to the steepness of the terrain (Tappeiner et al., 2020).

95% of the apple-growing area is used for the cultivation of only ten different apple varieties. This fairly monocultural apple growing underlines the agricultural value for the region as it is very much export-oriented, including wine and milk. In turn, South Tyrol's agriculture depends on the import of fertilisers and fodder, which highlights the region's dependency on the world economic situation. In order to be more resilient towards the volatility of market prices for agricultural commodities, protective measures were taken by founding a worldwide unique cooperative system, which is basically a union of farmers and producers to gain more negotiating power (Tappeiner et al., 2020).

Furthermore, farmers in South Tyrol have formed, for instance, an association called the *Maschienenring* (*eng.* machinery ring), which is an institution to facilitate the inter-farm use of machinery and services amongst members, as purchase and maintenance of machinery is very costly (Tappeiner et al., 2020).

Additionally, there is a high degree of parcelling in South Tyrol, meaning that the agricultural land is divided by many farmers and split into several private plantations and orchards. This may also be viewed as an argument that speaks in favour of developing a SDI as an umbrella platform for the exchange of agricultural geoinformation, such as spatial patterns of plant diseases, for the whole region. By means of implementing technologies in agriculture, it is expected to also lower production costs, which in mountain agriculture are mainly driven up by topographical challenges, such as the difficult terrain with steep slopes and few usable areas as well as the remoteness and accessibility of certain orchards. These technologies, however, require cooperative solutions in order to contribute to safety and ease of work (Tappeiner et al., 2020).

South Tyrol's vision of a sustainable agriculture 4.0 promotes the implementation of innovations, both technological and entrepreneurial (Zebisch et al., 2018), which require (a) the provision of financial subsidies creating incentives to acquire new technologies; (b) an investment into complementary training (in terms of operating these technologies); and (c) the offer of advisory services regarding sustainable agriculture (Zebisch et al., 2018; Tappeiner et al., 2020). On the other side of the production chain, it is also important to sensitise the consumers about agricultural sustainability, as consumerism has its fair share in defining the future of agriculture.

In terms of plant disease management, investing in new technologies poses a financial hurdle without a doubt. However, these technologies can possibly exert a positive long-term impact, as early detection of infected trees offers early scope for action, thus, reducing production costs, which are again lowered through the reduced use of large-scale pesticide

spraying (Tappeiner et al., 2020).

Yes, crop protection is important to ensure future food supplies but at what price? Future agriculture needs to drastically reduce the use of pesticides and fertilisers, become more climate-neutral and promote biodiversity (Tappeiner et al., 2020).

Sustainable agriculture must protect and preserve land, water, climate and genetic resources for future generations, ensure the health and welfare of all livestock, produce high-quality agricultural products, be economically viable and socially acceptable (Tappeiner et al., 2020). Thus, the SDGs need to be pursued in conjunction, as, for instance, ensuring food security cannot be realised only by implementing innovative technologies to end hunger, but the human footprint on natural resources, the contribution to greenhouse gases and, ultimately, adaptation to climate change need to be addressed simultaneously. Thus, expectations towards sustainable agriculture are high, but the need for change outweighs it. And implementing innovative strategies is part of steering towards sustainability.

Cartography bears the potential through precision maps that are already embedded in precision agriculture to foster the use of sensing systems and integrate maps into spatial decision making, particularly for plant disease control and plant health monitoring. Precision farming that employs cartographic principles in map making can prove efficient in minimizing crop losses and ensure food supplies. This requires knowledge sharing, adequate training as well as collaborative or participatory mapping approaches to empower farmers, who are willing and use the technology to deploy these themselves. Furthermore, Hjelmager et al. (2008) identified that by organising spatial data across disciplines and organisations, SDIs meet the need to create multi-participant, decision-supported environments in order to address the issues of sustainable development and improving quality of life.

'*Yet in the end, sustainable development is not a fixed state of harmony, but rather a process of change in which the exploitation of resources, the direction of investments, the orientation of technological development, and institutional change are made consistent with future as well as present needs. We do not pretend that the process is easy or straightforward. Painful choices have to be made. Thus, in the final analysis, sustainable development must rest on political will.*' (UNWCED, 1987)

7 Limitations and Paths of Future Research

In hindsight, it is definitely easier to point out certain risks or indicate shortcomings that one was not aware of when beginning to work on the thesis. In the following sections, an overview shall be given, briefly describing limitations encountered during the thesis work and suggesting possible paths for future research:

Data Collection

Early disease detection

- Further research is necessary to find an optimal time period for deploying an early disease detection in the field. Yuan et al. (2013), for instance, conducted a multi-temporal study, comparing classification results of data acquired at an early disease stage with data obtained at a later, more developed disease manifestation. Classification results imply that detecting plant diseases at a later stage achieved higher accuracy and thus seemed more reliable.
- Albetis et al. (2017) outdoor temperature is assumed to have an effect on the leaf spectral signatures, which implies that in-field detection may be biased as leaf spectral signatures are affected by environmental temperature, which typically increases during the growing season. Thus, comparability of leaf spectral signatures of different phenological stages need to aware of temperature influence.
- This also includes diurnal changes in the spectral signature, as the photosynthetic activity and thus the leaf metabolism varies across the day. How great is the impact of diurnal changes on the '*general*' leaf spectral signature?
- So far this thesis indicates that there are detectable spectral differences in May (at a fairly early phenological stage). At which phenological stage would it be technically possible and feasible to identify AP-induced spectral differences early in the field?

Instrument operability

- Instrument warm-up time and sampling logistics (spectroradiometer)
  - For optimal performance, SVC (2012) recommends switching on the spectroradiometer and leave the device running for approximately 15 minutes before commencing with the sampling

    '*During this period, the instrument should be placed in the environment where scanning will take place. This period allows the detector temperatures and other electronics to stabilize before taking spectral data.*' (SVC, 2012, p.51)
  - Al-Saddik et al. (2018) for instance allowed the spectroradiometer used in their study to warm up at least for 20 minutes prior to sampling to exclude any bias on the spectral signatures, potentially caused by the instrument itself

- The durability of LI-Ion batteries is seen as a limitation, although theoretically they are originally designed to provide over 3 hours operation following a full charge. However, to perform the sampling in one day with the spectroradiometer, three batteries were needed in total.
- As the spectroradiometer recorded an internal temperature of around 50°C under hot outdoor conditions in July, one cannot exclude necessarily an impact of the instrument's internal temperature on the sampled spectral signatures. There might be an influence.

Operating the UAV

- In terms of reproducibility of the methodological framework suggested in this thesis, the mayor hurdle seemed to be the operation of a UAV, which
  a) relies on optimal flying conditions, which might pose a challenge especially in mountain environments.
  b) a flying licences and equally important the financial budget for acquiring a UAV

Orchard activities and black hail nets

- Field campaigns were not only restricted by the weather conditions but also by the ongoing orchard management, such as spraying, that limited accessibility of the orchard for taking measurements on certain days
- Black hail net:
  - The annual estimates of the Hail Protection Consortium (*de.* Hagelschutzkonsortium) in South Tyrol do not indicate any significant increase in area affected by hail during 1981–2017. With climate change and rising temperatures, it is expected, though, that hail events become more intense. Consequently, hail nets are increasingly used in both fruit growing and viticulture (Zebisch et al., 2018)
  - The hail net was a major drawback for the purpose of this thesis, as the aerial UAV-based imagery of orchards was affected by the filtering effect of the net and distorts the spectral information below.
  - Perhaps it would be possible to model the spectral characteristics of the hail net in order to use a model-based approach for processing and diminishing or totally eliminating the filtering effect. This may seem a fairly complex task as the hail net does not appear as a flat surface with homogenous absorption features in the aerial images.
  - Deploying a ground-sensing approach using multi- and hyperspectral camera sensors either on a tripod, orchard vehicles in motion, or install permanent field sensors, covering all the vegetation periods would be an alternative approach.
    - Bendel et al. (2020), for instance, suggest a tractor-mounted system as a suitable method in viticulture since data could be collected in parallel to fieldwork.

  - Deery et al. (2014), describe proximal remote sensing buggies for field-based phenotyping.
- As Bock et al. (2020) already highlighted, crop motion due to wind can be a limiting issue though during ground and proximal sensing in the field.

Plant disease characteristics

- Upper leaves in a canopy may have different phytoplasma concentrations and therefore also show varying levels of symptom expression than lower parts of the crop stand. Consequently, there might also be a bias in scaling the findings from the ground to the airborne sensing approach, also bearing in mind that phytoplasma concentrations vary in the canopy throughout the year.
- Mixed infection, a plant suffering of multiple stress factors. Thus, the need to develop and deploy disease-specific camera sensors in the field to detect changes in specific spectral wavebands, particularly in the NIR and SWIR that can be related to specific phytoplasma-induced diseases

Data Processing

- According to Blackburn (2006), the maturation of sensor technology and growing operational deployment of ground-based, airborne and spaceborne instruments will greatly enhance the capabilities for routinely acquiring hyperspectral data and potentially, for quantifying plant pigments over a wide range of spatial scales.
- Therefore, scalability of data, which require standard conform data formats, will receive more attention in geospatial science than it already has, particularly for map development and spatial analysis
- Hence, Open standards will need to be increasingly adopted and further developed.
- The processing, analysis and visualisation of hyperspectral data will also gain further momentum when adopting data cubes in automatising plant disease identification and detection (for instance using rasdaman[1] or opendatacube[2])
  a) for real time,
  b) cloud-based, and/or
  c) cartographic web-map services

Data Analysis

Range of the electromagnetic spectrum used for analysis

- Similarly to Al-Saddik et al. (2018), the spectral range below 400 nm was not considered in the spectral analysis, due to high noise within the UV range. Additionally, the region outside of the Rikola hyperspectral camera, so below 500 nm would be interesting to include in the analysis in respect to photochemical pigments, such as anthocyanins and carotenoids.

[1] https://www.rasdaman.com/
[2] https://www.opendatacube.org/

Multi-class Classification

- Applying a multi-class classification instead of a binary classification (i.e. uninfected / infected), would be fascinating in terms of identifying latent trees and recovered trees from the other AP infected trees. Further, research and spectral analysis would be needed to investigate whether latent and/or recovered trees show different spectral properties from the AP infected and uninfected trees.
- Regarding the differentiation between recovered (and probably also latent trees) analysing the H_2O_2 accumulation within the plant as a defence mechanism against phytoplasma (Musetti et al., 2007) might be a first starting point for a multi-class classification or differentiation between symptomatic and symptomless plants
- Additionally, a multi-class classification could also be realised by mapping the severity of infection or visualising the likelihood of infection (i.e. uncertainty mapping)
- From a management perspective or a map user point of view, it would be interesting to know whether a multi-class classification would be meaningful, as it is imagined that a binary classification might be already sufficient, as the tree inevitably faces uprooting as soon as the infection is evident.

Disease specific VI

- Developing a AP specific VI would require further research activity and further testing of spectral ratios

Machine learning

- Entering deeper into the field of machine learning seems promising for developing a robust and reproducible model for image classification; this would require a comparison of different machine learning algorithms and evaluation of their classification performances

Data Visualisation

Data format

- Having touched upon data cubes as potential data formats for hyperspectral data analysis, this would also imply new opportunities in terms of data visualisation
  - Further testing and research on map interaction with data cubes would be promising as the data cube might become a more relevant data format in the future,
  - Further research is necessary on the visualisation of data cubes particularly in precision agriculture and for the development of precision maps,
    - With the focus on implementing multi-scale databases and their management for user interaction
    - These databases are also referred to as multi-resolution or multi-representation databases (MRDB) (Spaccapietra et al., 2000)

  - Meijers et al. (2020), for instance, suggest another format for web mapping using space-scale cube data for smooth user interaction

Cartographic generalisation

- Another aspect that was not addressed in this thesis is the Modifiable Areal Unit Problem (MAUP) which arises when data is aggregated spatially. It would be worthwhile investigating further to which extend MAUP occurs by choosing hexagons for aggregating the raster values

Map use

- User testing is definitely required in order to gain deeper insight into how particularly farmers perceive their orchard spatially, if and how a map could help their needs in spatial decision-making, and if a multiscale map is an effective visualisation approach in precision mapping
- Another feature that one could add to the visualisation would be the aspect of time, as several flights covering different phenological stages could be visualised and compared by implementing a time slider for instance; it would be interesting to analyse further the spectral variations in a phytoplasma-diseased tree over time
- Furthermore, it could be considered useful to provide ancillary information accompanying the web map in order to develop an interactive dashboard to the end-user

Data Sharing

Collaborative mapping in agriculture

- Further testing of the SDI and involvement of agricultural stakeholders in a precision mapping would be ideal in order to upscale the scope of the mapping effort from a single orchard to an entire region (potentially South Tyrol) and further improve the proposed methodological framework
- Additionally, the social perception of UAV-based precision mapping could be further investigated, as precision farming is commonly associated with intensive agriculture and less with organic, low or no chemical input farming – hence, precision mapping might be perceived as a means for mass production, which is not proposed here

8 Conclusion

This experimental research aimed at developing a cartographic understanding and a methodological framework for precision mapping. For this purpose, contemporary examples from different domains were reviewed with respect to their notion of and expectations towards a precision map. Despite the thematic amplitude in the drawn examples, precision mapping was closely related to sensor-based data acquisition, particularly to UAV-mapping and the classification of high-resolution imagery. However, map-making rests upon generalisation of spatial information, which is commonly overlooked in precision mapping. Hence, this study argues for adopting a multi-scale mapping approach in order to visualise different spatial granularities at respective levels of detail within a precision map.

Mapping is fundamental for spatial decision-making in agriculture and sets the basis for crop monitoring, including plant disease management. Plant pests endanger tree health and harvest, which is why an early disease detection is important in order to take adequate measures and minimise potential costs with further disease spread. As 'traditional' methods for plant disease detection, which include visual, in-field inspection of trees or biological testing either on-site or in the laboratory, are costly in terms of labour and time. Sensor-based methods, therefore, have become more attractive, as they allow a spectral analysis of different plant diseases, since plant pathogens cause biochemical and biophysical modifications, which can be identified from the leaf spectral signatures (Mahlein, 2016).

At the example of an AP infected orchard in South Tyrol, a non-invasive mapping method was established spanning the whole data lifecycle: adopting a ground and airborne, proximal sensing approach, hyperspectral data were collected on the leaf and orchard level. Relevant spectral bands were identified through PCA to differentiate between infected and uninfected leaves and the findings serve for future spectral analysis of AP and image classification deploying machine learning algorithms. Insights gained through the spectral data analysis served as the basis for the subsequent hyperspectral waveband selection and composition of adequate vegetation indices. A hexagonal grid structure, assimilating the tree rows, is used for cartographic generalisation of the image classifications as well as for the abstraction of the tree canopy shape by the individual hexagonal cell. Following Shneiderman's 1996 visualisation mantra '*Overview first, zoom and filter, then details-on-demand*', the multi-scale precision map is designed as a web map, which is embedded in the EDP, an open-source SDI geoportal maintained by Eurac Research's CSS. Understood as open science, this study follows the FAIR and open data principles and aims at making the data available for further reuse for future research.

This experimental study is expected to encourage future application of cartography in agriculture and foster cartographic understanding in precision mapping using multi- and hyperspectral data. Further research is required on the spectral analysis of AP, but also in terms of SDI-based collaborative mapping in the agricultural sector, as well as user-oriented precision mapping of plant diseases adopting multi-scale visualisations. The precision map is viewed as a cartographic tool that can be part of an environmentally sustainable disease and pest management programme with the potential to minimise yield losses and foster food security, if politically wanted and promoted.

Bibliography

Albetis, J., Duthoit, S., Guttler, F., Jacquin, A., Goulard, M., Poilvé, H., Féret, J.-B. & Dedieu, G. (2017). Detection of Flavescence dorée Grapevine Disease Using Unmanned Aerial Vehicle (UAV) Multispectral Imagery. *Remote Sensing*, *9*(4), 308. https://doi.org/10.3390/rs9040308

Al-Saddik, H., Simon, J. C. & Cointault, F. (2018). Assessment of the optimal spectral bands for designing a sensor for vineyard disease detection: the case of 'Flavescence dorée'. *Precision Agriculture*, *20*(2), 398–422. https://doi.org/10.1007/s11119-018-9594-1

Amici, A., Refatti, E., Osler, R. & Pellegrini, S. (1972). Corpi riferibili a micoplasmi in piante di melo affette dalla malattia degli scopazzi. *Rivista di Patologia Vegetale*, (8), 3–19.

Bache, S. M. & Wickham, H. (2020). *magrittr: A Forward-Pipe Operator for R* [R package version 2.0.1]. https://CRAN.R-project.org/package=magrittr

Baric, S., Berger, J., Cainelli, C., Kerschbamer, C., Letschka, T. & Via, J. D. (2010). Seasonal colonisation of apple trees by 'Candidatus Phytoplasma mali' revealed by a new quantitative TaqMan real-time PCR approach. *European Journal of Plant Pathology*, *129*(3), 455–467. https://doi.org/10.1007/s10658-010-9706-x

Baric, S., Kerschbamer, C., Vigl, J. & Via, J. D. (2007). Translocation of apple proliferation phytoplasma via natural root grafts – a case study. *European Journal of Plant Pathology*, *121*(2), 207–211. https://doi.org/10.1007/s10658-007-9256-z

Barker, D. H., Seaton, G. G. R. & Robinson, S. A. (1997). Internal and external photoprotection in developing leaves of the CAM plant Cotyledon orbiculata. *Plant, Cell and Environment*, *20*(5), 617–624. https://doi.org/10.1111/j.1365-3040.1997.00078.x

Barnes, C., Balzter, H., Barrett, K., Eddy, J., Milner, S. & Suárez, J. (2017). Individual Tree Crown Delineation from Airborne Laser Scanning for Diseased Larch Forest Stands. *Remote Sensing*, *9*(3), 231. https://doi.org/10.3390/rs9030231

Barthel, D., Dordevic, N., Fischnaller, S., Kerschbamer, C., Messner, M., Eisenstecken, D., Robatscher, P. & Janik, K. (2021). Detection of apple proliferation disease in Malus × domestica by near infrared reflectance analysis of leaves. *Spectrochimica Acta Part A: Molecular and Biomolecular Spectroscopy*, *263*, 120178. https://doi.org/10.1016/j.saa.2021.120178

Bendel, N., Backhaus, A., Kicherer, A., Köckerling, J., Maixner, M., Jarausch, B., Biancu, S., Klück, H.-C., Seiffert, U., Voegele, R. T. & Töpfer, R. (2020). Detection of Two Different Grapevine Yellows in Vitis vinifera Using Hyperspectral Imaging. *Remote Sensing*, *12*(24), 4151. https://doi.org/10.3390/rs12244151

Ben-Hur, A. & Weston, J. (2010). A User's Guide to Support Vector Machines. In O. Carugo & F. Eisenhaber (Eds.), *Data mining techniques for the life sciences* (pp. 223–239). Humana Press. https://doi.org/10.1007/978-1-60327-241-4_13

Bertamini, M., Grando, M. S. & Nedunchezhian, N. (2003). Effects of Phytoplasma Infection on Pigments, Chlorophyll-Protein Complex and Photosynthetic Activities in Field Grown Apple Leaves. *Biologia plantarum*, *46*(2), 237–242. https://doi.org/10.1023/b:biop.0000022258.49957.9a

Bertamini, M., Muthuchelian, K., Grando, M. S. & Nedunchezhian, N. (2002). Effects of Phytoplasma Infection on Growth and Photosynthesis in Leaves of Field Grown apple

(Malus Pumila Mill. cv. Golden Delicious). *Photosynthetica*, *40*(1), 157–160. https://doi.org/10.1023/a:1020156021629

Birtchnell, T. & Gibson, C. (2015). Less talk more drone: Social research with UAVs. *Journal of Geography in Higher Education*, *39*(1), 182–189. https://doi.org/10.1080/03098265.2014.1003799

Blackburn, G. A. (1998). Spectral indices for estimating photosynthetic pigment concentrations: A test using senescent tree leaves. *International Journal of Remote Sensing*, *19*(4), 657–675. https://doi.org/10.1080/014311698215919

Blackburn, G. A. (2006). Hyperspectral remote sensing of plant pigments. *Journal of Experimental Botany*, *58*(4), 855–867. https://doi.org/10.1093/jxb/erl123

Blattny, C., Seidl, V. & Erbenová, M. (1963). The Apple proliferation of various sorts and the possible strain differentiation of the virus. *Phytopathologia Mediterranea*, *2*(3), 119–123. http://www.jstor.org/stable/42683862

Bock, C. H. (2011). Detection and measurement of plant disease symptoms using visible-wavelength photography and image analysis. *CAB Reviews: Perspectives in Agriculture, Veterinary Science, Nutrition and Natural Resources*, *6*(027). https://doi.org/10.1079/pavsnnr20116027

Bock, C. H., Barbedo, J. G. A., Ponte, E. M. D., Bohnenkamp, D. & Mahlein, A.-K. (2020). From visual estimates to fully automated sensor-based measurements of plant disease severity: Status and challenges for improving accuracy. *Phytopathology Research*, *2*(1). https://doi.org/10.1186/s42483-020-00049-8

Bormann, F. H. (1966). The Structure, Function, and Ecological Significance of Root Grafts in Pinus strobus L. *Ecological Monographs*, *36*(1), 1–26. https://doi.org/10.2307/1948486

Bossomaier, T. & Hope, B. A. (2015). *Online gis and spatial metadata* (2nd ed.). CRC Press. https://doi.org/10.1201/b19465

Bovey, R. (1963). Observations and experiments on Apple proliferation disease. *Phytopathologia Mediterranea*, *2*(3), 111–114. http://www.jstor.org/stable/42683860

Brewer, C. A. & Buttenfield, B. P. (2009). Mastering map scale: Balancing workloads using display and geometry change in multi-scale mapping. *GeoInformatica*, *14*(2), 221–239. https://doi.org/10.1007/s10707-009-0083-6

Britannica, T. (n.d.-a). Chlorosis. *Encyclopedia britannica*. https://www.britannica.com/science/phloem

Britannica, T. (n.d.-b). Glycolysis. *Encyclopedia britannica*. https://www.britannica.com/science/glycolysis

Britannica, T. (n.d.-c). Jumping plant louse. *Encyclopedia britannica*. https://www.britannica.com/animal/jumping-plant-louse

Britannica, T. (n.d.-d). Phloem. *Encyclopedia britannica*. https://www.britannica.com/science/chlorosis-plant-disease

Britannica, T. (n.d.-e). Pleomorphism. *Encyclopedia britannica*. https://www.britannica.com/science/pleomorphism

Brovelli, M. A., Codrina, M. I. & Coetzee, S. (2019). Openness and Community Geospatial Science for Monitoring SDGs – An Example From Tanzania. In A. Rajabifard (Ed.), *Sustainable development goals connectivity dilemma : Land and geospatial information for urban and rural resilience* (pp. 313–324). CRC Press. https://doi.org/https://doi.org/10.1201/9780429290626

Candiago, S., Remondino, F., Giglio, M. D., Dubbini, M. & Gattelli, M. (2015). Evaluating Multispectral Images and Vegetation Indices for Precision Farming Applications from UAV Images. *Remote Sensing*, *7*(4), 4026–4047. https://doi.org/10.3390/rs70404026

Card, S. K., Mackinlay, J. D. & Shneiderman, B. (1999). *Readings in information visualization: Using vision to think*. Morgan Kaufmann Publ.

Carr, D. B., Olsen, A. R. & White, D. (1992). Hexagon Mosaic Maps for Display of Univariate and Bivariate Geographical Data. *Cartography and Geographic Information Systems*, *19*(4), 228–236. https://doi.org/10.1559/152304092783721231

Carraro, L., Ermacora, P., Loi, N. & Osler, R. (2004). The Recovery Phenomenon In Apple Proliferation-Infected Apple Trees. *Journal of Plant Pathology*, *86*(2), 141–146. http://www.jstor.org/stable/41998183

Carraro, L., Ferrini, F., Ermacora, P., Loi, N. & Labonne, G. (2008). Infectivity of *Cacopsylla picta* (Syn. *Cacopsylla costalis*), Vector of '*Candidatus* Phytoplasma mali' in North East Italy. *Acta Horticulturae*, (781), 403–408. https://doi.org/10.17660/actahortic.2008.781.57

Casagrande, G. (2017). Opportunities. *Small flying drones* (pp. 47–89). Springer International Publishing. https://doi.org/10.1007/978-3-319-66577-1_3

Casagrande, G. & Gusto, D. D. (2017). Concepts and Issues. *Small flying drones* (pp. 13–45). Springer International Publishing. https://doi.org/10.1007/978-3-319-66577-1_2

Christensen, N. M., Axelsen, K. B., Nicolaisen, M. & Schulz, A. (2005). Phytoplasmas and their interactions with hosts. *Trends in Plant Science*, *10*(11), 526–535. https://doi.org/10.1016/j.tplants.2005.09.008

Ciccotti, A. M., Bianchedi, P. L., Bragagna, P., Deromedi, M., Filippi, M., Forno, F. & Mattedi, L. (2007). Transmission of 'Candidatus Phytoplasma mali' by root bridges under natural and experimental conditions. *Bulletin of Insectology*, *60*(2), 387–388. http://www.bulletinofinsectology.org/pdfarticles/vol60-2007-387-388ciccotti.pdf

Close, D. C. & Beadle, C. L. (2003). The Ecophysiology of Foliar Anthocyanin. *The Botanical Review*, *69*(2), 149–161. https://doi.org/10.1663/0006-8101(2003)069[0149:teofa]2.0.co;2

Coetzee, S., Ivánová, I., Mitasova, H. & Brovelli, M. (2020). Open Geospatial Software and Data: A Review of the Current State and A Perspective into the Future. *ISPRS International Journal of Geo-Information*, *9*(2), 90. https://doi.org/10.3390/ijgi9020090

Congedo, L. (2021). Semi-Automatic Classification Plugin: A Python tool for the download and processing of remote sensing images in QGIS. *Journal of Open Source Software*, *6*(64), 3172. https://doi.org/10.21105/joss.03172

Curran, P. J. (1989). Remote sensing of foliar chemistry. *Remote Sensing of Environment*, *30*(3), 271–278. https://doi.org/10.1016/0034-4257(89)90069-2

Deery, D., Jimenez-Berni, J., Jones, H., Sirault, X. & Furbank, R. (2014). Proximal Remote Sensing Buggies and Potential Applications for Field-Based Phenotyping. *Agronomy*, *4*(3), 349–379. https://doi.org/10.3390/agronomy4030349

Delgado, J. A., Short, N. M., Roberts, D. P. & Vandenberg, B. (2019). Big Data Analysis for Sustainable Agriculture on a Geospatial Cloud Framework. *Frontiers in Sustainable Food Systems*, *3*. https://doi.org/10.3389/fsufs.2019.00054

Directorate-General for Internal Policies of the Union. (2014). *Precision agriculture : An opportunity for EU farmers - potential support with the CAP 2014-2020* (P. J. Zarco-Tejada, P. Loudjani & N. Hubbard, Eds.). European Parliament. https://op.europa.eu/en/publication-detail/-/publication/a8acb192-1c72-47b5-b8d8-2980afb3e138

Directorate-General for Parliamentary Research Services. (2019). *Precision agriculture and the future of farming in Europe: Scientific foresight study* (C. Daheim, K. Poppe & R. Schrijver, Eds.). European Parliament. https://op.europa.eu/en/publication-detail/-/publication/40fe549e-cb49-11e7-a5d5-01aa75ed71a1

Drecki, I. & Maciejewska, I. (2005). DEALING WITH UNCERTAINTY IN LARGE-SCALE SPATIAL DATABASES. *Proceedings of the 22nd International Cartographic Conference*. https://icaci.org/files/documents/ICC_proceedings/ICC2005/htm/pdf/oral/TEMA7/Session%204/IGOR%20DRECKI.pdf

Environmental Systems Research Institute. (2006). Spreading Data Improves Crop Yield: New zealand fertilizer application system uses gis/gps. *ArcNews*, *28*. Winter 2006/2007. https://www.esri.com/news/arcnews/winter0607articles/spreading-data.html

Epstein, A. H. (1978). Root Graft Transmission of Tree Pathogens. *Annual Review of Phytopathology*, *16*(1), 181–192. https://doi.org/10.1146/annurev.py.16.090178.001145

European Comission. (2018). *Turning FAIR data into reality : Final report and action plan from the European Commission expert group on FAIR data*. Publications Office of the European Union. https://doi.org/10.2777/54599

Fiella, I. & Peñuelas, J. (1994). The red edge position and shape as indicators of plant chlorophyll content, biomass and hydric status. *International Journal of Remote Sensing*, *15*(7), 1459–1470. https://doi.org/10.1080/01431169408954177

Filella, I., Serrano, L., Serra, J. & Peñuelas, J. (1995). Evaluating Wheat Nitrogen Status with Canopy Reflectance Indices and Discriminant Analysis. *Crop Science*, *35*(5), 1400–1405. https://doi.org/10.2135/cropsci1995.0011183x003500050023x

Food and Agriculture Organization of the United Nations. (1996). Rome Declaration on World Food Security and World Food Summit Plan of Action: World Food Summit, 13-17 November 1996, Rome, Italy, 43. http://www.fao.org/3/w3613e/w3613e00.htm

Food and Agriculture Organization of the United Nations. (2014). *Building a common vision for sustainable food and agriculture : Principles and approaches*. Food and Agriculture Organization of the United Nations. http://www.fao.org/3/i3940e/i3940e.pdf

Frank, A. U. & Timpf, S. (1994). Multiple representations for cartographic objects in a multi-scale tree—an intelligent graphical zoom. *Computers & Graphics*, *18*(6), 823–829. https://doi.org/10.1016/0097-8493(94)90008-6

Frisinghelli, C., Delaiti, L., Grando, M. S., Forti, D. & Vindimian, M. E. (2000). Cacopsylla costalis (Flor 1861), as a Vector of Apple Proliferation in Trentino. *Journal of Phytopathology*, *148*(7-8), 425–431. https://doi.org/10.1046/j.1439-0434.2000.00403.x

GeoNode Development Team. (n.d.). *GeoNode's Documentation* (O. S. G. Foundation, Ed.). https://docs.geonode.org/en/master/index.html

Geospatial Media. (2019, January 14). *Kuandeng Technology demonstrates high-precision maps in CES 2019* (Geospatial World, Ed.). https://www.geospatialworld.net/news/kuandeng-technology-demonstrates-high-precision-maps-in-ces-2019/

Giorno, F., Guerriero, G., Biagetti, M., Ciccotti, A. M. & Baric, S. (2013). Gene expression and biochemical changes of carbohydrate metabolism in in vitro micro-propagated apple plantlets infected by 'Candidatus Phytoplasma mali'. *Plant Physiology and Biochemistry*, *70*, 311–317. https://doi.org/10.1016/j.plaphy.2013.05.040

Gitelson, A. A. & Merzlyak, M. N. (1997). Remote estimation of chlorophyll content in higher plant leaves. *International Journal of Remote Sensing*, *18*(12), 2691–2697. https://doi.org/10.1080/014311697217558

Gitelson, A. A., Kaufman, Y. J. & Merzlyak, M. N. (1996). Use of a green channel in remote sensing of global vegetation from EOS-MODIS. *Remote Sensing of Environment*, *58*(3), 289–298. https://doi.org/10.1016/s0034-4257(96)00072-7

Gitelson, A. A., Merzlyak, M. N. & Chivkunova, O. B. (2001). Optical Properties and Nondestructive Estimation of Anthocyanin Content in Plant Leaves. *Photochemistry and Photobiology*, *74*(1), 38–45. https://doi.org/10.1562/0031-8655(2001)0740038opaneo2.0.co2

Graetz, N., Friedman, J., Osgood-Zimmerman, A., Burstein, R., Biehl, M. H., Shields, C., Mosser, J. F., Casey, D. C., Deshpande, A., Earl, L., Reiner, R. C., Ray, S. E., Fullman, N., Levine, A. J., Stubbs, R. W., Mayala, B. K., Longbottom, J., Browne, A. J., Bhatt, S., Weiss, D. J., Gething, P. W., Mokdad, A. H., Lim, S. S., Murray, C. J. L., Gakidou, E. & Hay, S. I. (2018). Mapping local variation in educational attainment across Africa. *Nature*, *555*(7694), 48–53. https://doi.org/10.1038/nature25761

Grefe, C. (2021). UN-Gipfel gegen Hunger – Es bleibne neun Ernten Zeit. *ZEIT ONLINE*, *38*. https://www.zeit.de/2021/38/un-gipfel-hunger-ernaehrung-nahrung-verteilungsproblem?

Haber, R. B. & McNabb, D. A. (1990). Visualization idioms: A conceptual model for scientific visualization systems (G. M. Nielson, B. Shriver & L. J. Rosenblum, Eds.). *Visualization in Scientific Computing*, 74–93. https://www.academia.edu/2205276/Visualization_idioms_A_conceptual_model_for_scientific_visualization_systems

Harvey. (1997). *Justice, Nature and the Geography*. John Wiley & Sons.

Hernández-López, D., Felipe-García, B., Sánchez, N., González-Aguilera, D. & Gomez-Lahoz, J. (2012). Testing the Radiometric Performance of Digital Photogrammetric Images: Vicarious vs. Laboratory Calibration on the Leica ADS40, a Study in Spain. *Photogrammetrie - Fernerkundung - Geoinformation*, *2012*(5), 557–571. https://doi.org/10.1127/1432-8364/2012/0139

Herzog, U., Wiedemann, W. & Trapp, A. (2010). *Apfeltriebsucht in Sachsen* (Vol. 19/2010). Sächsisches Landesamt für Umwelt, Landwirtschaft und Geologie. https://publikationen.sachsen.de/bdb/artikel/14993

Herzog, U., Wiedemann, W. & Trapp, A. (2012). *Phytoplasmen im sächsischen Obstbau* (Vol. 32/2012). Sächsisches Landesamt für Umwelt, Landwirtschaft und Geologie. https://publikationen.sachsen.de/bdb/artikel/15671

Hjelmager, J., Moellering, H., Cooper, A., Delgado, T., Rajabifard, A., Rapant, P., Danko, D., Huet, M., Laurent, D., Aalders, H., Iwaniak, A., Abad, P., Düren, U. & Martynenko, A. (2008). An initial formal model for spatial data infrastructures. *International Journal of Geographical Information Science*, *22*(11-12), 1295–1309. https://doi.org/10.1080/13658810801909623

Hotelling, H. (1933). Analysis of a complex of statistical variables into principal components. *Journal of Educational Psychology*, *24*(6), 417–441. https://doi.org/10.1037/h0071325

Huang, Y. & Brown, M. E. (2018). Advancing to the next generation precision agriculture: – global trends, challenges and opportunities. In R. Serraj & P. Pingali (Eds.), *Agriculture & food systems to 2050*. World Scientific. https://doi.org/10.1142/11212

Ingram, J. (2011). A food systems approach to researching food security and its interactions with global environmental change. *Food Security*, *3*(4), 417–431. https://doi.org/10.1007/s12571-011-0149-9

Institut für Wirtschaftsforschung. *Economy in Figures: Die Südtiroler Wirtschaft unter der Lupe* (Handelskammer Bozen, Ed.). German. Ed. by Handelskammer Bozen. 2016,

27. https://www.handelskammer.bz.it/sites/default/files/uploaded_files/Scuola_economia/20170104_economy_in_focus_dt.pdf

International Organisation for Standards, Open Geospatial Consortium & International Hydrographic Organization. (2018). *A Guide to the Role of Standards in Geospatial Information Management*. http://ggim.un.org/meetings/GGIM-committee/8th-Session/documents/Standards_Guide_2018.pdf

Izenman, A. J. (2008). *Modern Multivariate Statistical Techniques: Regression, Classification, and Manifold Learning*. Springer-Verlag. https://doi.org/10.1007/978-0-387-78189-1

Janik, K., Barthel, D., Oppedisano, T., Anfora, G., Angeli, G., Baldessari, M., Bianchedi, P., Campisano, A., Covelli, L., Dallago, G., Fischnaller, S., Ioriatti, C., Jarausch, W., Letschka, T., Mazzoni, V., Mittelberger, C., Moser, M., Öttl, S., Panassiti, B. & Weil, T. (2020). *Apple Proliferation - a Joint Review* (K. Janik, D. Barthel, T. Oppedisano & G. Anfora, Eds.). Fondazione Edmund Mach; Laimburg Research Centre. http://www.laimburg.it/downloads/Apple_Proliferation.pdf

Jarausch, B. (2007). http://www.apfeltriebsucht.de

Jarausch, B., Schwind, N., Jarausch, W., Krczal, G., Dickler, E. & Seemüller, E. (2003). First Report of Cacopsylla picta as a Vector of Apple Proliferation Phytoplasma in Germany. *Plant Disease*, *87*(1), 101–101. https://doi.org/10.1094/pdis.2003.87.1.101a

Kalluri, U. C., Payyavula, R. S., Labbé, J. L., Engle, N., Bali, G., Jawdy, S. S., Sykes, R. W., Davis, M., Ragauskas, A., Tuskan, G. A. & Tschaplinski, T. J. (2016). Down-Regulation of KORRIGAN-Like Endo-β-1,4-Glucanase Genes Impacts Carbon Partitioning, Mycorrhizal Colonization and Biomass Production in Populus. *Frontiers in Plant Science*, *7*. https://doi.org/10.3389/fpls.2016.01455

Kartte, S. & Seemüller, E. (1988). Variable response within the genus Malus to the apple proliferation disease / Unterschiedliche Reaktion auf die Apfeltriebsucht innerhalb der Gattung Malus. *Zeitschrift für Pflanzenkrankheiten und Pflanzenschutz / Journal of Plant Diseases and Protection*, *95*(1), 25–34. http://www.jstor.org/stable/43383267

Kartte, S. & Seemüller, E. (1991). Susceptibility of Grafted *Malus* Taxa and Hybrids to Apple Proliferation Disease / Anfälligkeit von veredelten *Malus*-Taxa und -Hybriden für die Apfeltriebsucht. *Journal of Phytopathology*, *131*(2), 137–148. https://doi.org/10.1111/j.1439-0434.1991.tb04739.x

Kim, R., Bijral, A. S., Xu, Y., Zhang, X., Blossom, J. C., Swaminathan, A., King, G., Kumar, A., Sarwal, R., Ferres, J. M. L. & Subramanian, S. V. (2021). Precision mapping child undernutrition for nearly 600,000 inhabited census villages in india. *Proceedings of the National Academy of Sciences*, *118*(18), e2025865118. https://doi.org/10.1073/pnas.2025865118

Klauser, F. & Pedrozo, S. (2015). Power and space in the drone age: A literature review and politico-geographical research agenda. *Geographica Helvetica*, *70*(4), 285–293. https://doi.org/10.5194/gh-70-285-2015

Kraak, M.-J. (2019). *Strategic Plan for 2019-2027* (tech. rep.). International Cartographic Association. https://icaci.org/files/documents/generalassembly2019/22-ica_strategic_plan_2019-2027.pdf

Kraak, M.-J. & Fabrikant, S. I. (2017). Of maps, cartography and the geography of the International Cartographic Association. *International Journal of Cartography*, *3*(sup1), 9–31. https://doi.org/10.1080/23729333.2017.1288535

Krczal, G., Krczal, H. & Kunze, L. (1988). *Fieberiella florii* (stål), a vector of apple proliferation agent. *Acta Horticolturae*, (235), 99–106. https://doi.org/10.17660/actahortic.1989.235.12

Kucheryavskiy, S. (2020). mdatools — R package for chemometrics. *Chemometrics and Intelligent Laboratory Systems*, *198*. https://doi.org/10.1016/j.chemolab.2020.103937

Laurie, G., Boulton, G., Campbell, P., Collins, B., Elias, P., Hall, W., O'Neill, O., Rawlins, M., Thornton, J., Vallance, P. & Walport, M. (2012). *Science as an open enterprise*. The Royal Society. https://royalsociety.org/-/media/policy/projects/sape/2012-06-20-saoe.pdf

Lee, I.-M., Davis, R. E. & Gundersen-Rindal, D. E. (2000). Phytoplasma: Phytopathogenic Mollicutes. *Annual Review of Microbiology*, *54*(1), 221–255. https://doi.org/10.1146/annurev.micro.54.1.221

Lepka, P., Stitt, M., Moll, E. & Seemüller, E. (1999). Effect of phytoplasmal infection on concentration and translocation of carbohydrates and amino acids in periwinkle and tobacco. *Physiological and Molecular Plant Pathology*, *55*(1), 59–68. https://doi.org/10.1006/pmpp.1999.0202

Li, D., Wang, X. & Sun, T. (2016). Energy-optimal coverage path planning on topographic map for environment survey with unmanned aerial vehicles. *Electronics Letters*, *52*(9), 699–701. https://doi.org/10.1049/el.2015.4551

Lichtenthaler, H. K. & Rinderle, U. (1988). The Role of Chlorophyll Fluorescence in The Detection of Stress Conditions in Plants. *C R C Critical Reviews in Analytical Chemistry*, *19*(sup1), S29–S85. https://doi.org/10.1080/15476510.1988.10401466

Liu, J. & Liu, J. (2018). Intelligent and Connected Vehicles: Current Situation, Future Directions, and Challenges. *IEEE Communications Standards Magazine*, *2*(3), 59–65. https://doi.org/10.1109/mcomstd.2018.1700087

Loi, N., Ermacora, P., Carraro, L., Osler, R. & Chen, T. A. (2002). Production of monoclonal antibodies against apple proliferation phytoplasma and their use in serological detection. *European Journal of Plant Pathology*, *108*(1), 81–86. https://doi.org/10.1023/a:1013901706383

Lokers, R., Knapen, R., Janssen, S., van Randen, Y. & Jansen, J. (2016). Analysis of big data technologies for use in agro-environmental science. *Environmental Modelling & Software*, *84*, 494–504. https://doi.org/10.1016/j.envsoft.2016.07.017

Lowe, A., Harrison, N. & French, A. P. (2017). Hyperspectral image analysis techniques for the detection and classification of the early onset of plant disease and stress. *Plant Methods*, *13*(1). https://doi.org/10.1186/s13007-017-0233-z

Mahlein, A.-K., Rumpf, T., Welke, P., Dehne, H.-W., Plümer, L., Steiner, U. & Oerke, E.-C. (2013). Development of spectral indices for detecting and identifying plant diseases. *Remote Sensing of Environment*, *128*, 21–30. https://doi.org/10.1016/j.rse.2012.09.019

Mahlein, A.-K. (2016). Plant disease detection by imaging sensors – parallels and specific demands for precision agriculture and plant phenotyping. *Plant Disease*, *100*(2), 241–251. https://doi.org/10.1094/pdis-03-15-0340-fe

Mattedi, L., Ciccotti, A. M., Bianchedi, P. L., Bragagna, P., Deromedi, M., Filippi, M., Forno, F. & Pedrazzoli, F. (2008). Trasmissione di Apple Proliferation attraverso anastomosi radicali. In C. Ioriatti & W. Jarausch (Eds.), *Scopazzi del melo - Apple Proliferation* (pp. 76–91).

Mattedi, L., Forno, F., Branz, A., Bragagna, P., Battocletti, I., Gualandri, V., Pedrazzoli, F., Bianchedi, P. L., Deromedi, M., Filippi, M., Dallabetta, N., Varner, M. & Ciccotti, A. M.

(2008). Come riconoscere la malattia in campo: Novità sulla sintomatologia. In C. Ioriatti & W. Jarausch (Eds.), *Scopazzi del melo - Apple Proliferation* (pp. 63–75).

McFarlane, H. E., Döring, A. & Persson, S. (2014). The cell biology of cellulose synthesis. *Annual Review of Plant Biology*, *65*(1), 69–94. https://doi.org/10.1146/annurev-arplant-050213-040240

McNeall, D. (2015). *Picking a colour scale for scientific graphics* (B. Figures, Ed.). https://betterfigures.org/2015/06/23/picking-a-colour-scale-for-scientific-graphics/

Meier, U. (2001). *Growth stages of mono- and dicotyledonous plants: Bbch-monograph* (U. Meier, Ed.; 2nd ed.). Biologische Bundesanstalt für Land- und Forstwirtschaft. https://www.politicheagricole.it/flex/AppData/WebLive/Agrometeo/MIEPFY800/BBCHengl2001.pdf

Meijers, M., van Oosterom, P., Driel, M. & Šuba, R. (2020). Web-based dissemination of continuously generalized space-scale cube data for smooth user interaction. *International Journal of Cartography*, *6*(1), 152–176. https://doi.org/10.1080/23729333.2019.1705144

Meireles, J. E., Schweiger, A. & Cavender-Bares, J. (2017). *Spectrolab: Class and methods for hyperspectral data in R* [R package version 0.0.10]. https://doi.org/10.5281/zenodo.3934575

Ministero delle Politiche Agricole e Florestali. (2006). Misure per la lotta obbligatoria contro il fitoplasma Apple Proliferation Phytoplasma. https://www.provinz.bz.it/land-forstwirtschaft/landwirtschaft/downloads/Decreto_ministeriale_23_febbraio_2006.pdf

Mittelberger, C., Yalcinkaya, H., Pichler, C., Gasser, J., Scherzer, G., Erhart, T., Schumacher, S., Holzner, B., Janik, K., Robatscher, P., Müller, T., Kräutler, B. & Oberhuber, M. (2017). Pathogen-Induced Leaf Chlorosis: Products of Chlorophyll Breakdown Found in Degreened Leaves of Phytoplasma-Infected Apple (Malus × domestica Borkh.) and Apricot (Prunus armeniaca L.) Trees Relate to the Pheophorbide a Oxygenase/Phyllobilin Pathway. *Journal of Agricultural and Food Chemistry*, *65*(13), 2651–2660. https://doi.org/10.1021/acs.jafc.6b05501

Moreland, K. (2016). Why We Use Bad Color Maps and What You Can Do About It. *Electronic Imaging*, *2016*(16), 1–6. https://doi.org/10.2352/issn.2470-1173.2016.16.hvei-133

Mulla, D. J. (2013). Twenty five years of remote sensing in precision agriculture: Key advances and remaining knowledge gaps. *Biosystems Engineering*, *114*(4), 358–371. https://doi.org/10.1016/j.biosystemseng.2012.08.009

Musetti, R., Marabottini, R., Badiani, M., Martini, M., di Toppi, L. S., Borselli, S., Borgo, M. & Osler, R. (2007). On the role of h2o2 in the recovery of grapevine (vitis vinifera cv. prosecco) from flavescence dorée disease. *Functional Plant Biology*, *34*(8), 750. https://doi.org/10.1071/fp06308

Nebert, D. D. (2004). *Developing Spatial Data infrastructure: The SDI Cookbook*. Global Spatial Data Infrastructure. http://gsdiassociation.org/images/publications/cookbooks/SDI_Cookbook_GSDI_2004_ver2.pdf

Nebiker, S., Lack, N., Abächerli, M. & Läderach, S. (2016). Light-weight multispectral UAV sensors and their capabilities for predicting grain yield and detecting plant diseases. *ISPRS - International Archives of the Photogrammetry, Remote Sensing and Spatial Information Sciences*, *XLI-B1*, 963–970. https://doi.org/10.5194/isprsarchives-xli-b1-963-2016

Negro, C., Sabella, E., Nicolì, F., Pierro, R., Materazzi, A., Panattoni, A., Aprile, A., Nutricati, E., Vergine, M., Miceli, A., Bellis, L. D. & Luvisi, A. (2020). Biochemical Changes in Leaves of Vitis vinifera cv. Sangiovese Infected by Bois Noir Phytoplasma. *Pathogens*, *9*(4), 269. https://doi.org/10.3390/pathogens9040269

Oerke, E.-C. (2006). Crop losses to pests. *The Journal of Agricultural Science*, *144*(1), 31–43. https://doi.org/10.1017/s0021859605005708

Oerke, E.-C., Mahlein, A.-K. & Steiner, U. (2014). Proximal Sensing of Plant Diseases. In M. L. Gullino & P. J. M. Bonants (Eds.), *Detection and diagnostics of plant pathogens*. *Vol. 5*I. *Detection and diagnostics of plant pathogens* (pp. 55–68). Springer Science+Business Media. https://doi.org/10.1007/978-94-017-9020-8_4

Okabe, M. & Ito, K. (2002). How to make figures and presentations that are friendly to color blind people. https://www.vwvj.be/sites/default/files/zien/zien_-_uit_voorbije_vorming/kleurzinonderzoekextratips.pdf

Open Geospatial Consortium. (n.d.). Glossary of Terms - O. https://www.ogc.org/ogc/glossary/o

Open Knowledge Foundation. (n.d.). *Open definition. defining open in open data, open content and open knowledge* (Open Knowledge Foundation, Ed.). https://opendefinition.org/od/2.1/en/

Osgood-Zimmerman, A., Millear, A. I., Stubbs, R. W., Shields, C., Pickering, B. V., Earl, L., Graetz, N., Kinyoki, D. K., Ray, S. E., Bhatt, S., Browne, A. J., Burstein, R., Cameron, E., Casey, D. C., Deshpande, A., Fullman, N., Gething, P. W., Gibson, H. S., Henry, N. J., Herrero, M., Krause, L. K., Letourneau, I. D., Levine, A. J., Liu, P. Y., Longbottom, J., Mayala, B. K., Mosser, J. F., Noor, A. M., Pigott, D. M., Piwoz, E. G., Rao, P., Rawat, R., Reiner, R. C., Smith, D. L., Weiss, D. J., Wiens, K. E., Mokdad, A. H., Lim, S. S., Murray, C. J. L., Kassebaum, N. J. & Hay, S. I. (2018). Mapping child growth failure in Africa between 2000 and 2015. *Nature*, *555*(7694), 41–47. https://doi.org/10.1038/nature25760

Osler, R., Loi, N., Carraro, L., Ermacora, P. & Refatti, E. (2000). Recovery in plants affected by phytoplasmas. *Proceedings of the 5th Congress of the European Foundation for Plant Pathology*.

Papp, L., van Leeuwen, B., Szilassi, P., Tobak, Z., Szatmári, J., Árvai, M., Mészáros, J. & Pásztor, L. (2021). Monitoring Invasive Plant Species Using Hyperspectral Remote Sensing Data. *Land*, *10*(1), 29. https://doi.org/10.3390/land10010029

Pastenes, C., Pimental, P. & Lillo, J. (2004). Leaf movements and photoinhibition in relation to water stress in field-grown beans. *Journal of Experimental Botany*, *56*(411), 425–433. https://doi.org/10.1093/jxb/eri061

Pedrazzoli, F., Ciccotti, A. M., Bianchedi, P. L., Salvadori, A. & Zorer, R. (2008). Seasonal colonisation behaviour of *Candidatus* Phytoplasma mali in apple trees in Trentino. *Acta Horticulturae*, (781), 483–489. https://doi.org/10.17660/actahortic.2008.781.70

Peñuelas, J., Gamon, J., Fredeen, A., Merino, J. & Field, C. (1994). Reflectance indices associated with physiological changes in nitrogen- and water-limited sunflower leaves. *Remote Sensing of Environment*, *48*(2), 135–146. https://doi.org/10.1016/0034-4257(94)90136-8

Peñuelas, J. & Filella, I. (1998). Visible and near-infrared reflectance techniques for diagnosing plant physiological status. *Trends in Plant Science*, *3*(4), 151–156. https://doi.org/10.1016/s1360-1385(98)01213-8

Pretty, J. (2008). Agricultural sustainability: Concepts, principles and evidence. *Philosophical Transactions of the Royal Society B: Biological Sciences*, *363*(1491), 447–465. https://doi.org/10.1098/rstb.2007.2163

QGIS Development Team. (2021). *Qgis geographic information system*. Version 3.18.2-Zürich. QGIS Association. https://www.qgis.org

R Core Team. (2021). *R: A Language and Environment for Statistical Computing*. R Foundation for Statistical Computing. Vienna, Austria. https://www.R-project.org/

Raposo, P. (2017). Scale and Generalization. *Geographic Information Science & Technology Body of Knowledge*, *2017*(Q4). https://doi.org/10.22224/gistbok/2017.4.3

Reich, B. J. & Haran, M. (2018). Precision maps for public health. *Nature*, *555*(7694), 32–33. https://doi.org/10.1038/d41586-018-02096-w

Řezník, T., Kubíček, P., Herman, L., Pavelka, T., Leitgeb, Š., Klocová, M. & Leitner, F. (2020). Visualizations of Uncertainties in Precision Agriculture: Lessons Learned from Farm Machinery. *Applied Sciences*, *10*(17), 6132. https://doi.org/10.3390/app10176132

Richards, J. A. & Jia, X. (2006). *Remote Sensing Digital Image Analysis* (4th ed.). Springer-Verlag Berlin Heidelberg. https://doi.org/10.1007/3-540-29711-1

Robinson, A. H., Morrison, J. L., Muehrcke, P. C., Kimerling, A. J., Passmore, L., Guptill, S. C. & Starr, E. (1995). *Elements of Cartography*. Wiley.

Robinson, A. C., Demšar, U., Moore, A. B., Buckley, A., Jiang, B., Field, K., Kraak, M.-J., Camboim, S. P. & Sluter, C. R. (2017). Geospatial big data and cartography: Research challenges and opportunities for making maps that matter. *International Journal of Cartography*, *3*(sup1), 32–60. https://doi.org/10.1080/23729333.2016.1278151

Roth, R. E., Brewer, C. A. & Stryker, M. S. (2011). A typology of operators for maintaining legible map designs at multiple scales. *Cartographic Perspectives*, (68), 29–64. https://doi.org/10.14714/cp68.7

RStudio Team. (2021). *RStudio: Integrated Development Environment for R*. RStudio, PBC. Boston, MA. http://www.rstudio.com/

Rui, D. (1950). Una malattia inedita: La virosi a scopazzi del melo. *Humus*, *6*(11), 7–10.

Rumpf, T., Mahlein, A.-K., Steiner, U., Oerke, E.-C., Dehne, H.-W. & Plümer, L. (2010). Early detection and classification of plant diseases with Support Vector Machines based on hyperspectral reflectance. *Computers and Electronics in Agriculture*, *74*(1), 91–99. https://doi.org/10.1016/j.compag.2010.06.009

Sandbrook, C. (2015). The social implications of using drones for biodiversity conservation. *Ambio*, *44*(S4), 636–647. https://doi.org/10.1007/s13280-015-0714-0

Savary, S., Ficke, A., Aubertot, J.-N. & Hollier, C. (2012). Crop losses due to diseases and their implications for global food production losses and food security. *Food Security*, *4*(4), 519–537. https://doi.org/10.1007/s12571-012-0200-5

Savary, S., Willocquet, L., Pethybridge, S. J., Esker, P., McRoberts, N. & Nelson, A. (2019). The global burden of pathogens and pests on major food crops. *Nature Ecology & Evolution*, *3*(3), 430–439. https://doi.org/10.1038/s41559-018-0793-y

Schaper, U. & Seemüller, E. (1982). Condition of the phloem and the persistence of mycoplasmalike organisms associated with apple proliferation and pear decline. *Phytopathology*, *72*, 736–742. https://www.apsnet.org/publications/phytopathology/backissues/Documents/1982Articles/Phyto72n07_736.PDF

Schaper, U. & Seemüller, E. (1984). Recolonization of the stem of apple proliferation and pear decline-diseased trees by the causal organisms in spring / Wiederbesiedlung des Sprosses von triebsuchtkranken Apfelbäumen und verfallskranken Birnbäumen

durch die Erreger im Frühjahr. *Zeitschrift für Pflanzenkrankheiten und Pflanzenschutz / Journal of Plant Diseases and Protection*, *91*(6), 608–613. http://www.jstor.org/stable/43382792

Schmid, G. (1975). Prolonged observations on spread and behaviour of proliferation disease in apple orchards. *Acta Horticulturae*, (44), 183–192. https://doi.org/10.17660/actahortic.1975.44.30

Schmidt, S., Vanas, V., Schweigkofler, W., Öttl, S., Berger, J., Cainelli, C. & Baric, S. (2009). Das Schwerpunktprojekt Apfeltriebsucht am Versuchszentrum Laimburg. *Obstbau Weinbau*, *46*(7/8), 272–277. http://www.laimburg.it/en/projects-publications/publications.asp#download-area-idx140940

Schowengerdt, R. A. (2006). *Remote Sensing*. Elsevier Science & Technology.

Seemüller, E., Kison, H. & Lorenz, K.-H. (1998). On the geographic distribution and prevalence of the apple proliferation phytoplasma in low-intensity orchards in Germany / Über die geographische Verbreitung des Apfeltriebsucht-Phytoplasmas in Deutschland und die Infektionshäufigkeit im Streuobstbau. *Zeitschrift für Pflanzenkrankheiten und Pflanzenschutz / Journal of Plant Diseases and Protection*, *105*(4), 404–410. http://www.jstor.org/stable/43215258

Seemüller, E., Kunze, L. & Schaper, U. (1984). Colonization behavior of MLO, and symptom expression of proliferation-diseased apple trees and decline-diseased pear trees over a period of several years / Besiedlungsverhalten von MLO und Symptomausbildung bei triebsuchtkranken Apfelbäumen und verfallskranken Birnbäumen im Verlauf mehrerer Jahre. *Zeitschrift Für Pflanzenkrankheiten Und Pflanzenschutz / Journal of Plant Diseases and Protection*, *91*(5), 525–532. http://www.jstor.org/stable/43382859

Seemüller, E., Schaper, U. & Zimbelmann, F. (1984). Seasonal variation in the colonization patterns of mycoplasmalike organisms associated with apple proliferation and pear decline / Jahreszeitliche Veränderungen in der Besiedlung triebsuchtkranker Apfelbäume und verfallskranker Birnbäume durch mykoplasmaähnliche Organismen. *Zeitschrift Für Pflanzenkrankheiten Und Pflanzenschutz / Journal of Plant Diseases and Protection*, *91*(4), 371–382. http://www.jstor.org/stable/43382875

Seemüller, E., Kiss, E., Sule, S. & Schneider, B. (2010). Multiple Infection of Apple Trees by Distinct Strains of 'Candidatus Phytoplasma mali' and Its Pathological Relevance. *Phytopathology*, *100*(9), 863–870. https://doi.org/10.1094/phyto-100-9-0863

Seemüller, E. & Schneider, B. (2007). Differences in Virulence and Genomic Features of Strains of 'Candidatus Phytoplasma mali', the Apple Proliferation Agent. *Phytopathology*, *97*(8), 964–970. https://doi.org/10.1094/phyto-97-8-0964

Shneiderman, B. (1996). The eyes have it: A task by data type taxonomy for information visualizations. *Proceedings 1996 IEEE Symposium on Visual Languages*. https://doi.org/10.1109/vl.1996.545307

Sieber, P., Schorderet, M., Ryser, U., Buchala, A., Kolattukudy, P., Métraux, J.-P. & Nawrath, C. (2000). Transgenic Arabidopsis Plants Expressing a Fungal Cutinase Show Alterations in the Structure and Properties of the Cuticle and Postgenital Organ Fusions. *The Plant Cell*, *12*(5), 721–737. https://doi.org/10.1105/tpc.12.5.721

Sims, D. A. & Gamon, J. A. (2002). Relationships between leaf pigment content and spectral reflectance across a wide range of species, leaf structures and developmental stages. *Remote Sensing of Environment*, *81*(2-3), 337–354. https://doi.org/10.1016/s0034-4257(02)00010-x

Sishodia, R. P., Ray, R. L. & Singh, S. K. (2020). Applications of Remote Sensing in Precision Agriculture: A Review. *Remote Sensing*, *12*(19), 3136. https://doi.org/10.3390/rs12193136

Soleon GmbH (Ed.). (n.d.). *Coanda x6*. https://www.soleon.it/de/modelle/coanda-x6

Spaccapietra, S., Parent, C. & Vangenot, C. (2000). GIS Databases: From Multiscale to MultiRepresentation. *Lecture notes in computer science* (pp. 57–70). Springer Berlin Heidelberg. https://doi.org/10.1007/3-540-44914-0_4

Spectra Vista Corporation. (2012). *SVC HR-1024i / SVC HR-768i. USER MANUAL*. Version Revision 1.5. Spectra Vista Corporation. 29 Firemens Way, Poughkeepsie, New York 12603. https://docplayer.net/35656764-Svc-hr-1024i-svc-hr-768i-user-manual.html

Spectra Vista Corporation. (2016). *Full Sky Irradiance Sphere. USER MANUAL*. Version Revision 2.0. Spectra Vista Corporation. 29 Firemens Way, Poughkeepsie, New York 12603 USA. Retrieved August 10, 2021, from https://spectravista.com/wp-content/uploads/2021/07/SVC-Irradiance-Sphere-User-Manual-Rev-2.0.pdf

Steyn, W. J., Wand, S. J. E., Holcroft, D. M. & Jacobs, G. (2002). Anthocyanins in vegetative tissues: A proposed unified function in photoprotection. *New Phytologist*, *155*(3), 349–361. https://doi.org/10.1046/j.1469-8137.2002.00482.x

Strauss, E. (2009). Phytoplasma Research Begins to Bloom. *Science*, *325*(5939), 388–390. https://doi.org/10.1126/science.325_388

Szabó, G., Bertalan, L., Barkóczi, N., Kovács, Z., Burai, P. & Lénárt, C. (2017). Zooming on Aerial Survey. In G. Casagrande, A. Sik & G. Szabo (Eds.), *Small flying drones: Applications for geographic observation* (pp. 91–126). Springer-Verlag GmbH. https://doi.org/10.1007/978-3-319-66577-1

Tappeiner, U., Marsoner, T. & Niedrist, G. (2020). *Landwirtschaftsreport zur Nachhaltigkeit. Südtirol 2020* (U. Tappeiner, T. Marsoner & G. Niedrist, Eds.). Eurac Research. Retrieved August 10, 2021, from https://webassets.eurac.edu/31538/1620815463-landwirtschaftsreport-2020.pdf

Tarroux, E., DesRochers, A. & Tremblay, F. (2014). Molecular analysis of natural root grafting in jack pine (pinus banksiana) trees: How does genetic proximity influence anastomosis occurrence? *Tree Genetics & Genomes*, *10*(3), 667–677. https://doi.org/10.1007/s11295-014-0712-6

Tchuenté, L.-A. T., Stothard, J. R., Rollinson, D. & Reinhard-Rupp, J. (2018). Precision mapping: An innovative tool and way forward to shrink the map, better target interventions, and accelerate toward the elimination of schistosomiasis (J. Keiser, Ed.). *PLOS Neglected Tropical Diseases*, *12*(8), e0006563. https://doi.org/10.1371/journal.pntd.0006563

Tedeschi, R. & Alma, A. (2004). Transmission of Apple Proliferation Phytoplasma by Cacopsylla melanoneura (Homoptera: Psyllidae). *Journal of Economic Entomology*, *97*(1), 8–13. https://doi.org/10.1603/0022-0493-97.1.8

Tedeschi, R. & Alma, A. (2006). Fieberiella florii (homoptera: Auchenorrhyncha) as a Vector of “candidatus Phytoplasma mali”. *Plant Disease*, *90*(3), 284–290. https://doi.org/10.1094/pd-90-0284

Tedeschi, R., Jarausch, B., Delic, D. & Weintraub, P. (2013). Actual distribution of fruit tree and grapevine phytoplasma diseases and their vectors in Europe and neighboring regions. *Phytopathogenic Mollicutes*, *3*(1), 3. https://doi.org/10.5958/j.2249-4677.3.1.002

Thenkabail, P. S., Lyon, J. G. & Huete, A. (2018). Fifty Year of Advances in Hyperspectral Remote Sensing of Ariculture and Vegetation - Summary, Insights, and Highlights of Volume IV. In P. S. Thenkabail, J. G. Lyon & A. Huete (Eds.), *Advanced Applications in Remote Sensing of Agricultural Crops and Natural Vegetation* (2nd ed., pp. 339–378). CRC Press. https://doi.org/https://doi.org/10.1201/9780429431166

Trakas, A. (2012). Standards: The foundation fro service-oriented mapping. In M. Jobst (Ed.), *SOMAP 2012 : Service-Oriented Mapping 2012* (pp. 27–38). JOBSTMedia Präsentation Managment Verlag.

Tsouvalis, J., Seymour, S. & Watkins, C. (2000). Exploring Knowledge-Cultures: Precision Farming, Yield Mapping, and the Expert–Farmer Interface. *Environment and Planning A: Economy and Space*, *32*(5), 909–924. https://doi.org/10.1068/a32138

Tucker, C. J. (1979). Red and photographic infrared linear combinations for monitoring vegetation. *Remote Sensing of Environment*, *8*(2), 127–150. https://doi.org/10.1016/0034-4257(79)90013-0

Tucker, C. J., Holben, B. N., Elgin, J. H. & McMurtrey, J. E. (1981). Remote sensing of total dry-matter accumulation in winter wheat. *Remote Sensing of Environment*, *11*, 171–189. https://doi.org/10.1016/0034-4257(81)90018-3

Underwood, E. (2003). Mapping nonnative plants using hyperspectral imagery. *Remote Sensing of Environment*, *86*(2), 150–161. https://doi.org/10.1016/s0034-4257(03)00096-8

United Nations General Assembly. (2015). Resolution a/res/70/1: Transforming our world: The 2030 agenda for sustainable development (21 october 2015). *United Nations*. https://www.un.org/ga/search/view_doc.asp?symbol=A/RES/70/1&Lang=E

United Nations Secretary-General & World Commission on Environment and Development. (1987). Report of the world commission on environment and development : Note / [Includes bibliographical references.], 374. https://digitallibrary.un.org/record/139811?ln=en

Unterthurner, M. & Baric, S. (2011). Sechs jahre erfahrung in einer modellanlage. *Obstbau Weinbau*, *48*(3), 77–78. http://www.laimburg.it/en/projects-publications/publications.asp?somepubl_action=300&somepubl_image_id=210310

Usery, E. L., Pocknee, S. & Boydell, B. (1995). Precision farming data management using geographic information systems. *Photogrammetric Engineering & Remote Sensing*, *61*(11), 1383–1391. https://www.asprs.org/wp-content/uploads/pers/1995journal/nov/1995_nov_1383-1391.pdf

Vancauwenberghe, G. & Valečkaitė, K. (2018). Assessing the openness of spatial data infrastructures (sdi): Towards a map of open sdi. *International Jounral of Spatial Data Infrastructure Research*, (13), 88–100. https://doi.org/10.2902/1725-0463.2018.13.art9

Wahabzada, M., Mahlein, A.-K., Bauckhage, C., Steiner, U., Oerke, E.-C. & Kersting, K. (2015). Metro maps of plant disease dynamics—automated mining of differences using hyperspectral images (D. A. Lightfoot, Ed.). *PLOS ONE*, *10*(1), e0116902. https://doi.org/10.1371/journal.pone.0116902

Wahabzada, M., Mahlein, A.-K., Bauckhage, C., Steiner, U., Oerke, E.-C. & Kersting, K. (2016). Plant phenotyping using probabilistic topic models: Uncovering the hyperspectral language of plants. *Scientific Reports*, *6*(1). https://doi.org/10.1038/srep22482

Walker, P. G. T., Griffin, J. T., Ferguson, N. M. & Ghani, A. C. (2016). Estimating the most efficient allocation of interventions to achieve reductions in plasmodium falciparum

malaria burden and transmission in africa: A modelling study. *The Lancet Global Health*, *4*(7), e474–e484. https://doi.org/10.1016/s2214-109x(16)30073-0

Wegmann, M., Leutner, B. & Dech, S. (2016). *Remote sensing and gis for ecologists*. Pelagic Publishing Ltd.

Weibel, R. (1997). Generalization of spatial data: Principles and selected algorithms. In M. van Kreveld, J. Nievergelt, T. Roos & P. Widmayer (Eds.), *Algorithmic foundations of geographic information systems* (pp. 99–152). Springer Berlin Heidelberg. https://doi.org/10.1007/3-540-63818-0_5

Weinstein, B., da Silva, A. R., Kouzoukas, D. E., Bose, T., Kim, G. J., Correa, P. A., Pondugula, S., Lee, Y., Kim, J. & Carpenter, D. O. (2021). Precision mapping of COVID-19 vulnerable locales by epidemiological and socioeconomic risk factors, developed using south korean data. *International Journal of Environmental Research and Public Health*, *18*(2), 604. https://doi.org/10.3390/ijerph18020604

Weintraub, P. G. & Beanland, L. (2006). INSECT VECTORS OF PHYTOPLASMAS. *Annual Review of Entomology*, *51*(1), 91–111. https://doi.org/10.1146/annurev.ento.51.110104.151039

White, T. (2017). Symbolization and the visual variables. *Geographic Information Science & Technology Body of Knowledge*, *2017*(Q2). https://doi.org/10.22224/gistbok/2017.2.3

Wickham, H. (2016). *Ggplot2: Elegant graphics for data analysis*. Springer-Verlag New York. https://ggplot2.tidyverse.org

Wickham, H., Averick, M., Bryan, J., Chang, W., McGowan, L. D., François, R., Grolemund, G., Hayes, A., Henry, L., Hester, J., Kuhn, M., Pedersen, T. L., Miller, E., Bache, S. M., Müller, K., Ooms, J., Robinson, D., Seidel, D. P., Spinu, V., Takahashi, K., Vaughan, D., Wilke, C., Woo, K. & Yutani, H. (2019). Welcome to the tidyverse. *Journal of Open Source Software*, *4*(43), 1686. https://doi.org/10.21105/joss.01686

Wickham, H., François, R., Henry, L. & Müller, K. (2021). *Dplyr: A grammar of data manipulation* [R package version 1.0.5]. https://CRAN.R-project.org/package=dplyr

Wilkinson, M. D., Dumontier, M., Aalbersberg, I. J., Appleton, G., Axton, M., Baak, A., Blomberg, N., Boiten, J.-W., da Silva Santos, L. B., Bourne, P. E., Bouwman, J., Brookes, A. J., Clark, T., Crosas, M., Dillo, I., Dumon, O., Edmunds, S., Evelo, C. T., Finkers, R., Gonzalez-Beltran, A., Gray, A. J., Groth, P., Goble, C., Grethe, J. S., Heringa, J., Hoen, P. A. ’., Hooft, R., Kuhn, T., Kok, R., Kok, J., Lusher, S. J., Martone, M. E., Mons, A., Packer, A. L., Persson, B., Rocca-Serra, P., Roos, M., van Schaik, R., Sansone, S.-A., Schultes, E., Sengstag, T., Slater, T., Strawn, G., Swertz, M. A., Thompson, M., van der Lei, J., van Mulligen, E., Velterop, J., Waagmeester, A., Wittenburg, P., Wolstencroft, K., Zhao, J. & Mons, B. (2016). The FAIR guiding principles for scientific data management and stewardship. *Scientific Data*, *3*(1). https://doi.org/10.1038/sdata.2016.18

Wood, C. L., Sokolow, S. H., Jones, I. J., Chamberlin, A. J., Lafferty, K. D., Kuris, A. M., Jocque, M., Hopkins, S., Adams, G., Buck, J. C., Lund, A. J., Garcia-Vedrenne, A. E., Fiorenza, E., Rohr, J. R., Allan, F., Webster, B., Rabone, M., Webster, J. P., Bandagny, L., Ndione, R., Senghor, S., Schacht, A.-M., Jouanard, N., Riveau, G. & Leo, G. A. D. (2019). Precision mapping of snail habitat provides a powerful indicator of human schistosomiasis transmission. *Proceedings of the National Academy of Sciences*, *116*(46), 23182–23191. https://doi.org/10.1073/pnas.1903698116

Yao, H., Huang, Y., Tang, L., Tian, L., Bhatnagar, D. & Cleveland, T. E. (2018). Using hyperspectral data in precision farming applications. In P. S. Thenkabail, J. G. Lyon & A. Huete

(Eds.), *Advanced applications in remote sensing of agricultural crops and natural vegetation* (2nd ed., pp. 3–35). CRC Press. https://doi.org/10.1201/9780429431166-1

Young, A. & Britton, G. (1990, January). Carotenoids and stress. In R. G. Alscher & J. R. Cumming (Eds.), *Stress responses in plants: Adatation and acclimation mechanims* (pp. 87–112). Wiley-Liss.

Yuan, L., Zhang, J.-C., Wang, K., Loraamm, R.-W., Huang, W.-J., Wang, J.-H. & Zhao, J.-L. (2013). Analysis of spectral difference between the foreside and backside of leaves in yellow rust disease detection for winter wheat. *Precision Agriculture*, *14*(5), 495–511. https://doi.org/10.1007/s11119-013-9312-y

Zarco-Tejada, P. J., Miller, J. R., Noland, T. L., Mohammed, G. H. & Sampson, P. H. (2001). Scaling-up and model inversion methods with narrowband optical indices for chlorophyll content estimation in closed forest canopies with hyperspectral data. *IEEE Transactions on Geoscience and Remote Sensing*, *39*(7), 1491–1507. https://doi.org/10.1109/36.934080

Zawadzka, B. J. (1976). Reaction of apple cultivars to infection by apple proliferation disease. *Acta Horticulturae*, (67), 113–120. https://doi.org/10.17660/actahortic.1976.67.12

Zebisch, M., Vaccaro, R., Bertoldi, G., Schneiderbauer, S., Schlögel, R., Kofler, C., Obojes, N., Niedrist, G., Seeber, J., Vigl, L. E., Weiß, M. L., Streifeneder, T., Hoffmann, C., Götsch, H., Minerbi, S., Alberton, M., Bortolli, I. D., Scuttari, A., Unterthiner, G., Laner, P., Renner, K., Cavallaro, F. & Tappeiner, U. (2018). *Klimareport - Südtirol 2018* (M. Zebisch, R. Vaccaro, G. Niedrist, S. Schneiderbauer, T. Streifeneder, M. L. Weiß, A. Troi & K. Renner, Eds.). Bolzano, Italy, Eurac Research. https://webassets.eurac.edu/31538/1618826782-klimareport-2018-de.pdf